Microstructure and mechanical properties of the enameloid of pacu and piranha fishes: The role of different diets

Auteur : Müller, Laura
Promoteur(s) : Ruffoni, Davide
Faculté : Faculté des Sciences appliquées
Diplôme : Master en ingénieur civil biomédical, à finalité spécialisée
Année académique : 2020-2021
URI/URL : http://hdl.handle.net/2268.2/11649

UNIVERSITY OF LIEGE
FACULTY OF APPLIED SCIENCES

Microstructure and mechanical properties of the enameloid of pacu and piranha fishes: The role of different diets

Master thesis conducted by

LAURA MÜLLER

with the aim of obtaining the degree of Master in Biomedical Engineering

Under the supervision of

DAVIDE RUFFONI
PHILIPPE COMPÈRE
YANN DELAUNOIS

Liège

Academic year 2020-2021

Abstract

An understanding of the relationship between the structure, mechanical properties and functions of teeth is required regarding the development of effective and durable bio-inspired synthetic dental materials. Many studies have investigated this relationship in many species. However, few studies have been conducted on the teeth of Serrasalmidae fishes. The family of Serrasalmidae, though, offers an excellent opportunity to study this relationship because of the diversity of their diet.

The tooth consists of three distinct layers which are called (going from the center of the tooth to the outside): the pulp, the dentin and the enamel/enameloid. In some fishes, including those of the family Serrasalmidae, an additional superficial layer called the cuticle is also present.

The topic of the present thesis is to investigate structural and mechanical adaptation of the enameloid in two Serrasalmidae fishes having different diets: the carnivorous *Pygocentrus nattereri*, preferentially feeding on soft prey, and the herbivorous pacu *Piaractus brachypomus*, preferentially eating hard shells.

Enameloid microstructure is first characterized. Microscopic analysis of fractured teeth as well as surface etching performed on teeth sections allow identifying precisely the structure of the enameloid in the two species. Comparison between the structures found in the two species highlights that despite their different diets, no structural differences are observed between species with different feeding strategies (slicing vs. crushing). The enameloid of both fishes possesses a two-part organization. The inner enameloid is characterized by hydroxyapatite fiber bundles oriented and curved in a random manner forming a very sophisticated interlocking structure. The outer enameloid is organized with hydroxyapatite bundles aligned with each other and oriented either parallel or perpendicular to the tooth surface, depending on the region analyzed.

Second, the potential correlation between microstructure and mechanical properties is investigated through the assessment of local fracture behavior. Indeed, fracture resistance is an essential feature allowing the enameloid and, in general, the tooth to avoid catastrophic failure when cracks nucleate on the outer surface due to repeated cycles of chewing. High load indentation tests in combination with scanning microscopy are used to explore fracture properties of the different teeth. Although the difference is not significant, a quantitative evaluation of the fracture toughness as well as a qualitative observation of the cracks morphology demonstrates that inner enameloid possesses a higher resistance to crack initiation and propagation than the outer enameloid. Furthermore, indentation-based cracks invariably propagate along the internal interfaces, especially at the interface between the hydroxyapatite bundles, and that several extrinsic toughening mechanisms, such as crack deflection/curvature and uncracked hydroxyapatite bundles are used by the enameloid to increase fracture resistance.

Novel addictive manufacturing routes such as freeze casting or magnetically assisted manufacturing may allow the fabrication of ceramic scaffolds replicating the structure seeing in the enameloid to improve fracture resistance of synthetic teeth.

Acknowledgements

This work gave me the opportunity to be immersed for the first time in the world of experimentation and research. As in any research work, many small challenges arose throughout this work and the experiments carried out and without the precious support of many people, I would definitely not have been able to complete this thesis. I would like here to express them all my gratitude.

First of all, I would like to express all my gratitude to my supervisor, Professor Davide Ruffoni, for giving me the opportunity to work on such an interesting project within his laboratory. I especially want to thank him for all the time he gave me during this year but also for his precious advice and his enthusiasm towards my work which motivated me a lot during the realization of this thesis. I also thank him for supporting me in projects adjacent to my thesis.

I also want to thank the members of my jury for taking the time to read this thesis and to listen to my defense.

I would like to thank personally all the other persons that have contributed to the realization of my thesis. I would like to thank, first of all, Yann Delaunois for the great support he gave me during the experiments, the analysis of the results and the writing of this thesis, for his explanation for the biological aspects that were sometimes unknown to me but also for his constant kindness and benevolence during this year. I would also like to thank Alexandra Tits who helped me a lot even though they didn't have to. With Astrid Cantamessa, they were always supportive and reassuring and gave me a lot of useful advice throughout the year. I would also like to thank all the rest of the MBBM team for their kindness and their friendly welcome that they reserved for me in their team during this year.

I am deeply grateful to my family who has given me unfailing moral support throughout this thesis but more importantly throughout my studies. I am particularly fortunate to have a family that has supported me through my ups and downs without fail. I would also like to thank my friends who have made my studies years filled with joy and laughter. Their help and encouragement have been invaluable throughout these years.

Contents

Introduction

Through natural selection, over millions of years of evolution, living organisms have developed specific biological materials whose structure and chemical composition allows them to perform and optimize specific functions while meeting the requirements of the environment and the ecology of the organism.

Many biological materials are composites consisting of a stiff and brittle inorganic component embedded into a soft and ductile organic matrix. These natural composites possess a hierarchical structure from the molecular to the macro level providing exceptional mechanical properties that surpass those of their relatively weak constituents. Understanding the design principles used by nature to meet the mechanical demands and respond to the dynamic stimuli of the environment of biological materials has become a growing research topic in recent years. One of the main reasons for this increase is the inspiration to develop new bio-inspired and bio-mimetic high-performance materials with advanced properties while using more environmentally friendly resources. Indeed, current man-made composites have inferior mechanical properties at equal density to those found in composites created by nature. Considerable examples of fascinating biological materials include the nacre of abalone shell that shows a fracture work 3000 times higher than that of the mineral component, the Spider silk with a tensile strength similar to that of high-quality steel or even wood that can bend without breaking [1].

Teeth are an interesting biological structure. They are adapted to their main function, which is the consumption and processing of food. Mechanically speaking, teeth must be able to withstand large compressive forces (due to contact with other teeth and food) without deforming or breaking [1].
The study of teeth and more precisely their outermost layer called enamel (or enameloid) is interesting to develop efficient bio-inspired synthetic dental materials [2]. Indeed, natural teeth have advantages over commercially available synthetic dental materials (ceramics, polymers,..). These artificial materials do not possess both high load-bearing capacity and high fracture resistance, which is possible in biological tooth enamel due to its hierarchical structure. In addition, their mechanical properties are very different from those of natural enamel. Ceramics are much harder and polymers softer than tooth enamel. This can, for example, lead to inhomogeneous abrasions of the surface of the synthetic tooth or of the natural tooth on the opposite jaw. The study of enamel could enable the development of bio-inspired and bio-mimetic materials using the same design principles as those used by nature and thus recreating the same or similar properties as natural teeth. The bio-inspired materials offer great potential for improving the performance and durability of dental materials [3].

This thesis focuses on the most mineralized layer of the tooth, called enameloid, of two fishes of the family Serrasalmidae, the carnivorous *Pygocentrus nattereri* and the herbivorous *Piaractus brachypomus*. It aims at studying structural and mechanical adaptation of this layer to different diets.

This work is divided into four main chapters. The first one is dedicated to the introduction of the concepts necessary to understand this work. Basic notions about the tooth, such as its functions, organization in the mouth, morphology and structure are described for different vertebrates. Also, more details are given about the outermost layer of the tooth called the enameloid/enamel, such as its development,

structure, chemical composition and mechanical properties. Then, the two fishes we are interested in and their family are presented. Finally, to close this chapter, a brief state of the art of current knowledge about the teeth of these two fishes is done in order to introduce the main aims of the master thesis in detail.

The second chapter focuses on the description of the experiments conducted throughout this master thesis. It describes how samples were prepared, worked and then analyzed. Surface etching and fractures were performed on teeth of both species and observed with a scanning electron microscope to study the enameloid structure. The fracture toughness of this layer was then studied using high load indentation tests followed by microscopic analysis.

The third chapter presents the results. The images of the structure and the high load indentations obtained with scanning electron microscope are observed and analyzed.

In the last chapter, the observations made in the previous chapter are related and discussed in relation to the literature in order to characterize the enameloid microstructure of the two species and to identify the role of this structure in the resistance to crack initiation and propagation. This chapter also includes a discussion about the limitations encountered in this master thesis and presents ideas of improvement for future works.

Chapter 1

Background

The objective of this chapter is to provide the necessary context for understanding the work conducted in this master thesis. First, generalities on teeth are presented for several vertebrates, such as their functions, morphology, structure and chemical composition. Further description is then made for the enamel/enameloid, the structure studied in this work. Second, the Serrasalmidae family and more specifically the two species we are interested in are presented with a reminder of the current knowledge about the teeth of these fishes. Finally, the purpose of this thesis is introduced.

1.1 Teeth

The tooth is a hard organ found in the mouth of the gnathostome vertebrates, a group mainly composed of the extant back-boned animals. This organ is absent in certain back-boned animal as birds, this is a secondary loss [4, 5]. Some invertebrates also have structures called "teeth" around their mouth openings. Like vertebrate teeth, these structures help the animal to eat [4, 6]. The main difference with vertebrate teeth comes from the origin, the mode of secretion or the composition. In this master thesis, the term "teeth" is associated with animals having a backbone.

Teeth are essential for feeding. They allow for a better diet because they are involved in the first step of transforming food into nutrients. They are used to grasp, hold, tear and grind food. Apart from their role in feeding, teeth can also have more derived functions as being formidable weapons of attack and tusk against predators or rivals. Beavers use them to gnaw on trees that they use then to build dams and as a food source. Teeth can also be used for grooming that has an important role to play in the health of certain taxa like lemurs [4, 7]. In the male and some female narwhal, a unique and spiraled tooth is present on the top of their upper lip. It is sexually selected and probably functions as a signal and weapon during contests between males but also as a signal during mate choice. This tooth could also have other functions such as environmental sensing and prey capture [8].

Dental structures vary between vertebrates in several aspects. Significant differences can be observed between mammals and non-mammals, notably in tooth development and renewal. Vertebrates also show great diversity in the number, shape and location of their teeth in the mouth. Although the general structure of the tooth is very similar in all vertebrates with a layered structure consisting of pulp, dentin and enamel/enameloid, some variations such as the nature of their attachment to the bone or the structure of the enamel/enameloid at the micrometer scale appear among the vertebrate classes [4, 9].

1.1.1 Replacement

The renewal of teeth and their life span in the mouth varies between lower and upper vertebrates.

- **Mammalian vertebrates**

The majority of existent mammals have diphyodontic dentition which means that their teeth are replaced only once [5, 10]. Humans, for example, have only two sets of teeth: the fists to appear are deciduous teeth (also known as primary or baby teeth) and the second one is permanent teeth (secondary or adult teeth) [5, 11]. Other mammals such as cetaceans are monophyodont and do not replace any of their teeth [12, 13].
Because of the limited ability of mammals to renew teeth, mammalian teeth wear out throughout their life. The thickness and microstructure of their outermost layer (enamel) have evolved to resist abrasion and extend the life of a tooth [5].

Some mammals use strategies to compensate for tooth wear. One solution frequently used is hypsodontia [5]. This refers to the dentition where the teeth have a high crown, possibly short root and prolonged or continuous growth. Note that the crown is the part of the tooth that protrudes from the gum as opposed to the root. The continued growth requires the availability of stem cells. This type of dentition is found in horses, cows, and rodents [5, 11] (Figure 1.1.C). A few groups of mammals such as wallabies, manatees, and silver rat, use another strategy. They have the ability to develop new molars distal to the last molar. When the anterior molars are worn out, they are removed, all the teeth are moved forward and the new molars are positioned in the jaw of the animal [5].

- **Non-mammalian vertebrates**

Lower vertebrates differ from mammals in their ability to renew their teeth throughout the life of the animal [11]. These vertebrates and their jaws grow during their lives. Their teeth are therefore continually replaced, with each new set being slightly larger than the previous one, in order to keep pace with the growth of the jaws. In addition to the increase in size, the number of teeth may also increase with age [4].

During the formation of a replacement tooth, an epithelial thickening develops in the surroundings of the functional tooth to form a tooth bud. This occurs because the epithelium contains epithelial stem cells which are responsible for the continual renewal of the tooth. The bud then develops into the mesenchyme and progress either on the surface of the bone (extraosseous replacement) or by entering the medullary cavity of the tooth-bearing bone (intraosseous replacement) [14]. The location of the replacement teeth formation differs from one specie to another. In most characiformes (order of fishes that contains the Serrasalmidae family), they develop intraosseously beneath the functional teeth, either in a cavity within the jaw bone or in a trench [15].

In many Characiformes, the renewal of all the teeth in each quadrant occurs simultaneously, with the teeth developing, erupting and shedding almost at the same time. This has the advantage for piranhas of allowing the establishment of an interlocking row of teeth [15].

1.1.2 Morphology and organization

Vertebrates present a great diversity in terms of tooth shape, tooth arrangement and presence of occlusion between the jaws.

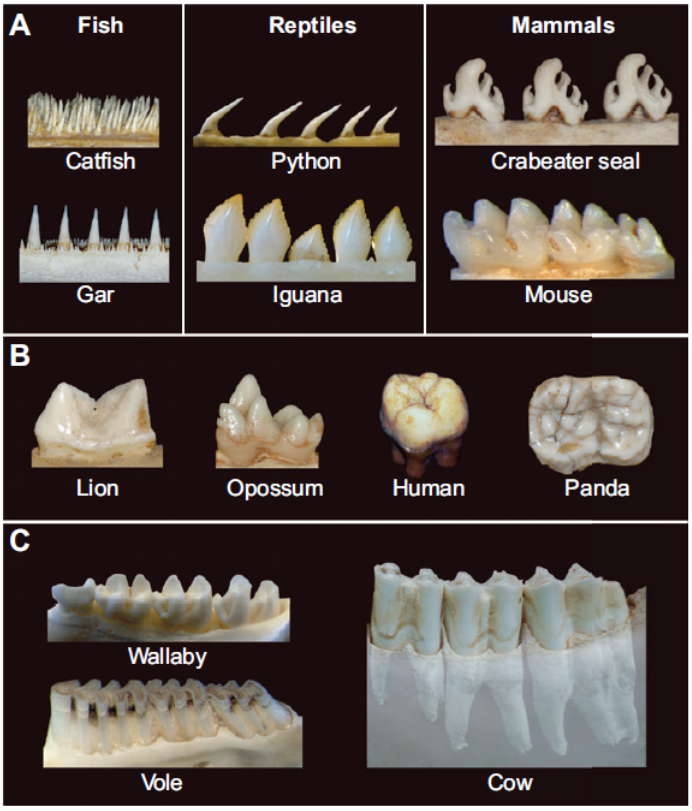

Figure 1.1: Diversity of morphology within vertebrate teeth [5].

The morphology of the tooth can vary in terms of size, but also in terms of the number, location and shape of the cusps (Figure 1.1). The cusp is an eminence of convex shape and variable volume present on the teeth surface. The teeth can be unicuspid or multicupsid. Moreover, the cusps can have different shapes, they can be individual bumps or elongated blades. They can also sometimes assemble to form complex crest patterns[5].
Mammals exhibit the most diverse multicuspid teeth with teeth generally more complex having a greater number of cusps (Figure 1.1.A). The molars of herbivorous mammals specialized in the consumption of plants such, as horses, are generally even more complex than the teeth present in animal-eating mammals, such as lions (Figure 1.1.B). Fishes and reptiles tend to have a greater number of simpler teeth [5] (Figure 1.1.A).

The arrangement of the teeth in the oral cavity also varies according to the classes of vertebrates. Mammals display a diverse and regionalized dentition, called heterodonty. They have teeth of various shapes within the same jaw: incisors, canines, premolars and molars (Figure 1.2). Their teeth are positioned in a single row in the anterior part of the mouth (mandible and maxilla) [4, 5].
Unlike mammals, the other vertebrates can have one or more rows of teeth in many places. In fishes, teeth can be located almost everywhere in the head: on the jaws, the palate, the floor of the mouth, the pharynx, the vomer, the gill arches and also the tongue. The lower vertebrates present a homologous dentition, i.e. composed of identical teeth [4, 10, 11].

Natural selection leads to the most optimized morphology and arrangements for the specific biological function of the teeth, i.e. the food consumption mode of the species to which they belong. Teeth are therefore characterized by the diet of the species, it conditions their shape, their arrangement and their number in the mouth in such a way as to maximize the efficiency of the decomposition of the food

consumed by the animal.

The teeth of herbivorous mammals are designed to crush and break up the vegetable matter. They are rough with very large surfaces, long crowns and short roots. Foliivores, which feed on leaves and stems, usually have elevated cusps connected by ridges to shear plants. The frugivorous species, especially those feeding on hard objects, tend to have blunter teeth that promote crushing. The jaws of the herbivorous species allow lateral movements during chewing [4, 16].
Carnivorous mammals have vertical up and down movements of their jaws, similar to that of a hinge. Their teeth have contact edges that are oriented parallel to the plane of motion, so the teeth are able to slide over each other [4, 17].
Insectivorous mammals feed on insects with chitinous and tough shells. Their teeth have many sharp, pointed cusps that interlock with opposing teeth acting like a mortar to break down the insect body [4].
Some mammals such as humans are omnivores. They eat either animal or plant foods. This more varied diet results in less specialized teeth [4, 17].

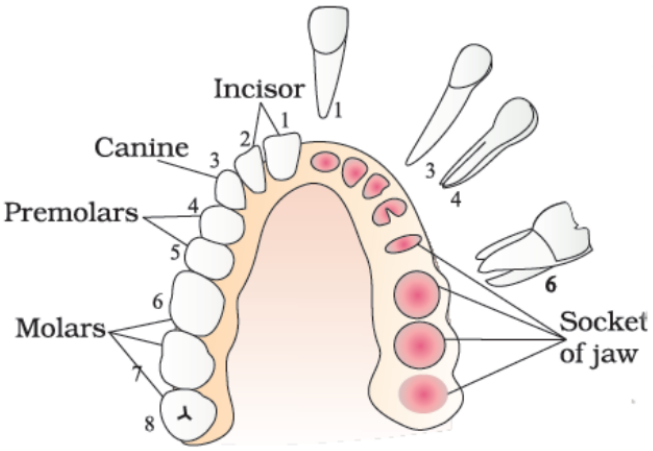

Figure 1.2: Types of teeth in the human mouth [18].

Because the size, shape, and organization of teeth in the mouth are related to the animal's diet, it is possible to determine from an animal skull the diet of living or fossil vertebrates [4, 16, 17].

Notice that the dentition of lower vertebrates does not present an occlusion between the opposing jaws. This absence is justified by the function of their dentition, which is generally limited to the capture, piercing and cutting of food into large fragments. Mammals, on the other hand, have a dental occlusion that allows them to better process food, which leads to an increase in the absorption of nutrients by the digestive system. The tooth is an important factor in the control of the occlusion. Indeed, an occlusion requires good contact between the cusps, pits and fissures of the teeth of the opposing jaws [19].

1.1.3 Structure and composition

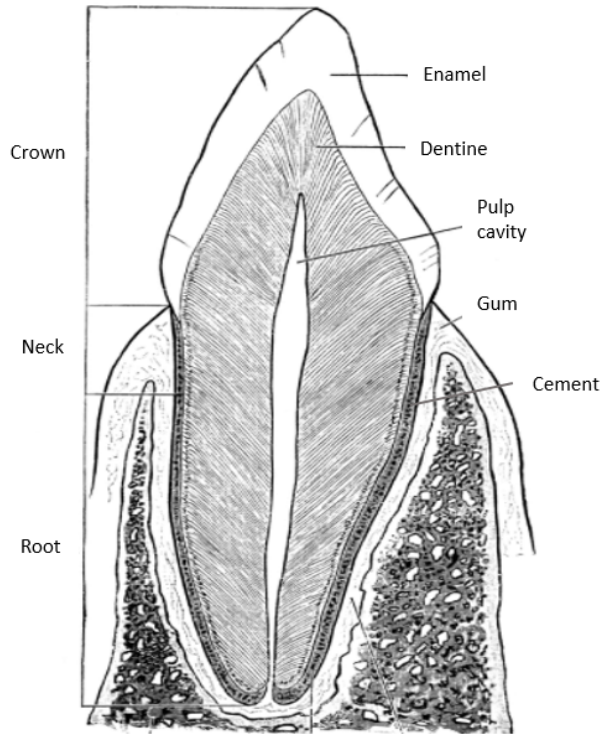

Figure 1.3: Section of canine teeth to illustrate the various parts and structures [20].

Teeth, composites of apatite and collagen, are the most mineralized component of vertebrate animals [1]. They have a hierarchical structure at different levels, from the nanoscale to the macroscopic scale. At length-scale between µm and mm, despite some differences, all the teeth have a general structure that consists of three main layers. The central part of the tooth is the dental pulp. It is surrounded and protected by a layer called dentin. The dentin is then covered on the crown by a hard and mineral-rich layer called the enamel in mammals and reptiles and the enameloid in amphibians and fish (Figure 1.3) [4, 21].

In addition, some families of fish including the family Serrasalmidae have a thin additional superficial layer that covers the enameloid. This layer is called the cuticle. It often presents a red pigmentation due to the presence of iron or iron oxide [21].

Mammalian teeth also have a root that allows the tooth to be anchored in the surrounding bone. This root is composed of four layers in the following order: dental pulp, dentin, enamel and a thin layer of cement. The root is not present in fish whose teeth are fixed with a connective tissue [4, 11].

1.1.3.1 Pulp

The pulp is the soft and sensitive central part of the tooth protected by the surrounding dentin [4]. It is a connective tissue, it contains thin type I collagen fibers and fibroblasts. It is rich in blood vessels and nerves [1, 15, 22]. Nerves transmit pain signals and blood vessels ensure the vascularization of the cells. The pulp tissue also contains immune cells and stem cells. The latter are able to differentiate into odontoblasts that secrete repair dentin in response to external stimuli (e.g. wear) [15].

In mammalian vertebrates, the dental pulp plays several crucial roles, providing nutrients to odontoblasts and producing both reparative responses to injury and immune responses to infection. These are essential roles in mammalian teeth as they cannot be replaced more than once in a mammal's lifetime. In non-mammalian vertebrates, teeth are generally replaced throughout life. It is therefore possible that the pulp has much more limited or absent support functions than in mammals [15].

1.1.3.2 Dentin

The dentin is the layer covering the dental pulp. This layer is synthesized by odontoblasts [9, 15, 22].

This layer has a composition close to that of bone. It is a mineralized layer containing crystallized apatite ($\sim$ 45 vol.%), type I collagen fibers ($\sim$ 30 vol.%), fluids and proteins [1, 15, 21, 23, 22, 24]. The dentin proteins include phosphoproteins and sialoprotein, which are two proteins coded by the same gene, but also bone sialoprotein, osteocalcin, osteopontin and dentin matrix protein-1. This last protein potentially plays a role in the differentiation of mesenchyme into odontoblasts [23].

The dentin is a porous structure characterized by numerous µm-sized dentinal tubules [4, 25, 26]. The diameter of the tubules varies according to the species. For example, the tubules present in fish dentin have a smaller diameter than those in human dentin. They host odontoblast processes whose cell bodies are located in the dental pulp [4, 21, 26].

1.2 Enameloid (or enamel)

The layer protecting and covering the dentin is called “enamel” in mammals and reptiles and “enameloid” in amphibians and fishes [21].

These tissues play a critical role in protecting the underlying dentin and pulp cavity from mechanical damages. They also allow the tooth to accomplish its functions, namely chewing for herbivorous species and biting and tearing for carnivorous species. To do so, enameloid and enamel enable the teeth to support large compressive and repeated loads without deforming and breaking [1, 2].

Although the chemical composition of enamel and enameloid is roughly similar, these two tissues have different microstructures. This difference in structure could be explained by the limited capacity of mammals to renew their teeth during their life unlike the lower vertebrates [5]. Indeed, the microstructure of the enamel of mammals must thus allow the tooth to survive throughout the life of the animal. The structural variation may also stem from differences in the formation of these two layers.

1.2.1 Development

The development of a tooth can be divided into a series of stages, in order, the dental lamina, bud, cap and bell stage [23] (Figure 1.4).

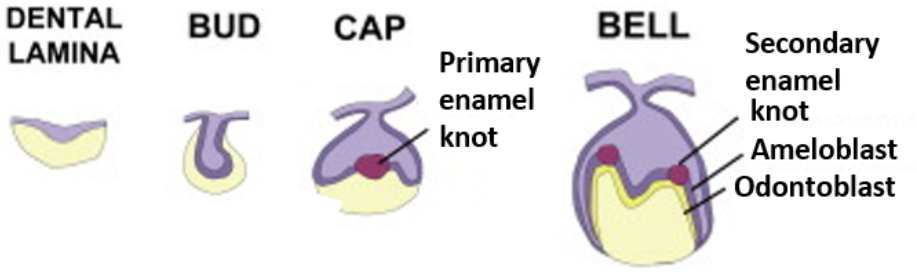

Figure 1.4: Stages of development of mammalian teeth. The yellow color represents the mesenchyme and the purple color represents the epithelium [27].

They lead to the formation of a tooth germ composed of the epithelium divided into the inner and outer dental epithelium and a mesenchymal dental papilla [15, 23, 27, 28] (Figure 1.5).

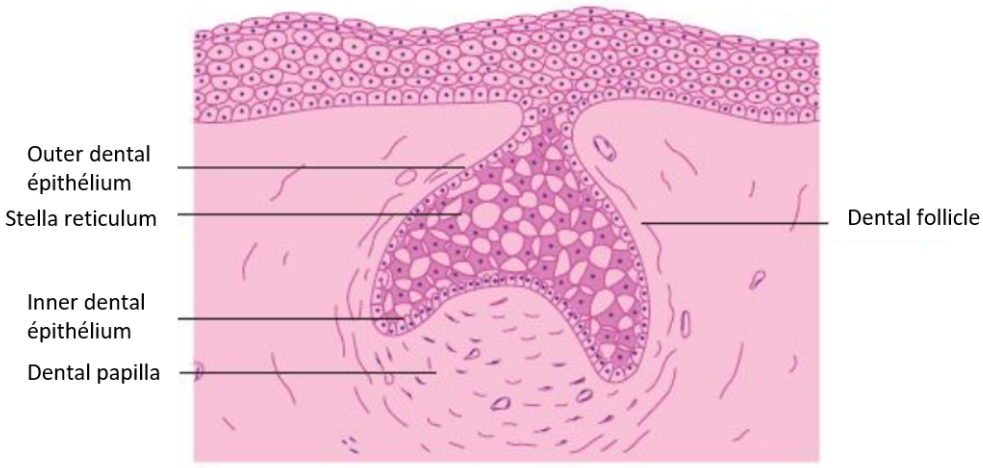

Figure 1.5: Dental tissue at the cap stage [29].

The main difference in the development of teeth in higher and lower vertebrates appears at the bell stage in the formation of enameloid and enamel. These two tissues do not have the same origin [21, 28].

- **Enamel**

The enamel is synthesized exclusively by inner dental epithelial cells.
From the bell stage, the inner dental epithelium and the adjacent outer layer of mesenchymal cells of the dental papilla differentiate. They then acquire the ability to secrete hard organic tissue matrices[15]. The outer layer of dental papilla cells differentiates into odontoblasts that secrete the dentin matrix. Immediately after predentin deposition, the inner dental epithelium differentiates into ameloblasts synthesizing the enamel matrix. Both are then mineralized to form enamel and dentin. As the enamel mineralizes, the matrix is gradually lost, so that the mature enamel contains only a small residue of organic matrix. Note that before tooth eruptions, ameloblasts die, therefore enamel is no longer being synthesized during the life of the organism [15, 22, 23].

- **Enameloid**

The enameloid also originates from inner dental epithelial cells but predominantly from mesenchymal cells.
As in mammals, from the bell stage, the outer layer of mesenchymal cells of the dental papilla differentiate into odontoblasts that have a major role in enameloid formation [15, 28]. However, in fishes, the differentiated inner dental epithelial cells cannot be called ameloblasts like the corresponding mammalian cells because their role in enameloid formation is minor [15].
The formation of the enameloid begins with the deposition of a thin layer of enameloid matrix at the interface between the inner dental epithelium and the dental papilla (Figure 1.6.a) [15, 28, 30]. This organic matrix contains numerous collagen fibrils secreted by odontoblasts that are organized in bundles and remain intimately linked to odontoblasts [25, 28, 30]. It also includes some proteins secreted by odontoblasts and the inner dental enameloid [28]. The thin organic matrix layer then gradually thickens, accompanied by an increase in fibril diameter [25].
Once the enameloid matrix is fully formed, dentin formation and enameloid mineralization begin [15, 25]. The latter begins at the junction between the enameloid and predentin and slowly expands to the apex of the enameloid cap [30]. This mineralization occurs by the deposition of fine crystals along the collagen fibrils. The orientation of these crystals is therefore imposed by the pattern of the collagen fibers of the matrix [4, 25] (Figure 1.6.c).

At the same time as enameloid mineralization, dentin formation begins with the deposition of a thin layer of dental matrix at the surface of the dental papilla. Before reaching considerable mineralization of the enameloid, the thin layer of dental matrix is unable to increase its thickness and to mineralize. Once the enameloid is sufficiently mineralized, the predentin thickens and organic substances are deposed [25]. The mineralization occurs starting from the part adjacent to the enameloid and extending to the pulp [15, 25].
The last step in the enameloid formation is the maturation stage (Figure 1.6.d). The cells of the internal dental epithelium are engaged in the degeneration and elimination of the organic matrix of the enameloid, which results in a considerable increase in the percentage of minerals [30].

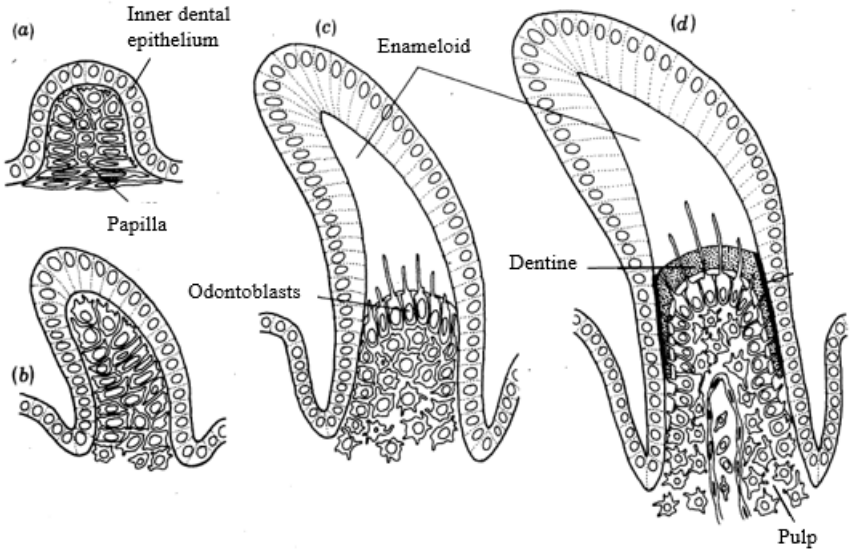

Figure 1.6: Stages of development of non-mammalian teeth. (a) Bell stage; (b) Enameloid matrix formation; (c) Enameloid mineralization; (d) Maturation [28].

1.2.2 Chemical composition

Enamel and enameloid have a similar composition. They are highly mineralized layers with a mineral content of 96 %vol µm-sized prismatic apatite crystals with a hexagonal cross-section shape and a very small amount of organic component and water [1, 2, 21, 31, 32]. The organic enamel matrix is mainly composed of proteins produced by the ameloblasts. Those are amelogenin, enamelin, ameloblastin and tuftelin [22, 33]. Amelogenins are the most abundant proteins in the enamel (90%). They are hydrophobic proteins and seem to be the main organizers of the deposition of enamel. The interaction of amelogenin with ameloblastin seems to play a role in the formation of the enamel. The functions of two other proteins, tuftelin and enamelin, are still not yet well understood [22, 23]. All the proteins present in enamel tend to be absent in the enameloid except for enamelin. The commune presence of enamelin in enamel and enameloid is probably responsible for the presence of the large hydroxyapatite crystals and the high levels of mineralization [33]. The organic enameloid matrix is composed mainly of collagen, which is not present in the enamel [19].

Enamel and enameloid are highly mineralized tissues composed of calcium phosphate mineral crystals, known as apatite [4, 9]. Apatite refers to a diversified group of phosphate minerals having the general formula: $Ca_{10}(PO_4)_6X_2$ where X is typically F (fluorapatite), OH (hydroxyapatite), or Cl (chlorapatite) [34].
Fluoroapatite and hydroxyapatite do not have the same mechanical properties: the first has a higher apparent modulus than hydroxyapatite, higher stiffness constants and higher elastic moduli. Fluorapatite

is therefore harder than hydroxyapatite [35].
Substitutions are common in the apatite lattice. Calcium can, for example, be replaced by sodium, strontium or magnesium and carbonate ions can replace phosphate [9, 34, 36]. These substitutions affect apatite properties such as lattice parameters, morphology, crystal size and stability (solubility) [9, 36]. A high fluorine content increases the stability and results in a reduction in carbonate content, and a greater crystallite size [9, 33, 36]. An increase in carbonate content provides greater solubility to the mineral. In seawater, carbonate-rich fluorapatite is the most dynamically stable phase [9].
In mammals, the mineral phase of enamel and dentin consists of hydroxyapatite. In many fishes, in addition to hydroxyapatite, the enamel and dentin contain varying concentrations of fluorapatite [37]. The presence of fluorine in dentin apatite depends on the fluorine concentration of the surrounding water. However, such dependence is not observed in enameloid and the fluoride content of the enamel is mainly associated with the fish species [37, 33].

1.2.3 Structure

The two tissues present a strong structural diversity among vertebrates. In most cases, amphibians and reptiles exhibit an aprismatic structure while the enamel of mammals is formed of prismatic structures [19]. The structure of enamel has been well described for the teeth of humans and some kinds of animals.

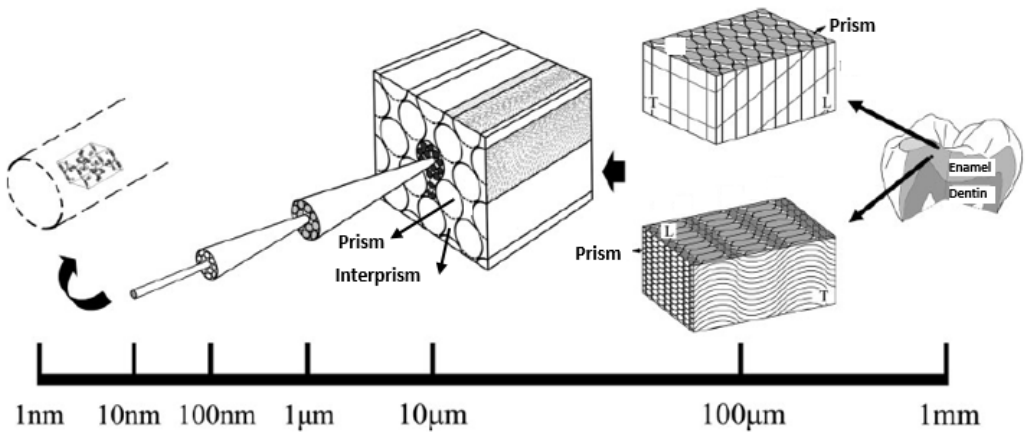

Figure 1.7: Schematic illustration of the human enamel hierarchical structure (from the nanometer to the millimeter scale). *Abbreviations: T, transverse plane; L, Longitudinal plane* [38].

The enamel structure found in humans is a complex hierarchical structure whose main structural elements are nano-sized fibril-like hexagonal hydroxyapatite crystallites ($Ca_5(PO_4)_3OH$) of 26 nm thickness (Figure 1.7). These are closely packed and run parallel to each other along their long axis to form mineral nanofibrils, whose diameter is 30-40 nm. These nanofibrils are aligned lengthways and aggregate into fibrils. Those are enveloped by an organic matrix and aligned in parallel to form thicker fibers called crystal fibers, whose diameter is 800 nm. Then, these crystal fibers cluster to each other in two different organizations called prism with a diameter of 6-8 µm (also called rod) and interprism. In the center of the prisms, the fibers are aligned lengthways and lie parallel to the rod axis. They deviate more and more like the distance from the center increase and finally near to the edge of the prism, they have an angle of 45° to the longitudinal axis of the rod. In the interprisms, the fibers are oriented perpendicularly to the rod axis. Between prisms and interprisms, there is a prism sheath consisting of organic matrix. Finally, in the outer third of the enamel thickness, the rods are arranged in parallel and oriented radially, intercepting the surface perpendicularly. In the inner two thirds of the enamel thickness, the

prisms undulate [38, 31].

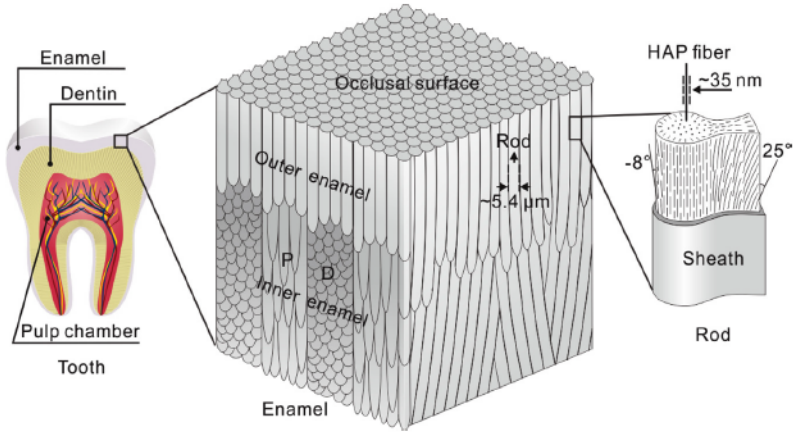

Figure 1.8: Schematic illustration of the hierarchical structure of the giant panda enamel [2].

The enamel structure of humans is similar to that of some other mammals such as rodents and carnivores. The main difference with the human enamel is the characteristic size of the structural units (e.g. diameter of the enamel rod or the diameter of hydroxyapatite fibers) [2].
Weng et al. (2016) [2] reported a structure similar to human enamel in the giant panda enamel. Indeed, it has a structure with enamel rods well aligned near the surface, these rods are then arranged obliquely to form alternating "X" shaped bands in the interior. In the rods, the nano-sized hydroxyapatite fibers are oriented along the long axis in the center and tilted gradually towards the sheaths at the periphery within rods (Figure 1.8).

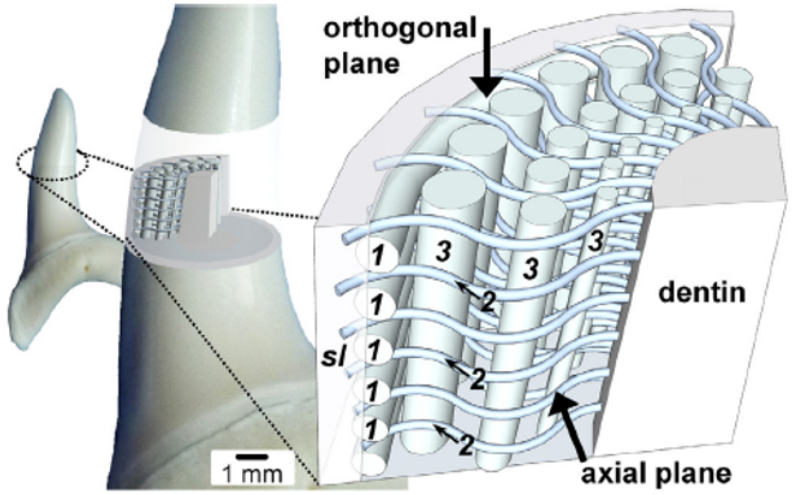

Figure 1.9: Schematic illustration of the fluoroapatite crystallite bundles organization in the shark outer enameloid. *Abbreviations: 1, Circumferential bundles; 2, Radial bundles; 3, Axial bundles* [3].

However, these structures are very different from that found in the enameloid of certain fishes such as sharks. In contrast to mammalian teeth, the smallest structural unit of shortfin mako shark (*I. oxyrinchus*) enameloid is fluoroapatite (Ca_5PO_4F) presented in the form of elongated fiber-like crystallites of roughly hexagonal cross-section with a length of 1 µm and a thickness of 50-80 nm. Each crystallite is surrounded by a layer of organic matrix and they are arranged in parallel forming very dense bundles, without holes, themselves surrounded by organic matrix. Due to the organization and

orientation of the bundles, the enameloid can be divided into two sub-layers. In the inner layer, the bundles are less well-ordered while in the outer part of the enamel, they are well organized. Three types of bundles can be distinguished in the outer part of the enameloid: axial bundles, circumferential bundles and radial bundles. The axial bundles are in the majority, they are oriented parallel to the longitudinal tooth axis (Figure 1.9, bundles n°3). These are invaded by radial bundles oriented perpendicular to the longitudinal axis of the tooth. The radial bundles start from the junction between the dentin and the enamel and extend to the superficial layer (Figure 1.9, bundles n°2). The last bundles are circumferential bundles that run parallel to each other and cover the entire contour of the dental crown (Figure 1.9, bundles n°1). These bundles are sometimes separated by the radial bundles passing between [3].

1.2.4 Mechanical properties

Biological materials generally possess mechanical properties that far exceed those obtained from the same compounds in man-made materials [1]. Enamel and enameloid as many biological materials are fibers composite materials composed of a stiff and brittle mineral phase embedded in a tough and ductile organic matrix. These biological materials are characterized by a structure that allows the combination of the best properties of the materials that compose it and therefore improves the overall mechanical properties of the biological material. The mineralized phase provides stiffness and the organic phase provides toughness [1]. These exceptional mechanical properties are optimally suited to the function of the material [3].

The small size and irregular shape of the enamel (and enameloid) makes the study of its mechanical properties challenging. Indentation is often adopted to determine their mechanical properties. The indentation technique consists of penetrating a tip, also called indenter of known geometry and mechanical properties, in a material in order to deduce its mechanical properties, including elastic modulus, hardness and fracture toughness [2, 32].

To enable the tooth to perform its function of taking food, the enamel (and enameloid) must be able to withstand a wide range of imposed and repeated stresses induced by contact with other teeth and food, while maintaining the shape of the teeth. It is characterized by great hardness. In particular, enamel is the hardest material in the human body [31].

The mechanical behavior of enamel (and enameloid) depends on the location, chemical composition, and orientation of apatite crystals which vary from one species to another [39]. Numerous studies have already investigated the hardness and Young's modulus of tooth enamel of several species using nanoindentation. Nanoindentation refers to an indentation in which charges of the order of tens of micronewtons (μN) are applied to allow penetration of the tip to depths between a few tens of nanometers (nm) and a few micrometers (μm).
Studies performed on human teeth reported that the hardness of enamel depends on microstructure (e.g. degree of prism alignment), composition (e.g. changes in chemistry, degree of mineralization), aging, carries, location, etc. [31]. The hardness (H) and Young's modulus (E) are not constant throughout the human enamel. They constantly decrease in traversing from the occlusal surface ($H > 6$GPa and $E > 115$GPa) to the enamel–dentin junction ($H < 3$GPa and $E < 70$GPa). Note that the occlusal surface is the upper surface of the teeth that is in contact with the teeth on the opposite jaw. This is due to the different orientations of the enamel prisms when traversing the distance between the enamel–dentin junction and the surface of the teeth resulting in a variation in the degree of biomineralization. The outer enamel is relatively richer in calcium and phosphorus content than the enamel at the junction with the dentin[31, 39]. The mechanical properties of the human enamel also varied from the lingual to the

labial side of the molar with higher stiffness and hardness on the lingual side than on the labial side [39].

Enameloid has also been studied in several fish species. Enax et al. have studied the hardness and the reduced elastic modulus of the enameloid of the shortfin mako shark (*Isurus oxyrinchus*) in two papers[3, 35]. They reported that the enameloid of this shark has a mean reduced elastic modulus of 103 GPa and a mean hardness of 4.9 GPa [3]. Despite the pronounced structural anisotropy of the enameloid of this shark, stiffness and hardness are essentially isotropic [3]. This layer has higher values of mechanical properties than that found in the dentin ($E \sim 30$ GPa and $H \sim 1$ GPa). This difference is due to the higher mineral content and higher crystallinity of enameloid [35]. Like many fishes, this shark has an additional superficial layer covering the enameloid and having different structures and compositions than the enameloid. Despite this, the reduced elastic modulus and hardness of this additional layer are comparable to those of the enameloid ($E \sim 91$ GPa and $H \sim 5.5$ GPa) [3].
As a comparison, the hardness and the reduced elastic modulus of the geological fluoroapatite crystal are respectively about 11 GPa and 148 GPa. It is therefore much harder but also more brittle than the enameloid that also contains an organic matrix [35]. This shows that even though biological materials have a hierarchical structure that allows the best properties of these compounds to be combined (stiffness and toughness), there is always a compromise (the hardness is lower than the one of fluorapatite). Note that although fluoroapatite is harder than hydroxyapatite, the shark teeth enameloid that contains fluoroapatite does not have a higher hardness than the enamel of human teeth that contains hydroxyapatite [35].
Chen et al. (2012) [32] have studied another type of shark, the great white shark (*Carcharodon carcharias*), and a piranha (*Serrasalmus manueli*). In dry conditions, the reduced modulus and hardness of piranha enameloid are 86.5 GPa and 4.1 GPa respectively. In the same conditions, the enameloid of the great white shark tooth has a reduced modulus of 84.4 GPa and a hardness of 4.1 GPa [32]. The different values obtained for the enameloid of the great white shark and of the shortfin mako shark may partly be caused by the methodology of the experiments but it is mainly due to differences in structure and composition between the enameloid of the two fishes [3]. Also in these two fishes, dentin has lower hardness and Young's modulus values. Indeed, the Young's modulus of the dentin is about 23 GPa for the piranha and about 20.4 GPa for the great white shark. The hardness value in piranha is about 0.8 GPa and about 0.7 GPa in the great white shark. In hydrated conditions, enameloid have lower modulus and hardness compared to those tested in dry conditions. The variation in values obtained in dry and hydrated conditions is much more significant in dentin because it is less mineralized and contains a higher amount of organic matter and water compared with enameloid. The hydration effect is therefore much more significant on the mechanical properties of dentin.

The high hardness and rigidity of enamel prevent the tooth from deforming under the high loads it undergoes repeatedly in the mouth. In addition, many small defects or cracks may form in the enamel and enameloid due to repeated contacts between the teeth as well as with another material, high cycle occlusion, temperature variations, corrosion or decay. Nevertheless, the mechanical function of the enamel is retained without catastrophic failure [31, 2]. It is therefore interesting to explore the toughness fracture of this material, which is defined as its ability to locally dissipate the high constraints that could cause the material to break.

Numerous studies have investigated the fracture toughness of the enamel of different species using high load indentations.
This interesting technique was notably well exploited by Weng et al. (2016) [2] to study the fracture mechanical properties of giant panda tooth enamel and the influence of the loading orientation and location on these properties. They used high load indentations to form cracks at the corner of the indent (Figure 1.10.A) and beneath the indent (Figure 1.10.C). From the measurement of the corner cracks length, it was possible to quantify the fracture toughness using a formula explained in Section 2.5.2.1.

The observation of the cracks both on the surface and under the indents revealed that cracks propagate preferentially along the internal interfaces such as the sheaths between enamel rods, and that extrinsic toughening mechanisms such as crack deflection/twisting and uncracked ligaments bridging, are used by the enamel to increase its toughness (Figure 1.10.B). A similar study to this one was carried out in the second part of this thesis.

The high load indentation technique has also been used on human enamel in several studies. Values ranging from 0.4 to 1.5 MPam$^{1/2}$ have been reported for the fracture toughness of the human enamel [40, 41, 42, 43]. The wide range of this property in the enamel is partially attributed to spatial variations in the chemistry and anisotropy of this layer [43]. This anisotropy was notably noticed by Cheng et al. (2010) [44] who performed indentations with a rotary indenter on frontal sections of human enamel (Figure 2.1). They concluded that the anisotropy is mainly due to the parallel arrangement of mineral crystals and enamel prisms that trigger crack propagation in a preferential orientation.

As a comparison, the fracture toughness of the hydroxyapatite is equal to 0.3 MPa m$^{1/2}$ [40, 2].

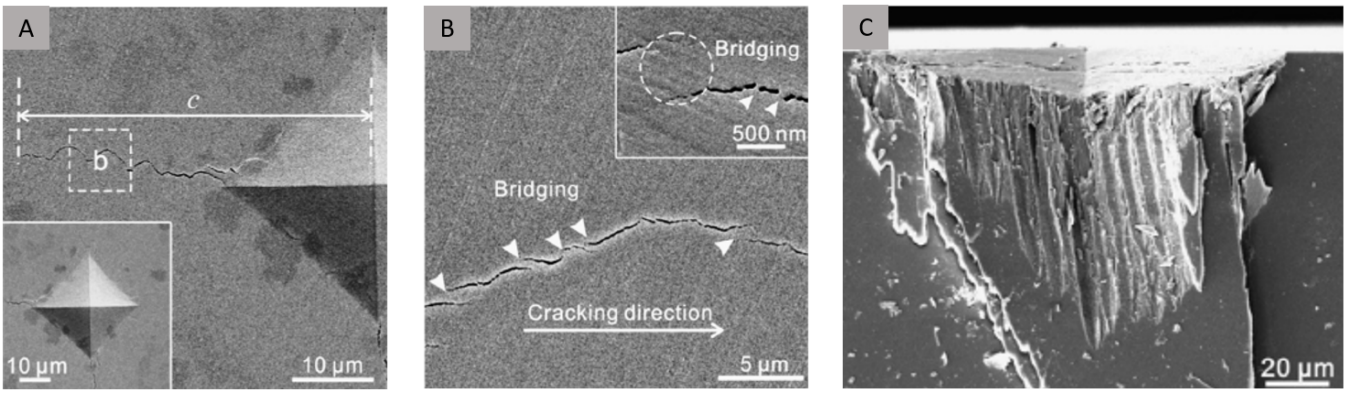

Figure 1.10: (A,B) SEM images of polished occlusal surface of giant panda tooth enamel after indentation under 2000 mN load along the longitudinal direction. (C) SEM image of giant panda tooth enamel beneath the indenter after indentation under 2000 mN load along longitudinal direction [2].

1.3 Serrasalmidae family

This thesis focuses on the enameloid of two fishes belonging to the Serrasalmidae family. This section aims to present this family and more precisely the two fishes in which we are interested.

The Serrasalmidae family is a monophyletic group of neotropical freshwater fishes belonging to the order Characiformes [45, 46, 47, 48]. Serrasalmidae species are widely distributed throughout the major South American river systems and inhabit a wide variety of habitats such as flooded forests, lowland floodplains, and headwater regions of rivers [45, 46, 47, 49]. This family includes seventeen genera including sixteen living genera and one fossil genus (Megapiranha) and more than 90 valid species [47, 45].

Fishes of the family Serrasalmidae have common characteristics such as a laterally compressed body, a long dorsal fin and an abdominal carina composed of pointed serrae from the modification of abdominal scales [49, 48].

Morphological and molecular phylogenies support a division of the family Serrasalminae into three main clades: the "piranhas" clade, the "pacus" clade and the "myleus" clade [49, 47, 45]. At the end of the

Cretaceous, the earliest separation of the family occurred and separated the "pacus" clade (*Colossoma*, *Mylossoma*, and *Piaractus*) from the rest of the family [49, 45]. The rest of the family was then split in two during the Eocene with the "piranhas" clade (*Metynnis, Pygopristis, Pygocentrus, Pristobrycon, Catoprion*, and *Serrasalmus*) [49, 45] and the "myleus" clade (*Mylesinus, Myleus, Myloplus, Ossubtus, Tometes*, and *Utiaritichthys*) [45] (Figure 1.11). However, the relationships within each of these clades remain uncertain [47] and the position of the genus *Acnodon* is problematic and uncertain, it can be placed as a sister group to the "piranhas" and "myleus" clades [49, 45].

This family possesses a wide diversity of diets ranging from herbivorous and frugivorous fishes to omnivorous or carnivorous species [21]. The three clades show in fact different trends in their feeding. Piranhas are group predators. They are predominantly carnivorous feeding on the flesh of other fishes. However, they can be facultative frugivorous or they also may feed on fins or even scratch the scales of other fish [45, 46]. Carnivorous species have a significant ecological role. As one of the main river predators, they help to balance fish populations by killing and feeding on weak, injured or diseased prey. They are also cleaning squads, feeding on cadavers of fishes and other vertebrates [46, 50, 51]. Unlike piranhas, pacus are predominantly herbivores feeding on seeds and fruits [45, 46]. Seed-feeding species serve a unique ecological function. Indeed, they allow for efficient seed dispersal over large distances in flooded forests and thus play an important role in maintaining tree diversity in lowland Amazonian forests [45, 46]. Finally, the "myleus" clade has an omnivorous diet [52].

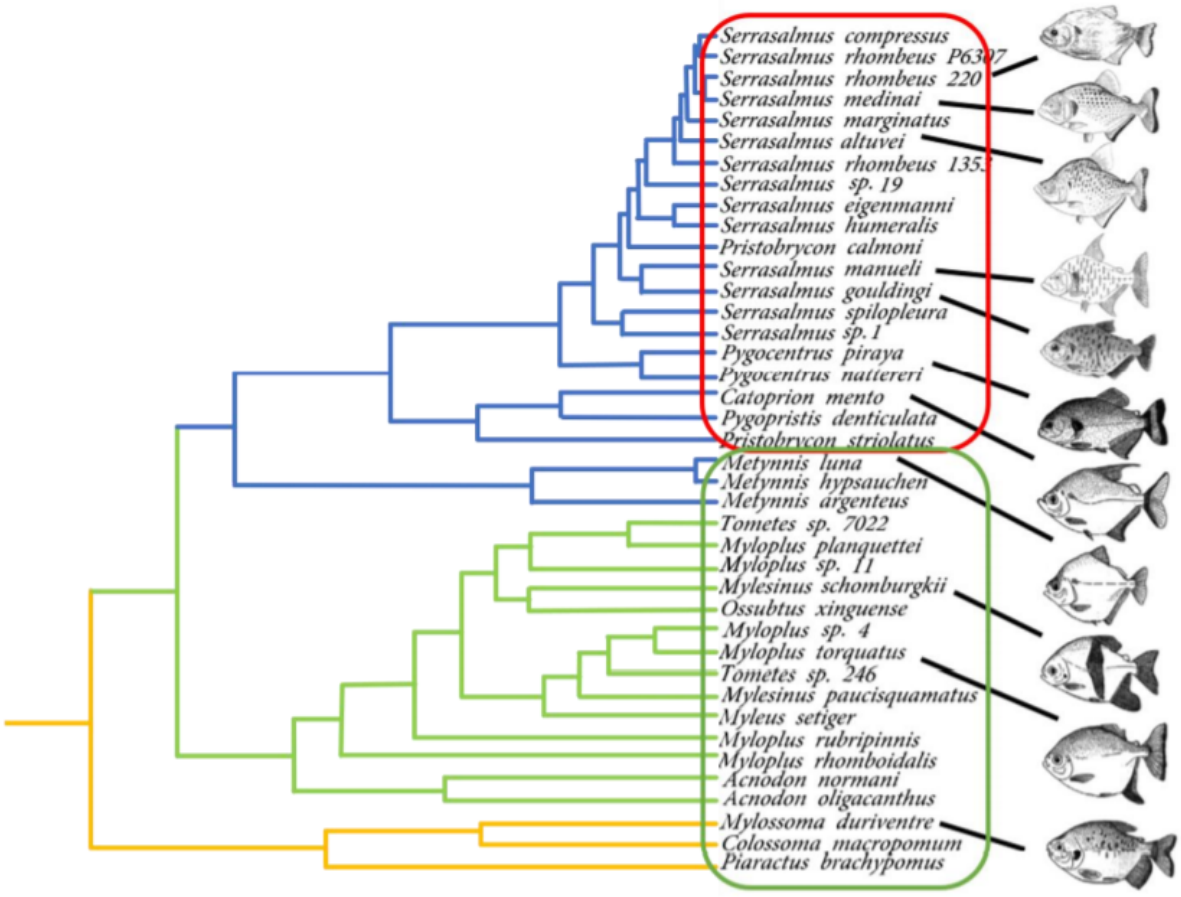

Figure 1.11: Phylogenetic tree of the family Serrasalmidae based on the analysis of 11 mitochondrial genes. The red and green frames represent respectively the carnivorous and herbivorous lineages. The colors represent the different clades: the "pacus" clade in yellow, the "myleus" clade in green and the "piranhas" clade in blue [45, 53].

The diversity of diets is reflected in the arrangement and morphology of the teeth [47, 49]. The teeth of carnivorous species are used to puncture and shear prey. They are generally tricuspid with a triangular, pointed, blade-like central cusp and two generally smaller lateral cusps. These sharp teeth are organized in a single row of teeth on each jaw and are strongly linked together via the small lateral cusps [15, 48, 49]. Scale-feeding piranhas, called lepidophagous, possess tuberculated teeth located on the external side of the premaxilla, allowing them to tear off scales [49]. The teeth of herbivores are used to cut pieces of plants or crush hard fruits and seeds. They have molariform teeth organized in one and two rows on the lower and upper jaws [54, 55, 56]. As in most fishes, the teeth of fishes of the Serrasalmidae family are constantly replaced throughout life [15].

1.3.1 Studied species

Two fishes of the family Serrasalmidae were studied in this thesis: the herbivorous pacu *Piaractus brachypomus* (Cuvier, 1818) and the carnivorous piranha *Pygocentrus nattereri* (Kner, 1858). These two species were chosen because of their different diets which means that their teeth have different functions.

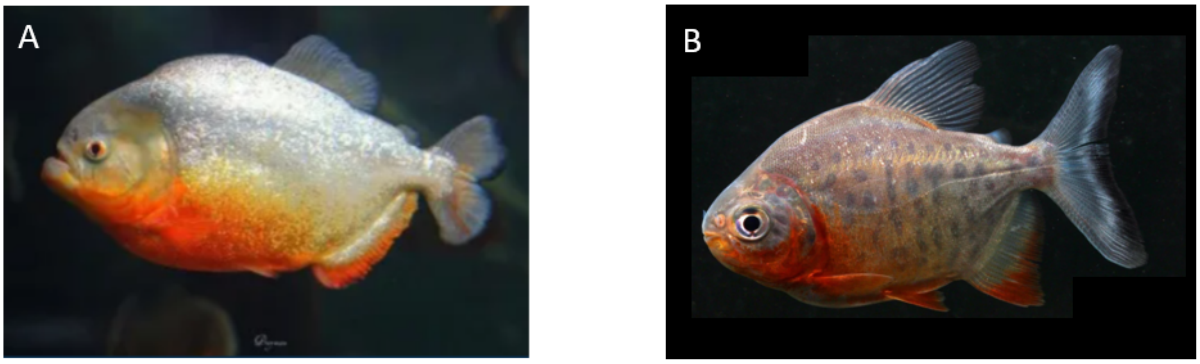

Figure 1.12: Studies species. (A) Piranha *Pygocentrus nattereri* [57]; (B) Pacu *Piaractus brachypomus* [58].

- ***Pygocentrus nattereri***

  P. nattereri (Figure 1.12.A), also known as the red-bellied piranha, is a fish that belongs to the order Characiformes and the family Serrasalmidae. In this family, it is placed in the clade of piranhas [49].
  P. nattereri is a freshwater fish native to the regions of South America. It is located east of the Andes, in the Parana-Paraguay and Amazon basin, but also in rivers of northeast Brazil and the Guianas [59, 60, 50]. As a result of aquaculture and aquarists, it has been introduced into other areas such as the southern United States [61].
  This fish has can grow to 50 cm [62].
  The *P. nattereri* has a varied diet which consists mainly of fins, scales, pieces or whole fish. It also feeds on insects, snails and plant material [50, 51]. Eating plants allows the fish to obtain food while it searches for prey [63].

- ***Piaractus brachypomus***

P. brachypomus (Figure 1.12.B), also known as the pirapitinga, is a fish of the order Characiformes belonging to the Serrasalmidae family. It is placed in the clade of pacus [49].
It is a freshwater fish native to the tropical regions of South America, found in the basins and floodplains of the Amazon and Orinoco rivers [64, 65]. It has been introduced in other regions, such as India or even Vancouver, as a result of the breeding of this species by humans for both aquaculture and aquarists [66, 67]. They are large fish that can reach a size of 88 cm and a weight of 25 kg [68, 69]. It is probably due to this large size that they are released into local waters because they exceed the size of the hobbyist's aquariums [67]. It is also probably because of its large size that it is an attractive candidate for sustainable aquaculture projects in many regions [70].
The diet of this species varies according to the season. Its diet consists mainly of seeds, fruits recently fallen from trees and riparian plants. However, during the dry season, *P. brachypomus* is able to feed on crustaceans, mollusks, or small fish [68, 70]. This species has a dentition with molariform teeth that are arranged in two rows on the premaxilla and dentary and separated from each other by small spaces. Behind the row on the dentary, a pair of conical teeth are also present [68, 69, 21].

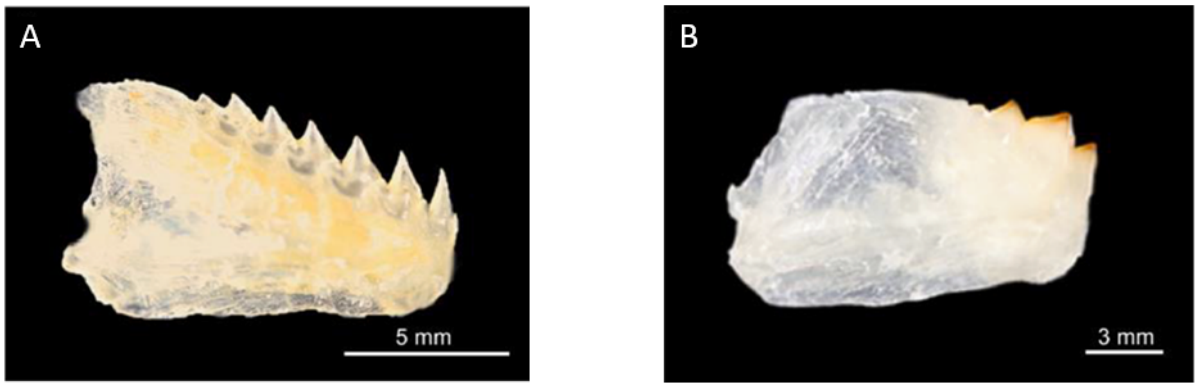

Figure 1.13: Photographs of the lower jaws in (A) the carnivorous piranha *P. nattereri*; (B) the herbivorous pacu *P. brachypomus* [21].

Yann Delaunois et al. (2020) [21] have studied the external morphology, internal structure and chemical composition of the teeth of these two species of the Serrasalmidae family having different feeding habits. Main results are discussed below:

► **External morphology**

Marked differences have been reported in the external morphology of the two species. Despite its varied diet, the dentition of the carnivore *P. nattereri* is strongly adapted to carnivory, allowing the animal to slice and tear fleshy meat. Their teeth are tricuspid with a broad, narrow, pointed primary cusp and two smaller secondary cusps (Figure 1.13.A). The herbivorous species has a dentition allowing them to chew and break hard food. The latter is composed of broad molariform teeth. Their teeth are tricuspid with a broad, well-developed primary cusp and two less developed secondary cusps. They also show red pigmentation on their surface which progresses towards the cusp cutting edges (Figure 1.13.B). Such pigmentation is not found in carnivorous species (Figure 1.13.A) [21].

► **Internal structure**

In order to analyze the internal structure and composition of the teeth, the environmental scanning electron microscopy (ESEM), energy dispersive X-ray microanalysis (EDX) and Raman microspectroscopy were used on polished surfaces of embedded jaws exposing a section of the tooth containing pulp, enameloid and dentin. Both species have an internal structure found consisting of five distinct layers, from the inner to the outer: pulp, dentin, enameloid and cuticle (Figures 1.14.A, 1.14.B and 1.15) [21].

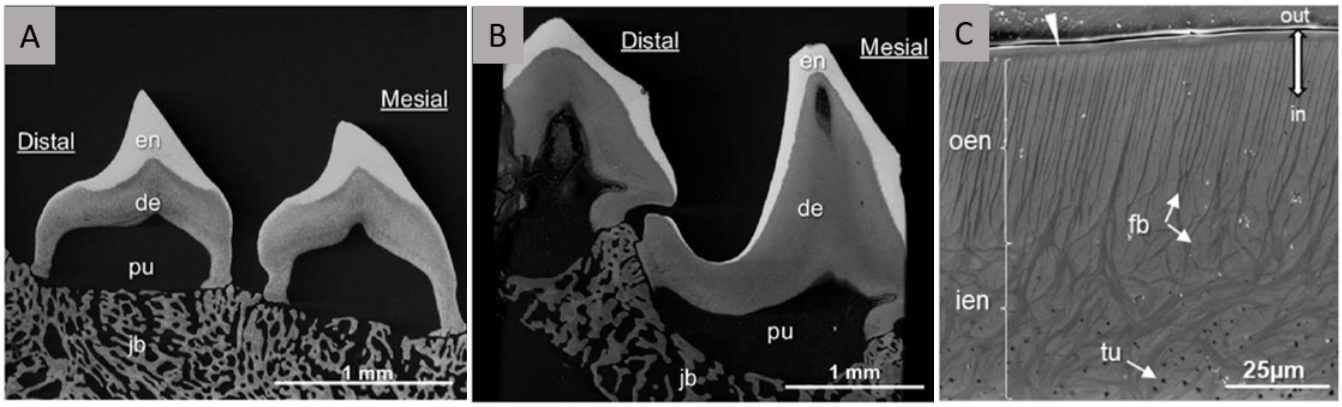

Figure 1.14: (A,B) SEM−BSE images of frontal polished sections of the oral teeth in (A) the herbivorous *P. Brachypomus* and (B) the carnivorous *P. Nattereri* showing their tooth morphology and internal microstructure. (C) SEM−GSE image of the enameloid layers in transversal section of serrasalmid teeth showing the internal organization of the enameloid. *Abbreviations: de, dentine; en, enameloid; ien, inner enameloid; oen, outer enameloid; jb, jaw bone; pu, pulp; tu, tubule; fb, collagen fibres*[21].

The microstructure of the dentin has been shown to be similar to that presented in Section 1.1.3.2. It is indeed characterized by the presence of numerous dentinal tubules extending from the pulp to the enamel. These present a diameter of about 1 µm and shelter the cytoplasmic extensions of the odontoblasts. Collagen fibers present in the dentin are randomly organized and interlaced between the tubules.

As in the shark, the enameloid of these two fish can be divided into two sub-layers with different structures, called the inner enameloid and the outer enameloid (Figure 1.14.C). The inner part has branched dentinal tubules whose number progressively decreases from the dentin to the outer enameloid where they are totally absent. Collagen fibers present in the inner enameloid are arranged in an interlocking network between the tubules. In the outer enameloid, the collagen fibers are organized in parallel bundles oriented perpendicularly to the tooth surface. The microscopy also pointed out the presence of mineral prism-like units between the parallel collagen fibers [21].

The two fishes also have a thin layer covering the outer enameloid called the cuticle. This one presents a bilayer organization with an inner part that seems less mineralized and more organic than the outer part. This is due to a higher presence of organic fibers in the internal cuticle in continuity with those of the outer enameloid. The thickness of this layer seems to vary according to the position in the tooth. It is thicker on the lingual side than on the vestibular side in both species. It also varies significantly between the two Serrasalmidae species. The herbivorous species has the thickest cuticle with an average thickness of 1.7 µm while the carnivorous *P. nattereri* has an average thickness of 0.8 µm.
This superficial layer often shown a red-pigmentation due to the presence of iron, especially in the herbivore species [21].

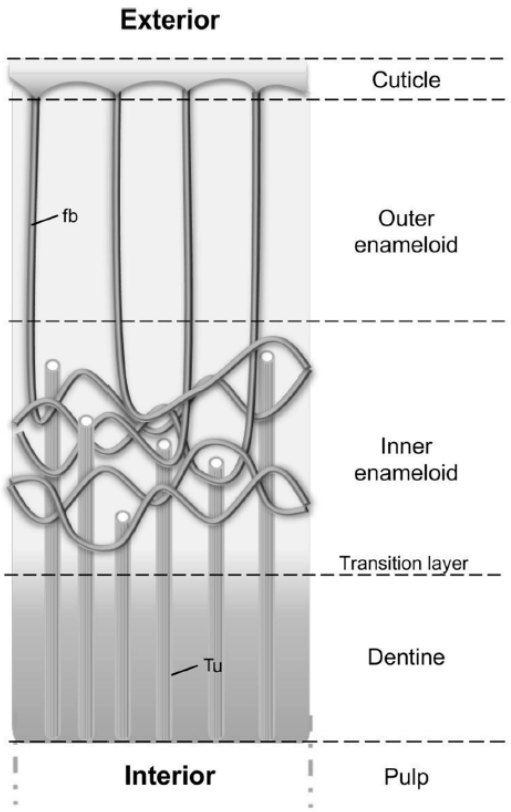

Figure 1.15: Schematic representation of a frontal cut of a Serrasalmidae fish tooth showing the succession and morphological features of the tooth layers. Lighter gray correspond to higher mineral proportion and dracker gray to lower mineral proportion; *Abbreviations: fb, collagen fibres; tu, tubules* [21].

► **Composition**

The serrasalmid teeth are mainly composed of hydroxyapatite which concentration varies between the different tooth layers but also between the two species. Both enameloid sub-layers contain the same mineral content with values ranging from 77 at.% (88 wt.%) in the herbivorous species to 80 at.% (91 wt.%) in the carnivorous species. The dentin is less mineralized with about 70 at.% (78 wt.%) mineral content in the carnivorous species. The cuticle is the lowest mineralized layer with a mineral proportion of 62 at.% (71 wt.%) in the carnivorous species [21] (Table 1.1).

Mineral proportion (at.%)		
	Herbivorous *P. brachypomus*	Carnivorous *P. nattereri*
Cuticle	68.5 ± 6.1	62.0 ± 11.9
Outer enameloid	77.1 ± 4.0	82.5 ± 3.5
Inner enameloid	76.7 ± 4.3	80.0 ± 5.3
Dentin	64.2 ± 5.6	71.4 ± 5.6

Table 1.1: Iron content in the tooth layers of the teeth of *P. brachypomus* and *P. nattereri* (mean ± standard deviation) [21].

Iron is also present in the cuticle of the two fishes and in the outer enameloid of the herbivorous species. It is probably present under the form of the substitution of Ca by Fe in the hydroxyapatite ((Ca, Fe)-phosphate). The iron content differs according to the location in the tooth: it is more abundant on the lingual side than on the labial side of the teeth. But it also varies between the two species: it is higher in the cuticle of the herbivorous species with a proportion up to 1.1 at.% (2.9 wt.%) than in the carnivorous

one. In addition, iron was recorded in the outer enameloid in the herbivorous species but not in the carnivorous species. This explains the more intense red-pigmentation at the surface of the herbivorous teeth (Table 1.2).
The presence of iron-enrichment in superficial tooth layers may be interpreted as mechanical support. It may harden the surface of the teeth, increase the resistance to friction and reduce abrasion during feeding.

Iron concentration (at.%)		
	Herbivorous *P. brachypomus*	Carnivorous *P. nattereri*
Cuticle	1.1 ± 0.4	0.3 ± 0.3
Outer enameloid	0.5 ± 0.3	0.0 ± 0.0
Inner enameloid	0.1 ± 0.2	0.0 ± 0.0
Dentin	0.1 ± 0.1	0.0 ± 0.0

Table 1.2: Iron content in the tooth layers of the teeth of *P. brachypomus* and *P. nattereri* (mean $\pm$ standard deviation) [21].

► Mechanical properties

A study on the elastic properties of the enameloid of these two fishes is in progress at the University of Liege by Ruffoni et al. Several static indentations performed on polished sections of the teeth of *P. brachypomus* and *P. nattereri* allow measuring the hardness (penetration resistance) and Young's modulus (elasticity) of their enameloid. The reported values of hardness range from 3 to 7 GPa and from 60 to 120 GPa for the Young's modulus in the enameloid of the two fishes (Figure 1.16). Note that no significant differences are reported in the elastic properties between the inner and outer enamel.

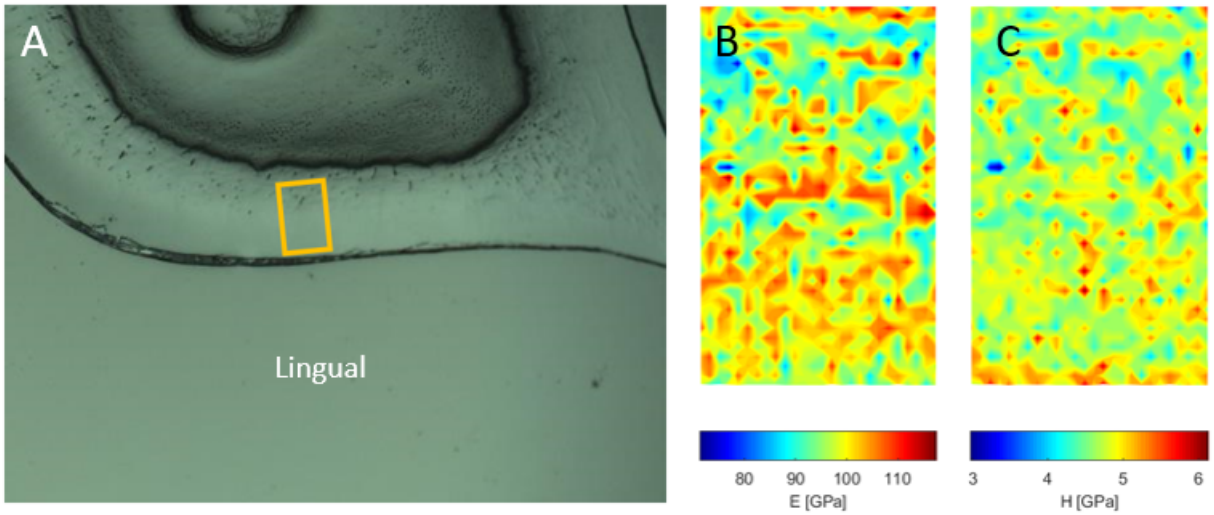

Figure 1.16: (A) Optic image of the polished transverse section of the oral teeth in the carnivorous *P. nattereri*. The yellow rectangle in (A) represents the 80 x 50 m grid on which 36 x 26 indentation points were made. (B) Values of the Young's modulus in the yellow rectangle of (A) obtained with static indentations. (C) Values of the hardness in the yellow rectangle of (A) obtained with static indentations.

1.4 Main aims of the master thesis

The thesis focuses on the enameloid of the teeth of two fishes presented in the section 1.3.1 having different diets: the carnivorous *Pygocentrus nattereri*, preferentially feeding on soft prey, and the herbivorous pacu *Piaractus brachypomus*, preferentially eating hard shells. The teeth of these two fishes have already been studied by Delaunois et al. (2020) [21] and Ruffoni et al. The results of their studies, concerning the external morphology, the chemical composition, the microstructure of the teeth as well as the elastic properties of the enameloid, are reported in Section 1.3.1. The purpose of this thesis is to further investigate the understanding of these teeth and more precisely of the enameloid of these teeth. It can be divided into two parts.

The prime objective is to further investigate the internal microstructure of the enameloid in the teeth of these two fishes. It is studied by means of a microscopic analyzing the surface of fractures of the transverse and frontal sections of teeth (Figure 2.1) as well as results of surface etching performed on polished tooth section surfaces. Using these techniques, the organization and arrangement of hydroxyapatite fibers or fiber bundles appear in relief and can be easily observed with a scanning electron microscope. They allow therefore a precise analysis of the internal microstructure of the enameloid. The structure found is compared between the two species with various feeding strategies (slicing vs. crushing) in order to observe whether additional structural differences between the species can be highlighted.

Secondly, the potential correlation between microstructure and mechanical properties is investigated through the assessment of local fracture behavior. Indeed, in addition to Young's modulus and hardness that have been computed already, fracture resistance is an essential feature. It allows the enameloid and, in general, the tooth to avoid catastrophic failure when cracks nucleates on the other surface due to repeated cycles of chewing. The second objective of this thesis is therefore to identify the role of the enameloid structure in the resistance to crack initiation and propagation of this material. This is done through the microscopic analysis of high load indentations performed on the enameloid of the two fish species, both in the outer enameloid and in the inner enameloid. This technique allows a quantitative evaluation of the fracture toughness but also a highlight of the different extrinsic toughening mechanisms used by the biological material.

Chapter 2

Materials and methods

The aim of this chapter is to describe the experiments performed in this master thesis. After samples preparation, a microscopic analysis of the fractured teeth and the result of a surface etching performed on frontal sections of the teeth was chosen to analyze the structure of the enameloid. Then, high load indentation tests were performed in the aim to investigate the fracture toughness of this layer.

2.1 Studied species

The experiments carried out during this master thesis have been performed on teeth from piranha *P. nattereri* and pacu *P. brachypomus*, two fish species belonging to the same family (Serrasalmidae). Teeth from aquarium subadult fish kept alive at the University of Liege were used for the surface etching. The fractures and indentation tests were carried out on the teeth of larger adult fish caught in Brazil.

2.2 Surface etching

2.2.1 Sample preparation

Surface etching was performed on three teeth (Two teeth of the herbivorous species and one tooth of the carnivorous species) already embedded in low viscosity agar epoxy resin (Agar Low Viscosity Resin, Agar Scientific, UK), oriented and polished to expose a frontal section of the teeth (vertical cuts parallel to the lingual-labial direction) (Figure 2.1). These samples were made four years earlier by Yann Delaunois, a final year student doing his master thesis at the University of Liege on the same fishes. As the samples were several years old, they had to be re-polished due to dust deposits, possible scratches or erosion of the mineral in contact with air which could occur after a few years. However, the samples were thin slides and therefore had to be re-embedded before polishing.

2.2.2 Sample embedding

The samples were this time embedded in epoxy resin (EpoFix resin Kit, Struers Inc., Germany) which has the particularity of hardening rapidly.

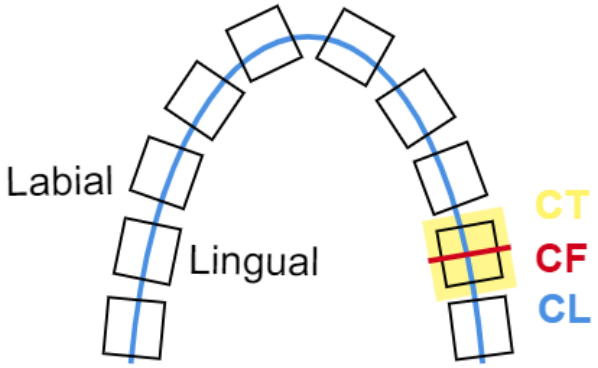

Figure 2.1: Diagram representing the different types of cuts. *Abbreviations: C.L., longitudinal cut; C.F., frontal cut; C.T., transverse cut.*

2.2.3 Sample grinding polishing

Samples were grinded in three steps with carbide papers: P800 at 50 rpm until reaching the tooth tissue and exposing a frontal section, P1500 at 20 rpm for three minutes and then P2500 at 20 rpm for three minutes.
Polishing was then performed on silk cloth with a 3 µm diamond spray (diamond suspension in alcohol) at 45 rpm for six minutes and then with a 1 µm diamond spray at 35 rpm for seven minutes. The two diamond sprays were each applied to a silk cloth 15 min before use to allow alcohol to evaporate.
The grinding and the polishing were performed with a polisher (METASERV 250, Buehler, Switzerland), under ethylene glycol irrigation, to ensure proper lubrication and removal of particles produced by grinding.
The samples were finally cleaned with ethanol and numbered in order to recognize them.

2.2.4 Surface etching

The frontal sections exposed were etched in 0.5M EDTA in HEPES buffer, pH 8.0 for 2h. After etching the samples were rinsed thrice in DDH_2O, pH 7.3, thrice in pure ethanol and air-dried. Etching with EDTA was not effective, the decalcification was not intense enough to make the bundles appear well-separated from one another, as can be seen in Figure 2.2.
Samples were therefore etched a second time in 3.7 vol% Hydrochloric acid (HCl) for 2s. They were then rinsed twice in DDH_2O pH 7.3, thrice in pure ethanol, and air dried. As can be seen in Figure 3.1 and 3.2, this etching was effective and allowed to show the orientation of the apatite crystals bundles.
Note that these two methods of etching were chosen on the basis of the success reported by Pupa Gilbert in her article on human enamel [71].

2.2.5 Sample observation

After the two types of etchings, the samples were observed using a Scanning Electron Microscope (type XL-30 ESEM-FEG, FEI/Philips Inc., Holland) under low-vacuum conditions (0.3 and 0.4 Torr in water vapor) without coating and with an acceleration voltage of 15 kV.

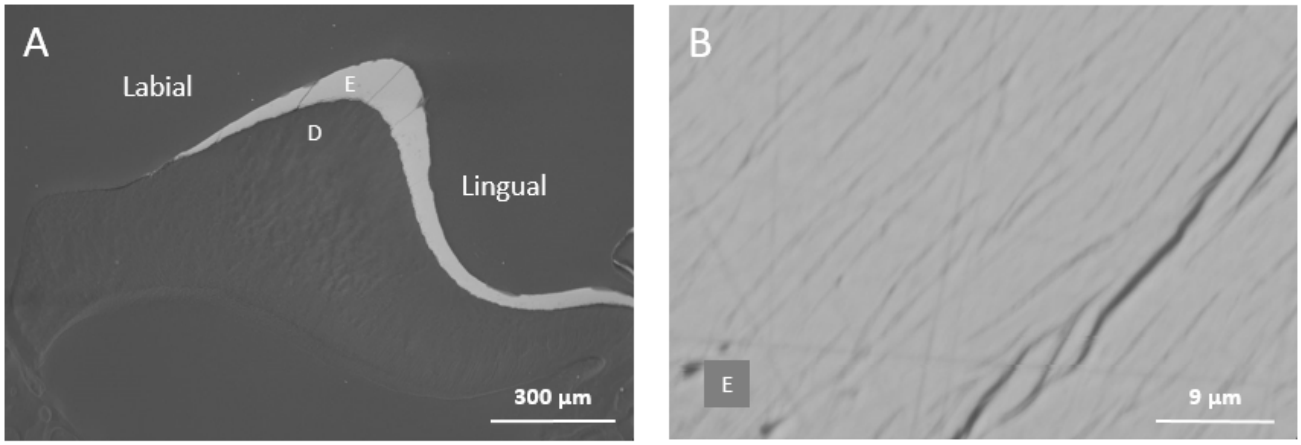

Figure 2.2: SEM−BSE images of frontal sections of an oral tooth of the carnivorous *P. nattereri* after EDTA etching. *Abbreviations: E, enameloid; D, dentin*.

2.3 Fracture

2.3.1 Sample preparation

The fractures were performed on teeth coming from the lower left jaw.
A piranha *P. nattereri* and a pacu *P. brachypomus* were euthanized using the method described by Huby et al. (2019) [72]. The jaws of the different species were extracted by dissection from the dead fish, separated into four parts (left and right lower jaw, left and right upper jaw) and maintained in 70% ethanol after manual cleaning. All teeth present on the left lower jaw of each species were then isolated from the jaw with a low speed diamond band saw (distilled water) and conserved in 70% ethanol.

2.3.2 Sample fracture

Two isolated teeth from each species were fractured. These fractures were performed in order to obtain a frontal and a transverse section fractures for each species (Figure 2.1).
Frontal section fractures were obtained thanks to a compression of the tooth in the labial-lingual axis in a vice.
The transverse section fracture of the herbivorous tooth was obtained in two steps. The first step was to create a horizontal notch approximately one fourth the width of the tooth with a scalpel at approximately mid-tooth height. In the second step, a scalpel was used as a lever to open the notch and a hammer blow to induce the fracture. The resulting fracture consists of a cap containing enameloid that has broken out of the rest of the teeth.
For the transverse section fracture of the carnivore tooth, two small horizontal notches were made on each side of the tooth at approximately mid-tooth height. A pair of forceps were then used to create a balancing movement towards the front of the tooth and provide a transverse fracture.

The obtained samples were dehydrated in a series of ethanol baths of increasing concentration. The dehydration was performed with a 90% ethanol bath (20 minutes) and then two 100% ethanol baths (20 minutes). The samples were then dried by critical point drying.

2.3.3 Sample observation

To allow observation of fracture surfaces, samples were placed on a support in order to expose the fracture to the electron beam in the microscope. The fracture surfaces were metalized with silver using sputtering machine (SCD030, Balzers Liechtenstein) to avoid charging phenomena.
Scanning electron microscope in secondary electron mode was used to visualize the internal structure within the fractures. The environmental scanning electron microscopes type XL-30 ESEM-FEG, FEI/Philips Inc., The Netherlands and type Quanta 600 FEI ESEM, FEI/ USA were operated under high-vacuum conditions with an acceleration voltage of 15 kV. The images obtained are presented in Section 3.1.2.

2.4 Indentation

2.4.1 Sample preparation

The indentation tests were performed on teeth coming from a lower left jaw. The teeth were isolated from the jaw in the same manner as explained in Section 2.2.1.

The following protocol was chosen based on the success reported by Ludwig Boltzmann Institute of Osteology in Vienna. This protocol allows obtaining very smooth surfaces and reducing the risk of the formation of microcracks that could modify the mechanical properties of the sample.

2.4.2 Sample dehydration

Five isolated teeth (two teeth from the herbivore species and three from the carnivore species) were used to perform high load indentation tests. These teeth were dehydrated in ascending grades of ethanol, acetone and methyl methacrylate (MMA) solutions. The dehydration was carried out in 11 days at room temperature with successive baths of 1 day in the following solutions:

- day 1: ethanol 80%
- day 2: ethanol 96%
- day 3: ethanol 100%
- day 4: ethanol 100%
- day 5: ethanol 100% + acetone (1:1)
- day 6: acetone
- day 7: ethanol 100% + acetone (1:1)
- day 8: ethanol 100%
- day 9: ethanol 100%
- day 10: methyl methacrylate
- day 11: methyl methacrylate

It is important to note that dehydration makes the teeth more rigid and must therefore be taken into account when analyzing the results.

2.4.3 Sample embedding

Samples were then embedded in resin which is a mixture of 400 ml of methyl methacrylate (MMA), 7g of Benzoylperoxid (BPO) and 100 ml of Nonylphenylpolyethyleneglycol acetate for 500 ml of resin. Benzoylperoxid is delivered with 25% water and must be dried for 24 hours at 30 to 35°C in the incubator before solving it in methyl methacrylate. Benzoylperoxid is used as a starter for polymerization.

Nonylphenylpolyethyleneglycol acetate was then added to the obtained mixture. The latter serves as a softener.
Teeth were placed into molds and oriented so that at least a transverse section and a frontal section of the teeth could be obtained for each species (Figure 2.1). The resin was then added and the molds were sealed covered using paraffin to avoid evaporation and leak of the resin.
The molds containing the teeth and the resin are then stored in the refrigerator (4°C) for two days and then transferred into the incubator for hardening for five days (two days at 34°C, two days at 42°C and one day at 50°C). The gradual increase in temperature is intended to prevent the formation of bubbles which can happen when the temperature becomes initially too high. Note that the polymerization reaction is exothermic and therefore produces heat. Too many samples in the incubator could cause the temperature to rise too quickly and lead to bubble.
After 5 days of incubation, the resulting resin block was removed from the mold.

2.4.4 Sample cutting, grinding polishing

The top and the bottom of the obtained resin blocks were cut with a diamond saw (low-speed, distilled water). The top of the block is cut in order to remove the part of the resin that was not polymerized and remained soft. The bottom of the block is cut in order to obtain a section of the tooth at the desired level allowing the visualization of the pulp, the dentin and the enameloid in both frontal and transverse sections of the teeth .
The samples were then grinded with carbide papers P1500 at 20 rpm for three minutes and then P2500 at 20 rpm for three minutes. Polishing was then performed in the same way as described in Section 2.1.3.
The grinding and the polishing were performed with the automatic polishing machine (METASERV 250, Buehler, Switzerland) under ethylene glycol irrigation to ensure proper lubrication and removal of particles produced by grinding. A force of 5 N was applied by the machine on the sample in order to obtain uniform polishing.
The samples were finally cleaned with benzine and silk fabric.

2.4.5 Indentation

The indentor used to study the fracture toughness is the TI 980 TriboIndenter (Hysitron, USA). The tip used in this thesis is a pyramidal diamond indenter with a triangular base called a Berkovich indenter. Several indentations were performed on the polished surfaces of the frontal sections of herbivorous and carnivorous species and of the transverse sections of carnivorous species. They were carried out at different locations in the enameloid (in an area close to the dentin and close to the external surface) with increasing loads of 100 mN between each indentation, starting from 100mN to 1100mN. The choice of applied forces was made based on the results of previous studies using high load indentations on biological materials [2, 73]. Above 1100 mN, the results were no longer reproducible and large uninterpretable damage appeared both in the inner and the outer enameloid.

2.4.6 Sample observation

After indentations, all samples were analyzed with a scanning electron microscope in backscattered electron mode (type XL-30 ESEM-FEG, FEI/Philips Inc., The Netherlands) operated under high-vacuum conditions with an acceleration voltage of 12.6 kV.

2.5 Observation and analysis techniques and equipment

2.5.1 Scanning electron microscope

The scanning electron microscopes FEI ESEM-FEG XL-30 (Philips, Nederlands) and FEI ESEM QUANTA 600 (FEI, USA) with a secondary electron (SE) detector and a backscattered electron (BSE) detector are used in this thesis.

The scanning electron microscope is an electron microscopy technique capable of imaging the surface of a sample with high quality and spatial resolution. It is based on the interaction of electrons with matter and can provide qualitative information about the sample, including its topography, morphology and composition [74]. A schematic representation of a scanning electron microscope is shown in Figure 2.3.

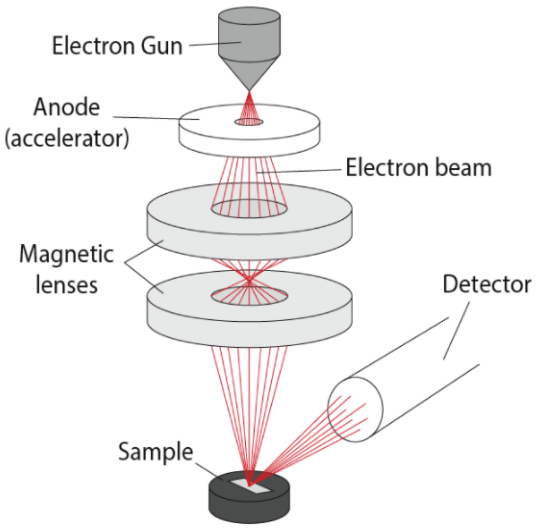

Figure 2.3: Schematic representation of a Scanning Electron Microscope [75].

The Electron Gun produces an electron beam. A filament, usually made of tungsten, is either heated (thermoelectric emitter) or exposed to a strong electric field (field emitter) to produce the electrons [74].

The resulting electron beam is focused by magnetic lenses to ensure that the beam hitting the sample is very narrow. This electron beam also passes through pairs of scanning coils, typically placed just before the final lens, which deflects the beam so that it scans the sample surface. The lenses and the scanning coils form an assembly called the electronic column [74, 75].

The interaction between the electron beam and the sample generates the emission of a variety of signals such as secondary electrons, backscattered electrons, photons (X-rays) and visible light. Each of these phenomena can be detected by specialized detectors and provide different types of information about the sample [74].

In this thesis, the observation of the fracture was done with secondary electron (SE) detector, which detects secondary electrons that are emitted when the primary electrons transferred some of their energy to the electrons of the sample atoms (Figure 2.4). These secondary electrons generally have low energy and because of this, they are emitted from atoms located close to the surface of the sample (from the

depth of approximately 550 nm). They are very sensitive to variations in the sample surface and thus allow revealing its topography [74]. The surface etching and the high load indentations results were observed using backscattered electron (BSE) detector because it provides images of the elementary composition of the sample (Figure 2.4). Indeed, this detector receives backscattered electrons that are reflected after the interactions between the primary beam electrons and the nuclei of the sample atoms. The backscattered electrons depends strongly on the atomic number of elements of the sample and allow providing images visualizing the variation of the surface composition in gray level [74].
In the rest of this thesis, the terms SEM−SE and SE or SEM−BSE and BSE refer to the techniques and images acquired by these detectors.

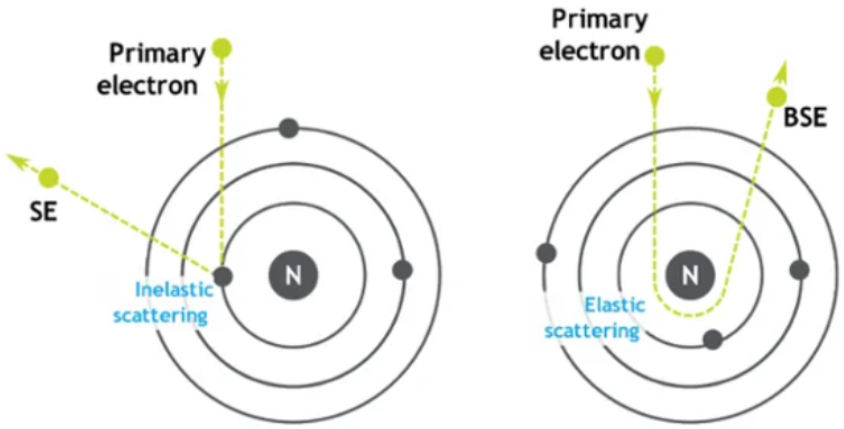

Figure 2.4: Secondary electrons and backscattered electrons [76].

The microscope must also be equipped with a vacuum pump system [74].

2.5.2 Indenter

The TI 950 TriboIndenter (Hysitron, USA) linked to the Triboscan program is used to study the mechanical properties of the enameloid. This machine enables nano-to-micro indentations which makes it possible to obtain mechanical properties such as the Young's modulus, the hardness and the fracture resistance [77]. The two firsts are obtained from load-displacement curves, while the fracture resistance is estimated from the analysis and the length of indentation cracks when high load indentations are performed [78]. In this thesis, the indenter is used to evaluate the fracture toughness of the enameloid of *P. brachypomus* and *P. nattereri* teeth.

2.5.2.1 Fracture toughness

Performing accurate fracture toughness measurements of brittle materials can often be a challenge. The high load indentation technique is an attractive option for evaluating the fracture toughness of brittle materials with small sizes or with short distance variations in the microstructure. This technique shows simplicity and rapidity of experiments [79, 80]. It is increasingly used to study toughness resistance of hard tissue and biological materials such as enameloid, bone,...[2, 44, 79].

This high load indentation technique allows the study of both crack initiation and propagation. It is based on the formation of cracks that emanate from the indent corners when high load indentations are performed. Diamond indenters with Vickers, Berkovich or cubic corner geometry can be used for such tests [78, 79, 80, 81]. In this thesis, only the Berkovich tip is used, it consists of three flats faces that

intersect at the tip of the indenter (Figure 2.5.a).

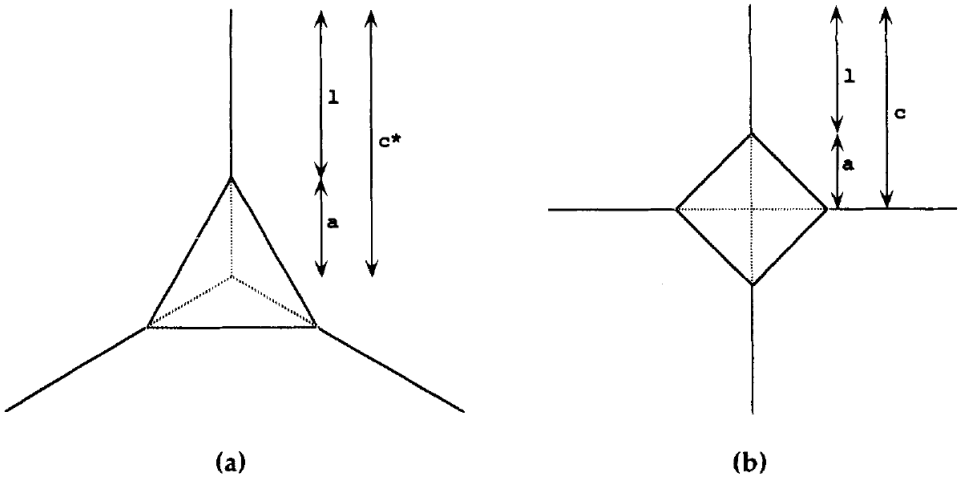

Figure 2.5: Illustration of indentation crack geometry with (a) a Berkovich tip (b) a Vickers tip (Top view). *Abbreviations: a, characteristic dimension of the plastic indent; l, final radial crack length; c = a + l* [81].

During the loading phase, a plastic indentation is created. The characteristic size of the indentation measured from the center to the top of the indent depends on the peak load and is given by [80]:

$$a = \left(\frac{P}{\alpha H}\right)^{1/2} \tag{2.1}$$

Where

- a is the characteristic size of the indentation measured from the center of the indent to the corner of the indent
- P is the peak load
- H is the hardness
- α is a non-dimensional geometric parameter that is equal to 1.3 in the case of a Berkovich tip [80].

When the peak load is sufficiently high, radial cracks emanate from the tips of the indenter on the surface which extend further as the load increases (Figure 2.5.a). During unloading, residual stress fields develop and cause the extent of the cracks [80, 82].

The crack initiation resistance can be evaluated by calculating the ratio between the total number of radial cracks initiated at the corner of the indent divided by the number of possible initiation sites, which is equal to three in the case of the Berkovich tip [80].

The fracture toughness of a material can be determined by performing measurements of the size of these cracks, assuming the mode of fracture is understood (Palmqvist or halfpenny crack model) (Figure 2.6). Indeed, the final crack length measured from the indent center to the end of the crack can be related to the fracture resistance of the material [81, 82]. Many expressions have been proposed that depend on indenter geometry and indentation crack morphology [78, 79]. The following two are the most widely used and cited in the literature.

The Lawn equation is given by the following, assuming a halfpenny crack configuration (Figure 2.6.b) [78, 81, 82]:

$$K_c = k\left(\frac{E}{H}\right)^{1/2}\left(\frac{P}{c^{3/2}}\right) \tag{2.2}$$

Where

- K_c is the fracture toughness
- E is Young's modulus
- H is the hardness
- c is the total length measured from the center of the indent to the end of the crack
- P is the peak load
- k is a geometrical constant related to the geometry of the indenter [82, 81, 78]. Anstis et al. (1981) adjusted the equation using numerous brittle materials whose fracture toughness is known and Vickers indenters (Figure 2.5.b). They found that the value of k is equal to 0.016 [78, 82].

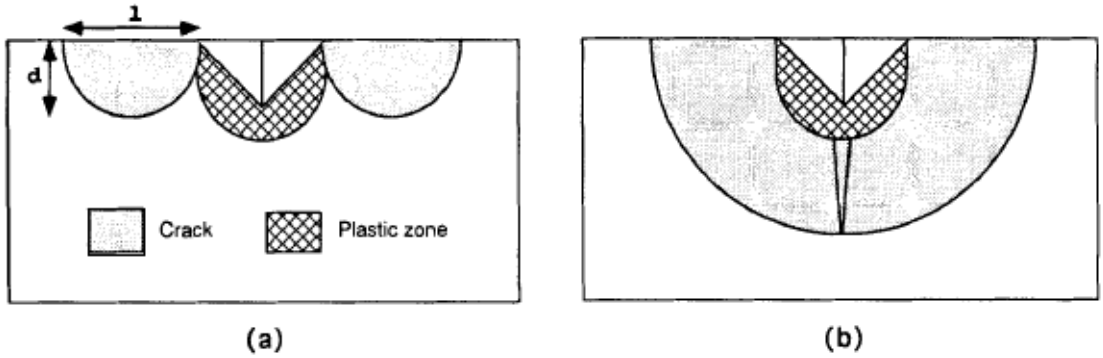

Figure 2.6: Cross-section view of (a) Palmqvist crack model (b) halfpenny crack model [81].

The fracture toughness equation for the Palmqvist crack model (Figure 2.6.a) proposed by Laugier is the following [82, 81, 78]:

$$K_c = \chi\left(\frac{a}{l}\right)^{1/2}\left(\frac{E}{H}\right)^{2/3}\left(\frac{P}{c^{3/2}}\right) \tag{2.3}$$

Where

- K_c is the fracture toughness
- a is the characteristic size of the indentation measured from the center of the indent to the corner of the indent
- l is the length of the crack measured from the corner of the indent to the end of the crack
- E is Young's modulus
- H is the hardness
- P is the peak load
- c is the total length measured from the center of the indent to the end of the crack

- $\chi = 0.015$ is a constant determined by fitting using Vickers indenters [82, 81].

Anstis et al. and Laugier, respectively, fitted experimentally the constants k and χ using four-sided Vickers pyramidal indenters. Dukino et al. (1992) then adjusted the Laugier equation for the three-sided Berkovich indenter and obtained $\chi = 0.016$ [78, 81]. This equation will be the focus of this thesis.

However, care should be taken when using the high load indentation technique for the fracture toughness measurement for biological materials. Firstly, unexpected cracks, not due to indentations, may occur during sample preparation. Furthermore, these methods have never been proven to be effective in evaluating the fracture toughness of materials that exhibit ascending R-curve behavior. Finally, the materials for which these techniques were designed are brittle materials. However, due to the low percentage of organic matrix contained in biological materials, they are less hard than these brittle materials. This makes this technique subject to even greater errors than would normally be expected when used on biological materials [79].

2.6 Statistical testing

The high load indentation tests are performed in the enameloid of both fish species but also at two locations within the enameloid (in a zone close to the dentin and a zone close to the surface). In order to evaluate if either the differences in the obtained toughness fracture values between the two species and between the two locations are significant or not, it is necessary to perform a statistical analysis. This analysis is performed on Matlab and is as follows.
To determine whether two independent data sets are significantly different, a two-sample t-test (TTEST2 function on Matlab) should be performed. However, this test can only be carried out if two conditions are met. The first condition is that the compared populations should follow a normal distribution. The Kolmogorov-Smirnov test (KSTEST function on Matlab) can be applied to check this condition. The second condition is that the compared populations must have the same variance. This can be checked by applying a two-sample F-test (VARTEST2 function on Matlab). If these two conditions are met, the t-test can be performed. Otherwise, i.e. if one of those criteria is not met, another test determining whether the two data sets are significantly different or not, called a Mann-Whitney U-test (RANKSUM function on Matlab), can be performed. However, with this test, the null hypothesis being tested is slightly different, it is now a matter of seeing if a randomly selected value in one population is lower or higher than a randomly selected value in the other population [83].

Chapter 3

Results

The purpose of this chapter is to objectively describe the images obtained using SEM techniques. The results acquired with the fractured teeth and the surface etching performed on frontal sections of the teeth allowed a precise analysis of the microstructure of the enameloid. The local fracture behavior of this layer was then studied through the observation of microscopic images of the high load indentation tests.

3.1 Microstructure

Two different approaches are used to characterize the microstructure. Firstly, the observation of the etching results gives a general view of the enameloid microstructure. In a second step, the observation of the fractures provides additional features on the microstructure of the enameloid but it also reveals insights into the cuticle and the microstructure of the dentin.

3.1.1 Surface etching

Polished frontal sections of teeth from carnivorous and herbivorous species were etched with hydrochloric acid (HCl) to study enameloid structure. The etching removes a slight thickness of the mineral part on the surface allowing to highlight the organization and arrangement of the mineral bundles.

The images observed below are SEM−BSE images in which the higher the proportion of mineral the higher the signal. Delaunois et coll. (2020) [21] reported that enameloid has similar compositions in the two species studied and it is mainly composed of hydroxyapatite crystals. From this knowledge, we can deduce that the observed higher brightness corresponds to hydroxyapatite crystals.

The observation of SEM−BSE images of the polished and etched frontal sections reveals that the teeth of the two fishes have different shapes. The tooth of *P. nattereri* has a slender central cusp, high and thin over its entire height (Figure 3.1.A) while the *P. brachypomus* tooth has a squat shape with a base wider than the tip (Figure 3.2.A). The two teeth exhibit also variations in the enameloid distribution. There is a gradient of enameloid thickness that increases from the base to the tip. This gradient is, however, weaker in the tooth of the carnivorous species where the enameloid thickness increases slowly up to the tip (Figure 3.1.A), while in the herbivorous species, the enameloid is more strongly concentrated on the top of the tooth and its thickness decreases rapidly as it descends towards the base (Figure 3.2.A).

The polished and superficially etched frontal section of the carnivorous species (Figure 3.1) shows that the enameloid of this species is composed of numerous mineral bundles whose arrangement differs greatly over the thickness of the enameloid. As a result of this difference in bundles organization from the outside to the inside, the enameloid can be divided into two sub-layers, called the outer and inner enameloid. In the outer part, hydroxyapatite fiber bundles are aligned parallel to each other. However, their orientation depends on the location within the tooth: on the lingual side of the tooth, they are pointed towards the top of the tooth while on the labial side, bundles are oriented perpendicular to the external surface of the tooth. In contrast, the inner enameloid comprises well-disorganized crystallite bundles. They are crossed, oriented and curved in a random manner.

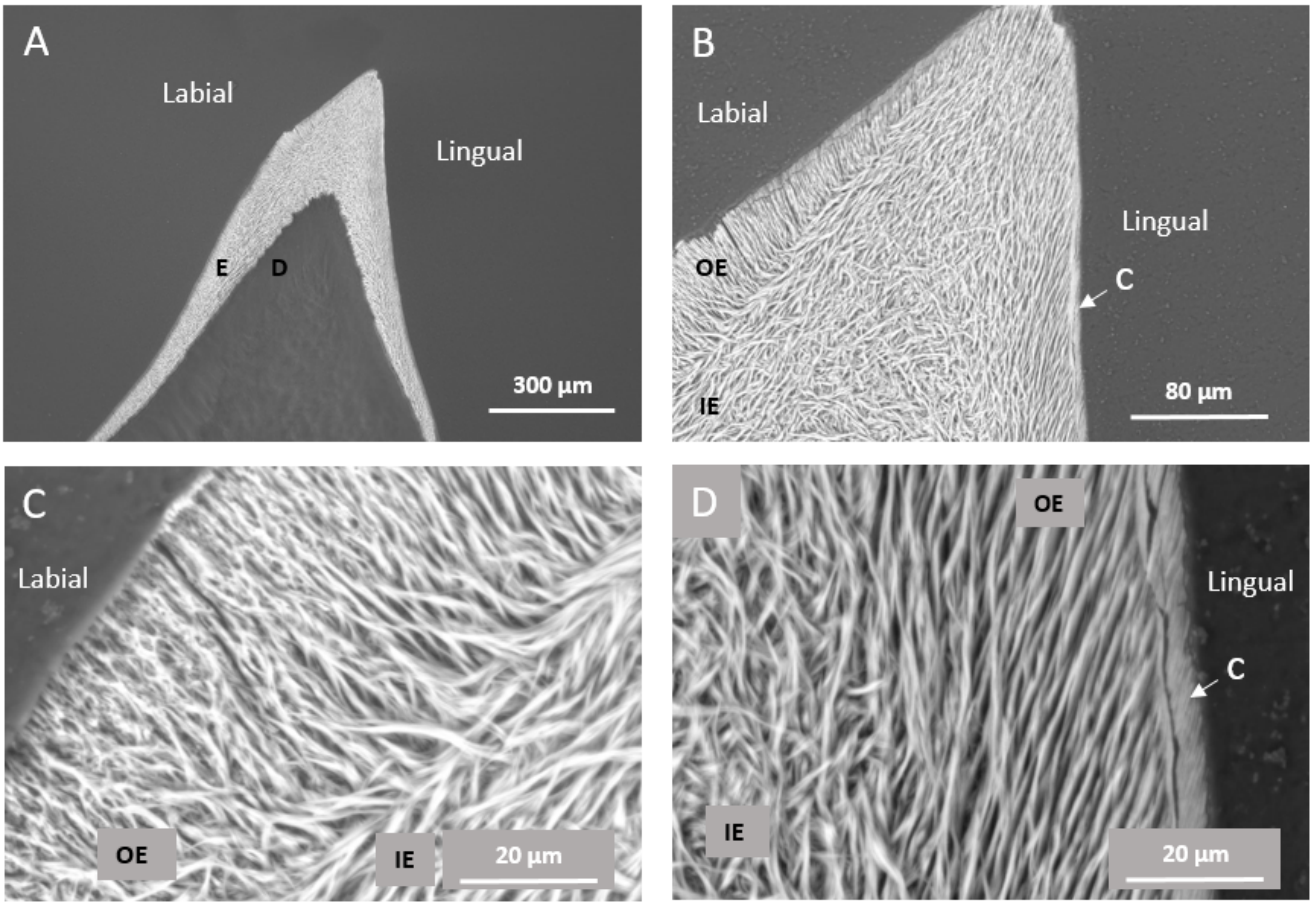

Figure 3.1: SEM−BSE images of the frontal section of an oral tooth of the carnivorous *P. nattereri* after HCl etching. *Abbreviations: D, dentin; E, enameloid; OE, outer enameloid; IE, inner enameloid; c, cuticle.*

The observation of Figure 3.2, showing the result of a surface etching performed on a frontal section of the herbivorous species, displays the same general arrangement of the bundles as the one highlighted in the carnivorous species. Indeed, the two-part organization of the enameloid is also revealed in the herbivorous species, with the well-organized mineral bundles of the outer enameloid transforming into a less ordered region on the inside (Figure 3.3).
However, there are slight differences between the structure of enameloid of these two fishes. In herbivorous species, the demarcation between the two sub-layers is less marked than in carnivorous species. Moreover, on the labial side of the carnivorous tooth, the bundles of the inner enameloid are randomly organized but with a region of preferential orientation parallel to the interface between the inner and outer enameloid (Figure 3.3.A), and such behavior has not been highlighted in the herbivorous sample.

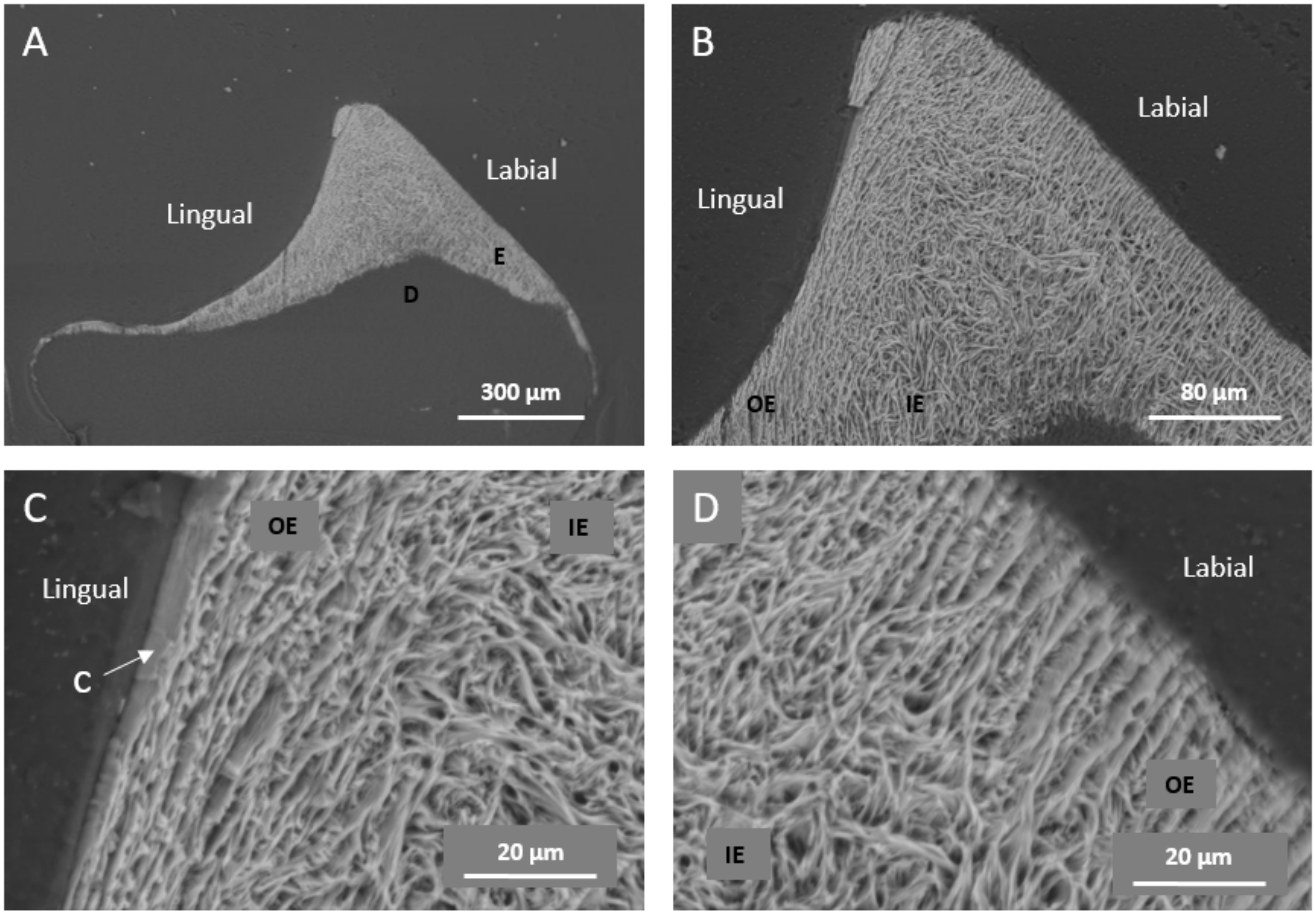

Figure 3.2: SEM−BSE images of frontal sections of an oral tooth of the herbivorous *P. brachypomus* after HCl etching. *Abbreviations: OE, outer enameloid; IE, inner enameloid; D, dentin; c, cuticle*.

The diameter of the mineral bundles visible on the etching images of the carnivorous and herbivorous species are, respectively, 1.847 ± 0.4971 µm (mean $\pm$ standard deviation) and 1.0149 ± 0.2716 µm. The bundles in the outer enameloid on the labial side of the carnivorous tooth seem to have smaller diameters than the bundles in the outer enameloid on the lingual side of the tooth (Figures 3.1.C and 3.1.D). However, this may be a result of etching as the solution may have been left for longer on the lingual side of the tooth resulting in more material being removed. That being said, this decrease in the diameter of the outer enameloid bundles on the lingual side is not observed in the herbivore species (Figures 3.2.C and 3.2.D).

It can also be noticed that the cuticle is still present on the lingual side in both species on almost the entire height of the tooth, while it has disappeared on the labial side (Figures 3.1.C, 3.1.D and 3.2.D).

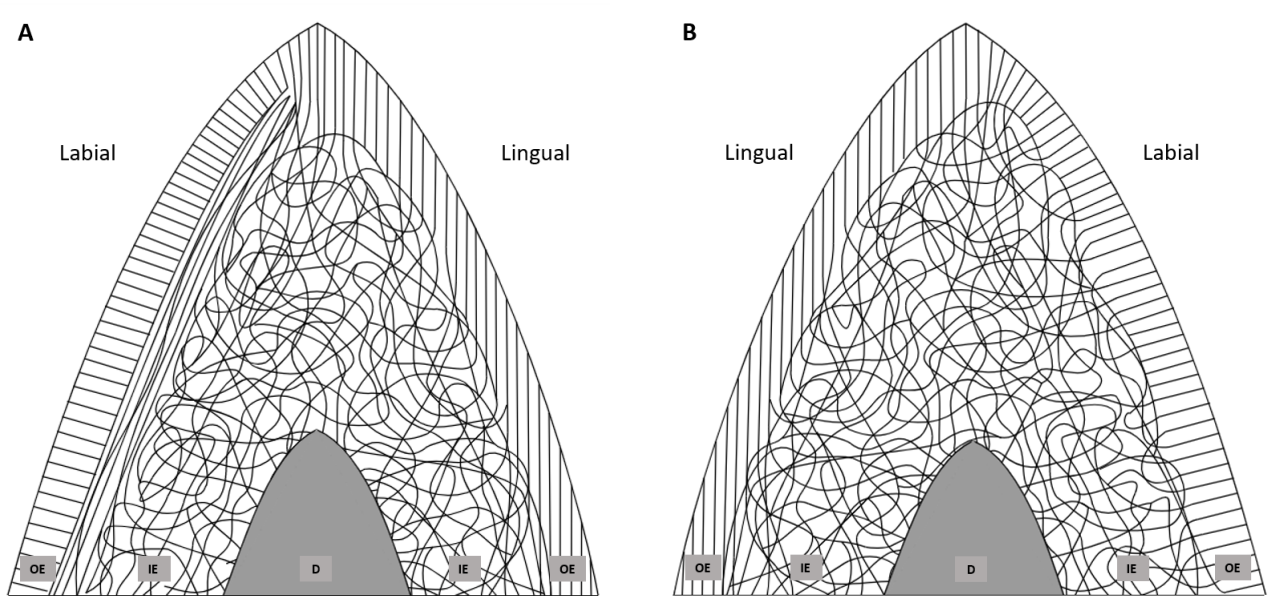

Figure 3.3: Schematic representation of a frontal section on oral tooth in (A) the carnivorous *P. nattereri* and (B) the herbivorous *P. brachypomus*, denoting the orientation of the bundles in the enameloid. *Abbreviations: OE, outer enameloid; IE, inner enameloid; D, dentin.*

3.1.2 Fractures

In this subsection, fractured samples are investigated in order to reveal additional features of the microstructure of the enameloid. It is important to note that the tooth sections obtained after the fractures are not totally frontal or transverse but generally a combination of both, as can be seen in Figure 3.5.A. To have the best understanding of the images shown in this section, their location will be indicated on a broader picture of the fracture.

3.1.2.1 Enameloid

SEM−SE images of the fractured tooth samples reveal that in the enameloid, the hydroxyapatite crystal fibers are tightly packed parallel to each other along their long axis to form larger bundles (Figures 3.4.E and 3.4.F). These bundles are arranged in two different organizations through the thickness of the enameloid, totally disordered inner enameloid and well-organized outer enameloid with bundles oriented parallel and perpendicularly to the surface. These two sub-layers of the enameloid are clearly visible in Figure 3.4.C showing a near-surface zoom into the frontal section fracture in a tooth of the carnivorous species.

Figures 3.4.E and 3.4.F illustrate the organization of bundles in the outer enameloid of the carnivorous species. In this sub-layer, the bundles have a rectangular shape whose length is unknown. Their cross-section is a rectangle whose width (side of the rectangle perpendicular to the surface) is larger than the thickness (side of the rectangle oriented parallel to the surface). They are aligned lengthways and oriented mostly parallel to the surface (Figure 3.4.E). These parallel bundles are invaded by thinner bundles oriented perpendicular to the surface of the tooth (Figure 3.4.F). A similar shape and organization of bundles in the outer enameloid is also found in the herbivore species (Appendix B, Figure 5.2).
By comparing the two sides (labial and lingual) of the fracture of the frontal section of a carnivorous tooth, it seems that the bundles organization in the outer enameloid is not exactly the same from one side to the other. Indeed, in Figure 3.4.C, the proportion of bundles perpendicular to the surface in the outer enameloid seems to be higher than on the other side (Figure 3.4.E), with as many bundles parallel

as perpendicular. However, from Figure 3.4.C, no information on the thickness of the bundles can be obtained due to the orientation of the cut.

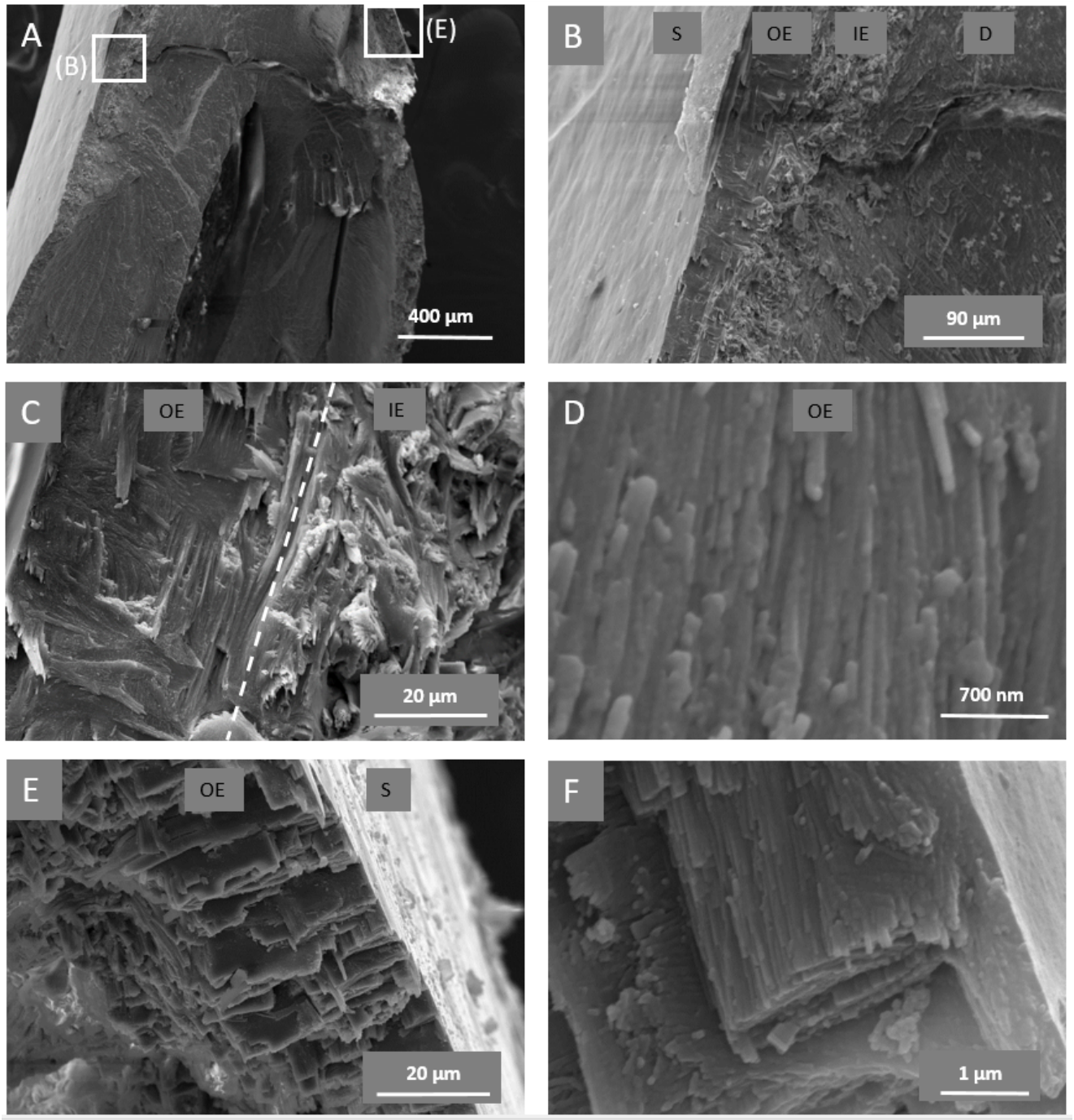

Figure 3.4: SEM−SE images of frontal section fractures of an oral tooth of the carnivorous *P. nattereri*. (B,C,D) Zooms in the region B of (A) showing the dentine, inner and outer enameloid; (E,F) Zooms in the region E of (A) showing the outer enameloid. *Abbreviations: S, surface; OE, outer enameloid; IE, inner enameloid; D, dentin*.

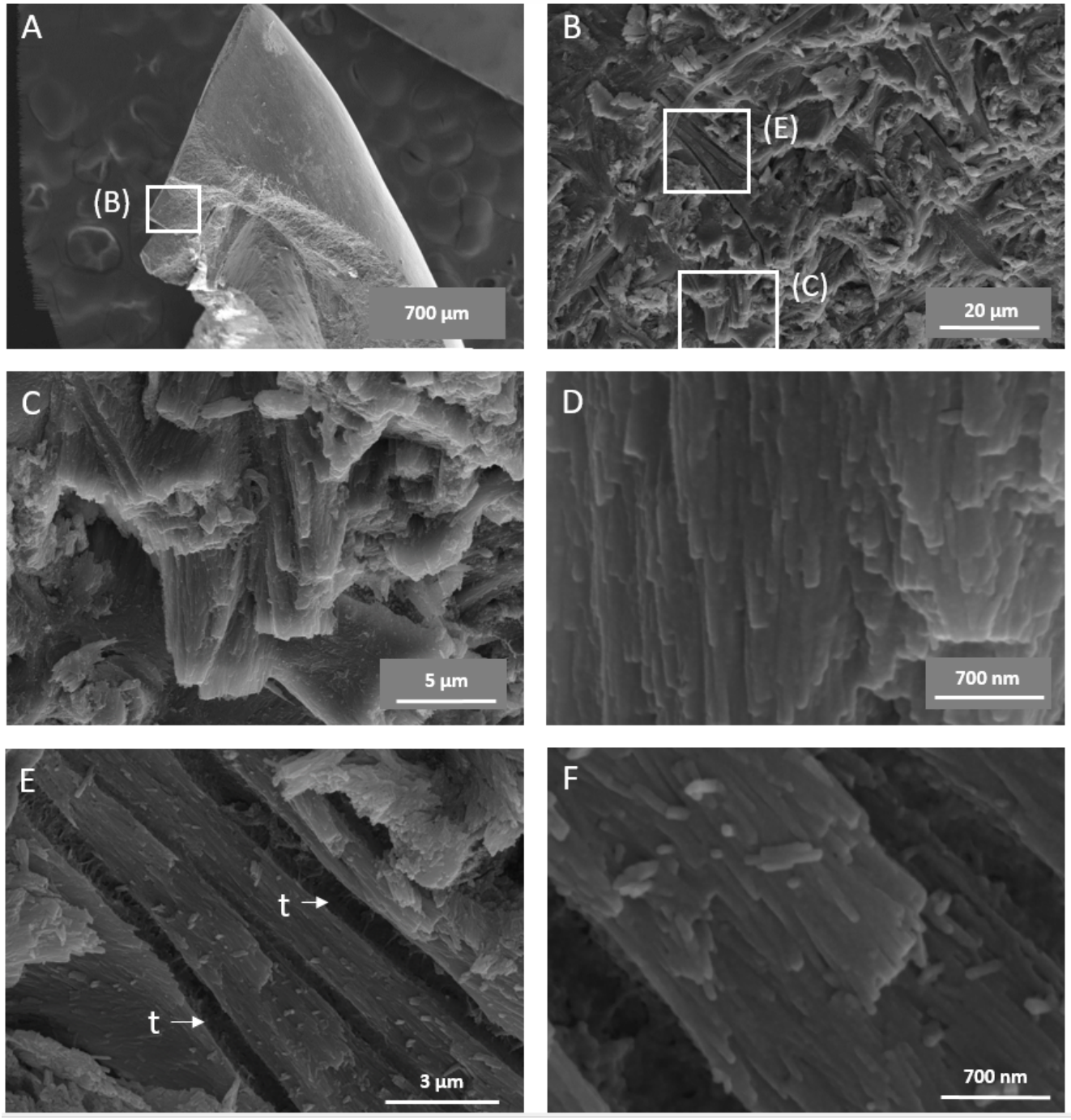

Figure 3.5: SEM−SE images of section fractures of an oral tooth in the herbivore *P. brachypomus*. (B) Zoom in the region B of (A) showing the inner enameloid; (C,D) Zooms in the region C of (B) showing some bundles of the inner enameloid; (E,F) Zooms in the region E of (B) showing some tubules of the inner enameloid. *Abbreviation: t, tubule*.

In Figure 3.5, the organization of the inner enameloid in the herbivorous species is very different from that found in the outer enameloid. Although the hydroxyapatite fibers are also aggregated in bundles, these are not as regular with well rectangular sections as in the outer enameloid. Moreover, unlike the outer enameloid, the inner region is completely disordered. The bundles are oriented in all directions, bend and intertwine. The same observations can be made in the inner enameloid of the carnivorous species (Appendix B, Figures 5.4.A, 5.4.C and 5.4.D).
Some tubules are also present in the inner enameloid (Figures 3.5.E and 3.5.E). These tubules appear to be cylindrical and have an average diameter of 0.67 $\pm$ 0.11 µm (mean $\pm$ standard deviation) in the herbivorous species. Around them, the hydroxyapatite fibers are aligned and oriented parallel to the longitudinal axis of the tubes.

It can also be noticed from Figure 3.7.B that the fracture is straight and directed perpendicular to the surface in the outer enameloid whereas it does not seem to enter the inner enameloid but follows the interface between the two sub-layers of the enameloid.

3.1.2.2 Dentin

The dentin structure is similar in both species and is characterized by the presence of numerous dentinal tubules (Figure 3.6). These appear to be cylindrical and have an average diameter of about 1.2 µm ± 0.12 µm (mean ± standard deviation) in the herbivorous species. In the same species, the tubules of the dentin have therefore a larger average diameter than those of the inner enameloid. They are aligned parallel to each other and directed perpendicular to the enameloid-dentin junction (Appendix B, Figure 5.5). Unlike the tubules found in the inner enameloid, they are not surrounded by hydroxyapatite fibers aligned parallel to the tubules. In dentin, the fibers seem to assemble to create the wall of the tubules, while the areas between the tubules exhibit small round structures.

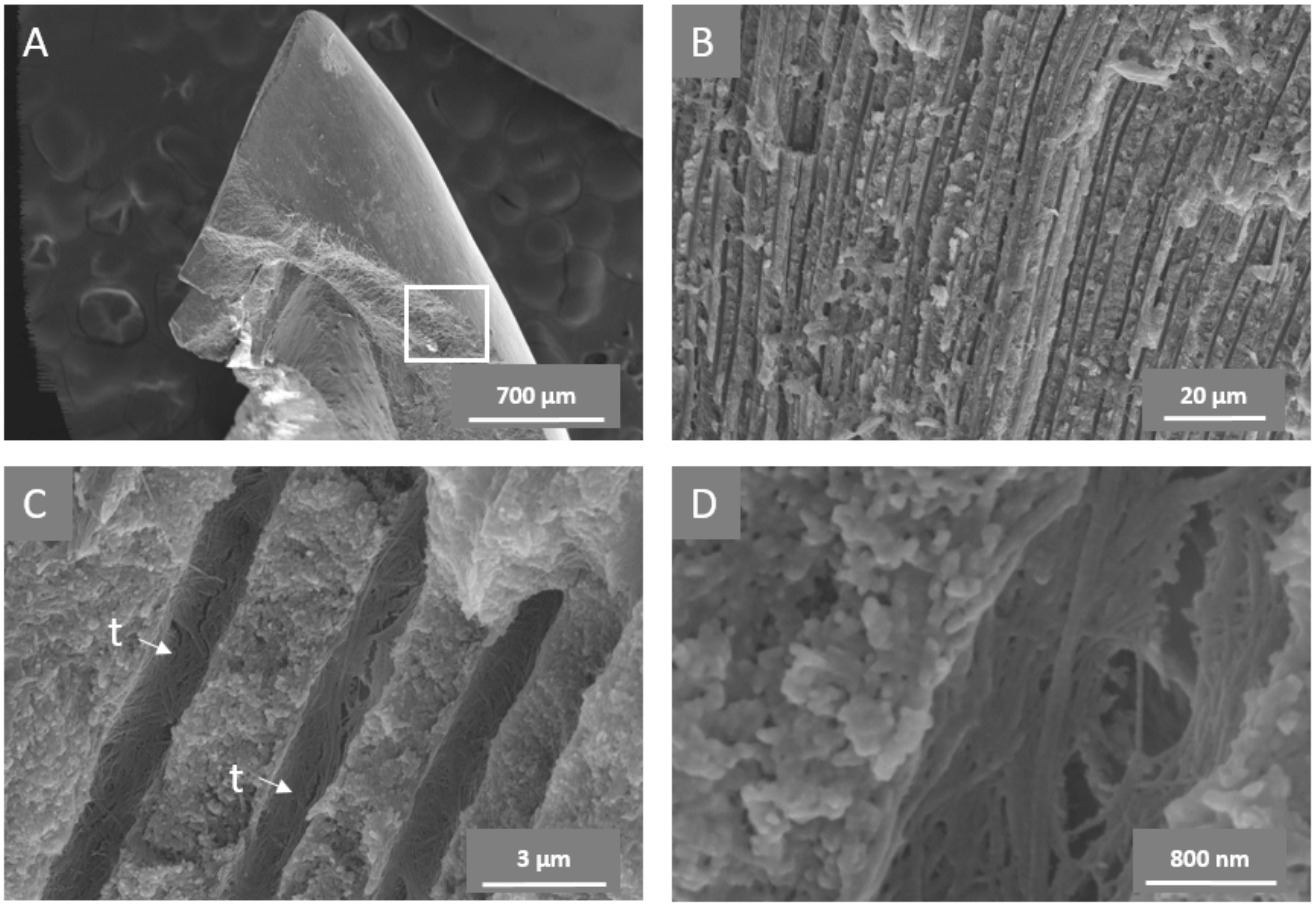

Figure 3.6: SEM−SE images of section fractures of an oral tooth of the herbivorous *P. brachypomus*. (B,C,D) Zooms in the square of (A) showing the tubules of the dentin. *Abbreviation: t, tubule*.

3.1.2.3 Cuticle

Unfortunately, no information on the internal structure of the cuticle could be extracted from the fracture images. However, Figures 3.7.C and 3.7.D indicate that the cuticle is detaching from the rest of the tooth.

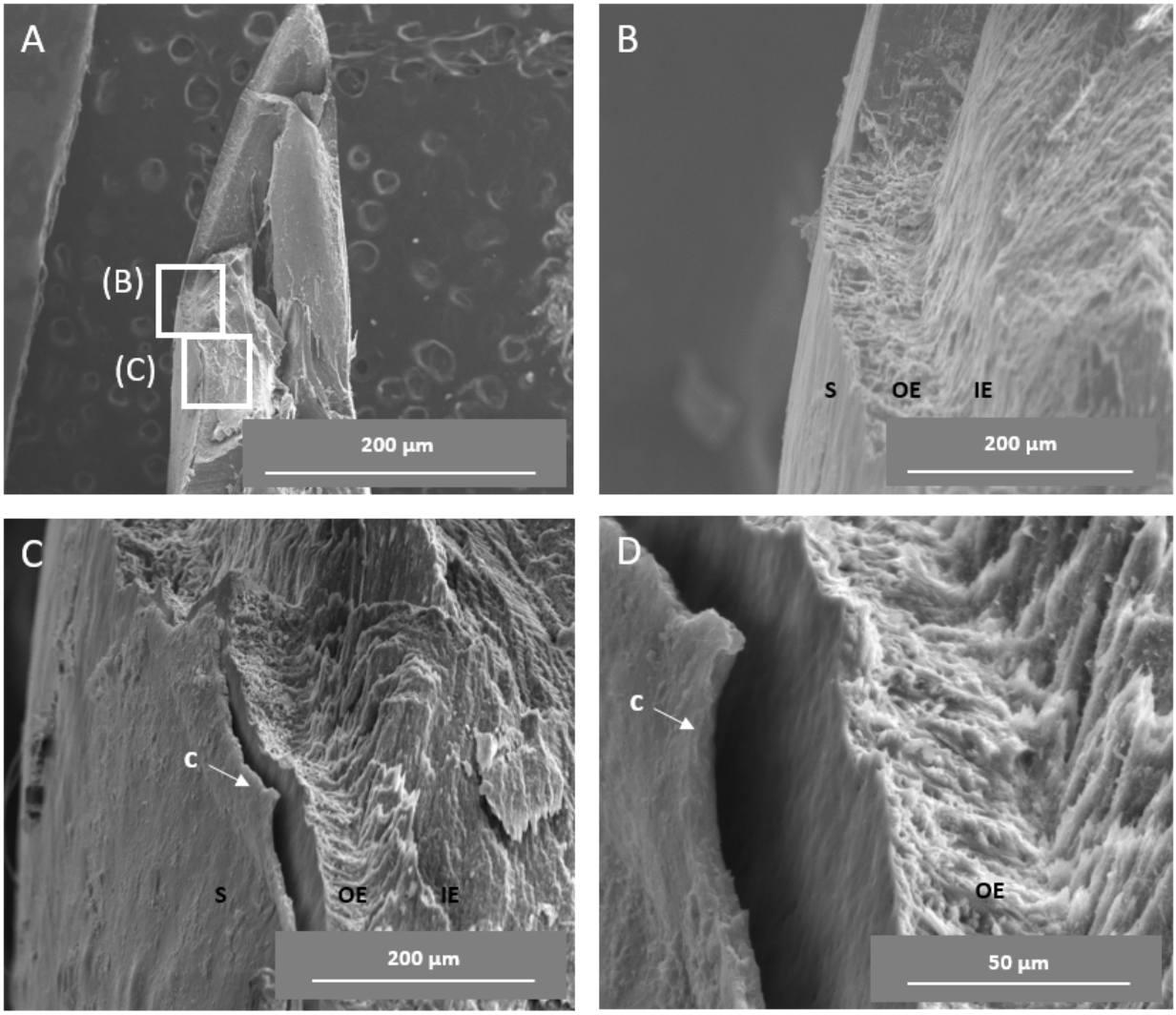

Figure 3.7: SEM−SE images of section fractures of an oral tooth of the carnivorous *P. nattereri*. (B) Zoom in the region B of (A). (C,D) Zooms in the region C of (A) showing the detachment of the cuticle. *Abbreviations: S, external surface; OE, outer enameloid; IE, inner enameloid; c, cuticle*.

3.2 High load indentations

The high load indentation technique is employed to investigate the local fracture behavior of the enameloid. Indentations initiate the formation of cracks at the corners of the indentations. By measuring the lengths of these indentation cracks and observing their propagation patterns, the resistance to crack initiation and propagation can be evaluated.

As can be visualized in Figure 3.9.A, the indentation of the sample produces radial cracks emanating from the corners of the indent due to the stress concentration induced.
The number of cracks initiated at the indent corners depends on the applied load and the location (inner or outer enameloid) of the indentation. The resistance to crack initiation can be deduced by calculating the ratio between the total number of radial cracks initiated at the corner of the indent divided by the number of possible initiation sites, which is equal to three in the case of the Berkovich tip [80].

The fraction of cracked indent corners as a function of the peak load is plotted and fitted wit a 3th-degree polynomial (Polynomial curve fitting) in Figure 3.8 for both species. It is important to indicate that cracks from indentations with significant damage on the side of the notch were not included in this calculation (Figure 3.9.B). This explains why the peak load on the x-axis does not reach 1100 mN in the two graphs.
If the initiation load is defined as the load at which the fraction of cracked corners is equal to 50 % [80], the one of the inner enameloid is greater than that of the outer enameloid in both species.

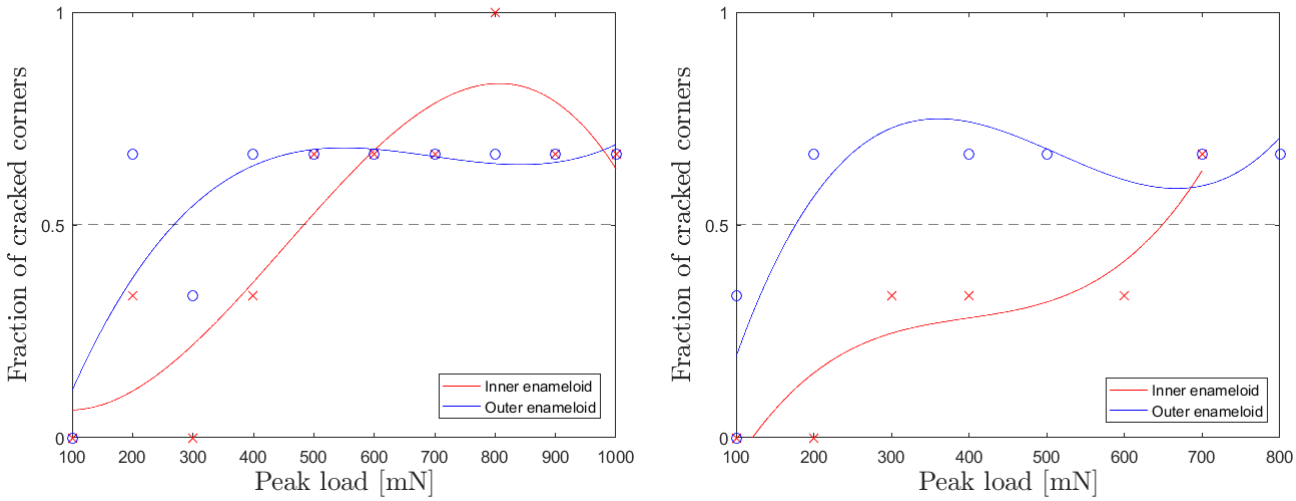

Figure 3.8: Cracking frequency in inner and outer enameloid of the herbivorous *P. brachypomus* (left graph) and the carnivorous *P. nattereri* (right graph).

In addition to crack initiation resistance, the fracture toughness K_c can be evaluated approximately from the average length of the radial cracks and the dimension of the plastic indent, using the following formula:

$$K_c = \chi\left(\frac{a}{l}\right)^{1/2}\left(\frac{E}{H}\right)^{2/3}\left(\frac{P}{c^{3/2}}\right) \tag{3.1}$$

Where P is the peak load, a is the characteristic dimension of the plastic indent measured from the center of the indent to the corner of the indent and χ is a geometric constant of indenter equal to 0.016 in the case of a Berkovich tip [81].

E and H corresponds respectively to the Young's modulus and the hardness of the enameloid. An ongoing study at the University of Liege has revealed, using nanoindentation tests, that Young's modulus values range from 60 to 120 GPa and hardness values from 3 to 7 GPa. This range of Young's modulus values was confirmed by a modulus mapping performed as a side aspect of this thesis and whose results are presented in Section 4.2.1. In the fracture toughness measurements, $H = 5$ GPa and $E = 100$ GPa were used as the average value of Young's modulus and hardness for the inner and outer enameloid of both species.

For each indent, the average length of the radial cracks was estimated by averaging the length of cracks emanating from each of the indent tips with c denoting the average length of the radial cracks measured from the crack tip to the center of the indent and l the average length of the radial cracks measured from the crack tip to the indent tip (Figure 3.9.A).

Some of the indentations show significant damage along their edges (Figure 3.9.B). Since there is no published standard saying that fracture toughness can be calculated from such indentations, they were not considered in the fracture toughness measurement in this thesis. Moreover, in biological materials, the cracks emanating from indentations are not necessarily straight as in brittle materials with linear elastic fracture mechanics behavior [2], some cracks are deflected from the indent corner, curved or bridged (Figure 3.10). In this thesis, the length of cracks that are directed in the direction of the indentation tip (not deflected) are used even though these cracks have curvatures and bridging occurring during crack propagation.

Fracture toughness was measured for all the indentations having the characteristics described above and reported for each of the two sub-layers of the enameloid and for each of the two fishes in Table 3.1.

Fracture toughness K_c [MPa m$^{1/2}$]		
	Herbivorous *P. brachypomus*	Carnivorous *P. nattereri*
Outer enameloid	0.56 ± 0.03	0.48 ± 0.17
Inner enameloid	0.69 ± 0.14	0.63 ± 0.12

Table 3.1: Fracture toughness obtained for the inner and outer enameloid of the teeth of *P. brachypomus* and *P. nattereri* (mean $\pm$ standard deviation).

Although the difference between the fracture toughness values obtained between the inner and outer enameloid was not significant following a statistical analysis explained in Section 2.6 (p-value = 0.4 in the herbivorous species and p-value = 0.09 in the carnivorous species), greater average fracture toughness is nevertheless observed in the inner enameloid than the outer enameloid.
The same statistical analysis shows that the difference in toughness fracture values between the carnivorous and herbivorous species is not significant (p-value = 0.25 in the outer enameloid and p-value = 0.55 in the inner enameloid). However, the average fracture toughness of the herbivore species is greater than that of the carnivore.

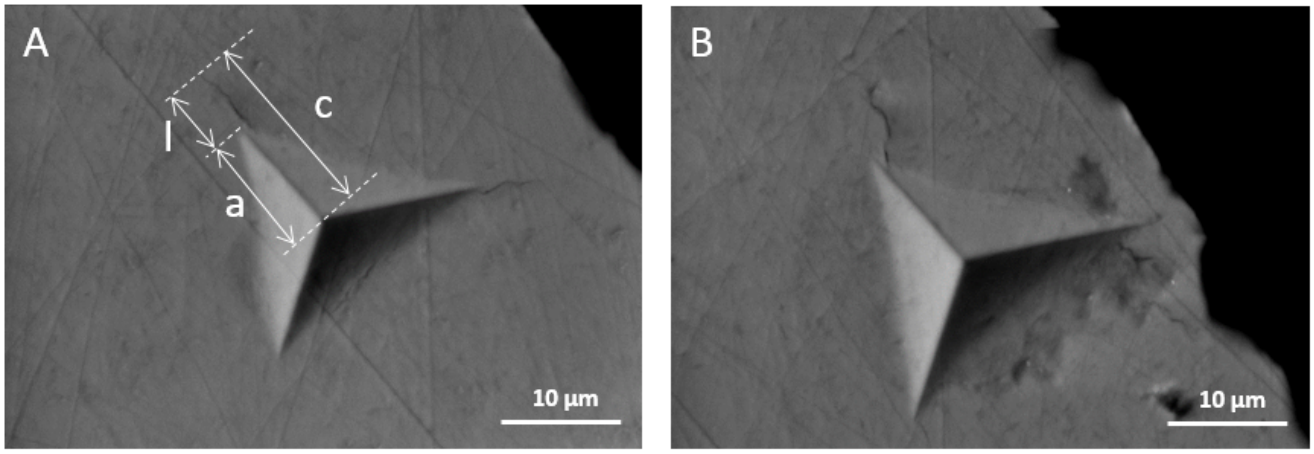

Figure 3.9: SEM−BSE images of the polished frontal sections of the outer enameloid in the herbivorous *P. brachypomus* after indentations under (A) 800 mN and (B) 1000 mN load. The crack lengths c and l as well as the dimension of the indent a used to calculate indentation toughness are denoted in (A). (B) shows an indentation with large damage on the side of the indent, not used in the toughness fracture approximation. *Abbreviations: c, length of the radial cracks measured from the crack tip to the center of the indent; l, length of the radial cracks measured from the crack tip to the indent tip; a, characteristic dimension of the plastic indent.*

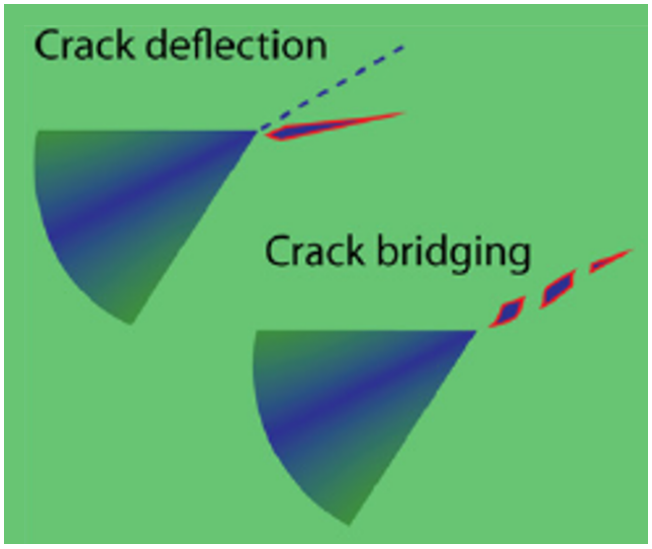

Figure 3.10: Schematic representation of a crack deflection and a crack bridging

Figure 3.11 shows representative indentation morphologies in the outer and inner enameloid under low and high loads. Cracks appear already at low loads in the outer enameloid of both species while they are not or almost not present in the inner enameloid for same loads. It can also be noticed that cracks appearing in the outer enameloid of carnivorous species at low loads are longer than those appearing in herbivorous species for the same loads.
At higher loads, cracks become wider and longer in the outer enameloid than those present at lower loads (Figures 3.11.C and 3.11.D). Cracks appear also in the internal enameloid at high loads. These cracks remain very thin but can be long.

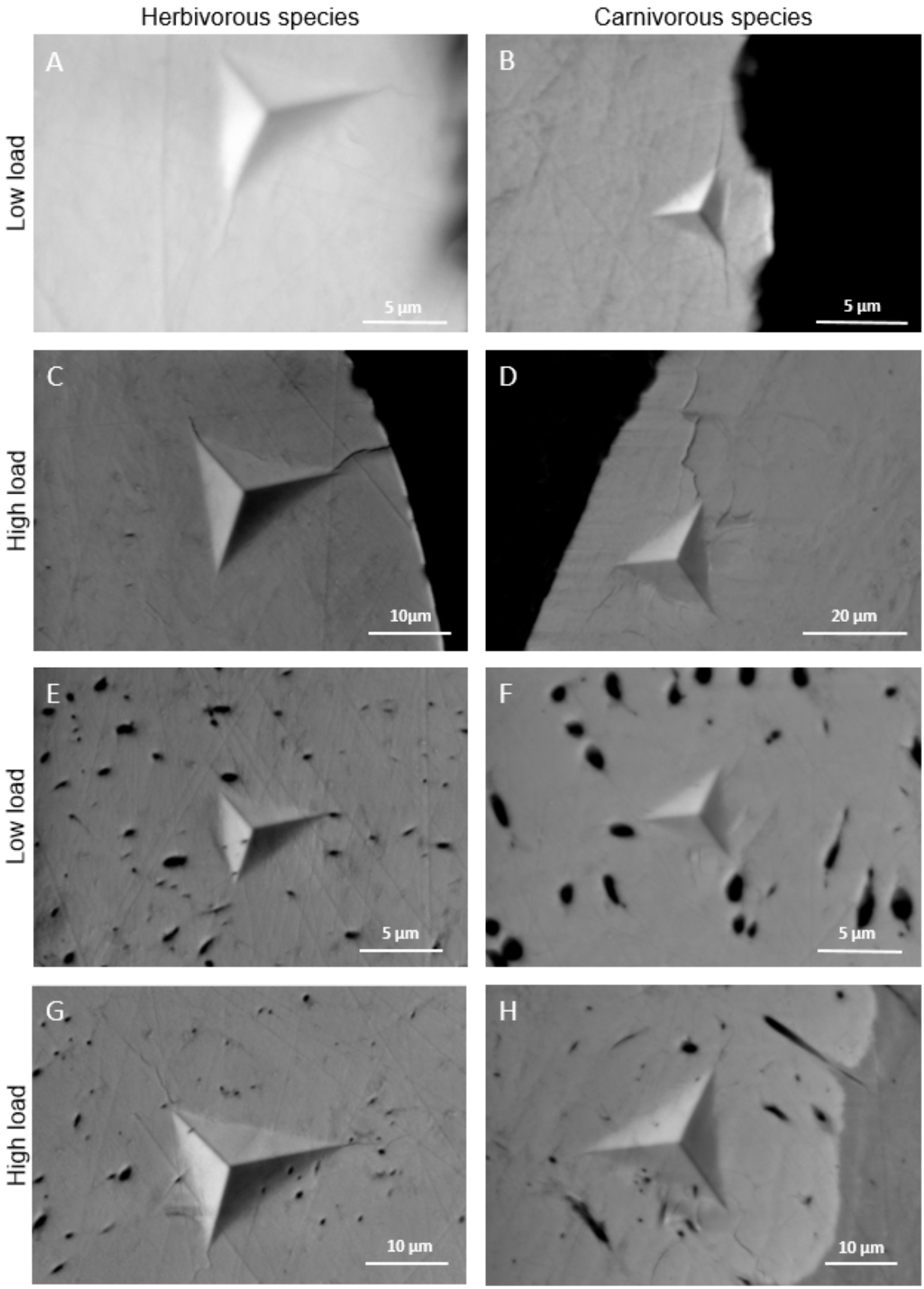

Figure 3.11: SEM−BSE images of the polished frontal sections of teeth (A,C,E,G) in the herbivorous *P. brachypomus* and (B,D,F,H) in the carnivorous *P. nattereri* after indentations under (A) 200 mN, (B) 200 mN, (C) 600 mN, (D) 700mN, (E) 300 mN, (F) 200 mN, (G) 800 mN and (H) 700 mN load.

Figures 3.12.A and 3.12.B show that some locations in the tooth are favorable to the formation of very large and extensive cracks, even at low loads.

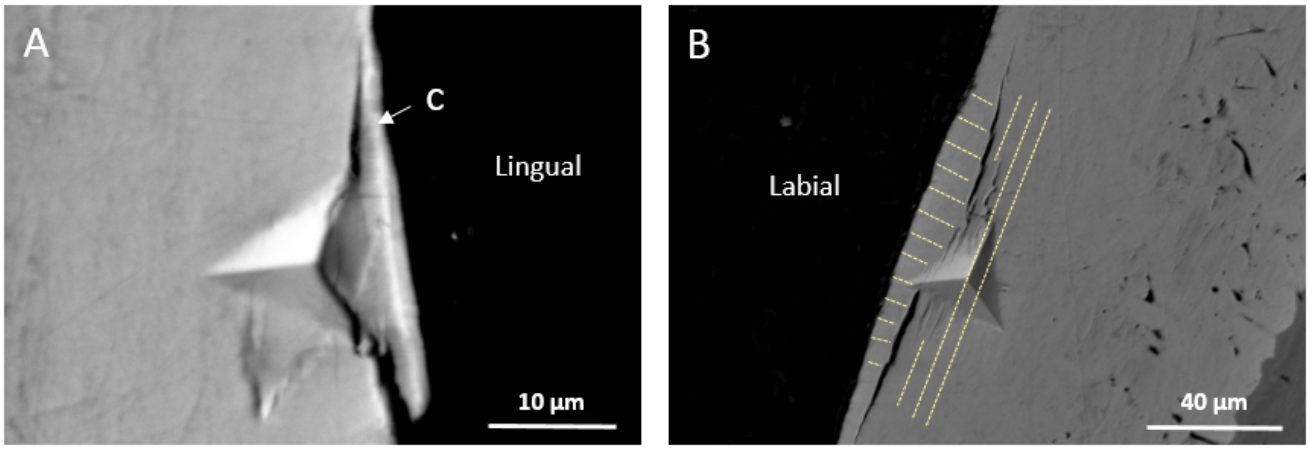

Figure 3.12: SEM−BSE images of the polished frontal sections of the outer enameloid in the carnivorous *P. nattereri* after indentations under (A) 200 mN and (B) 1100 mN load. The orientation of the bundles close to the indentation is denoted with yellow dotted lines in (B). *Abbreviation: c, cuticle*.

A more detailed analysis of the cracks present in each of the two sub-layers leads to the following observations:
A common observation between the two sub-layers is the presence of cracks bridging. They can be observed in the outer enameloid of the two species, as shown in Figures 3.13.B and 3.14.B, but also in the inner enameloid of the two species, this is illustrated in Figures 3.15.B, 3.16.C and 3.16.E.

In the outer enameloid, it can be observed that when indentations are performed on the labial side, the larger cracks emanating from the indent are in a straight line and oriented perpendicular to the surface while cracks emanating from indent carried out on the lingual side of the tooth are in a straight line but oriented preferentially parallel to the surface. This generally leads to a marked deflection of the large cracks at the top of the indent (Figures 3.13 and 3.14). In addition to these large cracks oriented perpendicular or parallel to the surface, smaller cracks sometimes appear oriented in other directions (Figures 3.13.A and 3.14.A).

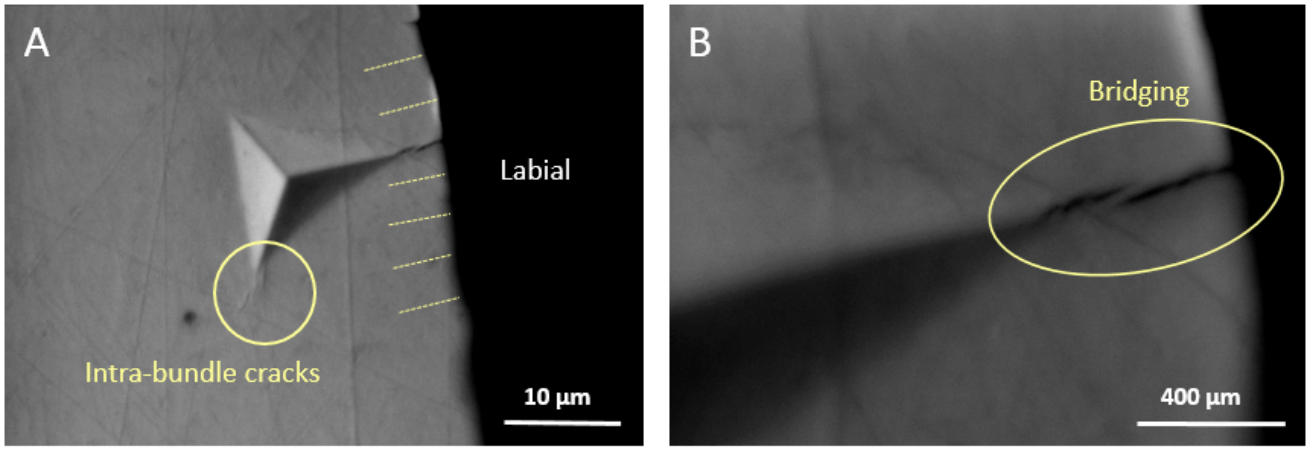

Figure 3.13: SEM−BSE images of the polished frontal section of the outer enameloid in the herbivorous *P. brachypomus* after indentations under 400 mN load. The orientation of the bundles close to the indentation is denoted with yellow dotted lines in (A). The circled region in (A) denotes intra-bundle cracks. The crack at the right corner of the indent of (A) is magnified in (B). The circled region in (B) denotes crack bridging.

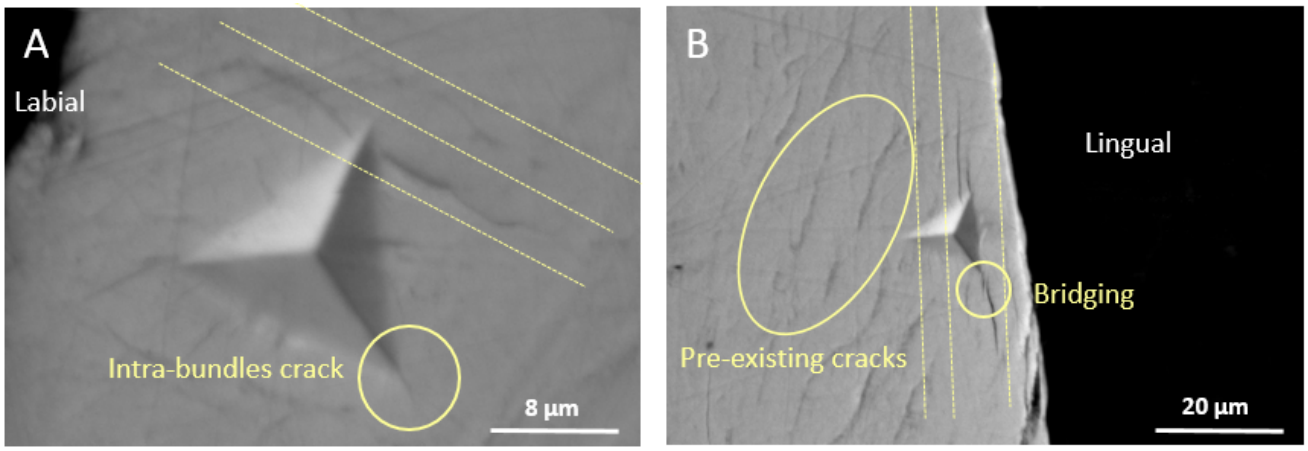

Figure 3.14: SEM−BSE images of the polished frontal section of the outer enameloid in the carnivorous *P. nattereri* after indentations under (A) 400 mN and (B) 200 mN load. The orientation of the bundles close to the indentations is denoted with yellow dotted lines in (A) and (B). The circled region in (A) denotes a intra-bundle crack. The circled region in (B) shows pre-existing cracks and crack bridging.

In the inner enameloid, the fissures are not all in straight lines, they are sometimes curved. These cracks curving are observed in the internal enameloid of both species, as can be seen in Figures 3.16.B, 3.16.D, 3.16.F and 3.15.B. Moreover, some cracks develop far from the indent (Figures 3.16.A and 3.15.A). Finally, the dentinal tubules present in the inner enameloid and visible as black dots on the SEM−BSE images intercept sometimes cracks emanating from the indents. In this case, we observe that either when a large crack penetrates the tubule, it comes out narrower as shown in Figure 3.16.E in the circled area, or when a small crack penetrates the tubule, it is stopped in it.

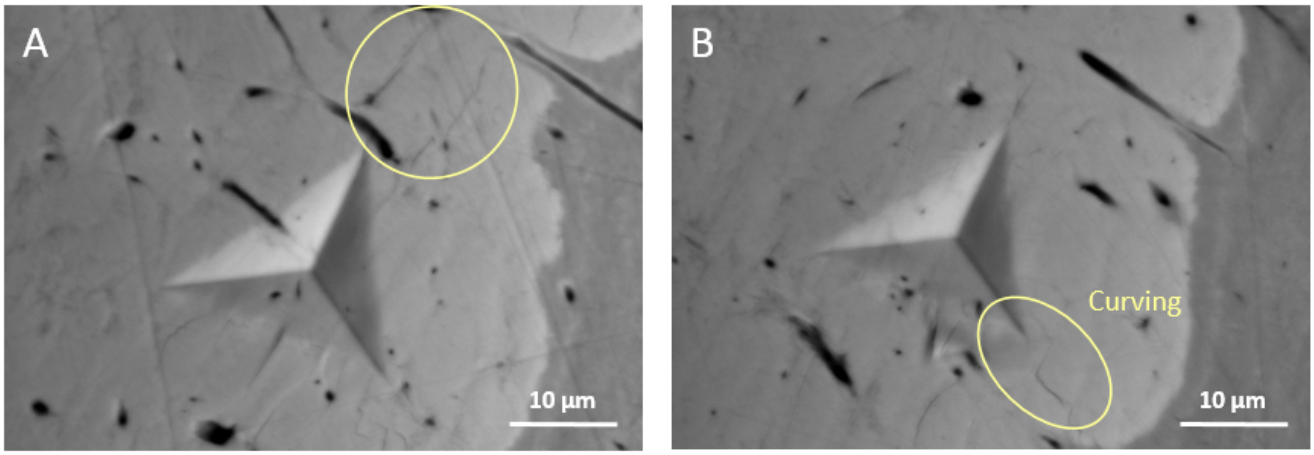

Figure 3.15: SEM−BSE images of the polished frontal section of the inner enameloid in the carnivorous *P. nattereri* after indentations under (A) 800 mN and (B) 1000mN load. The circled region in (A) denotes cracks located away from the indent. The circled region in (B) denotes crack curving.

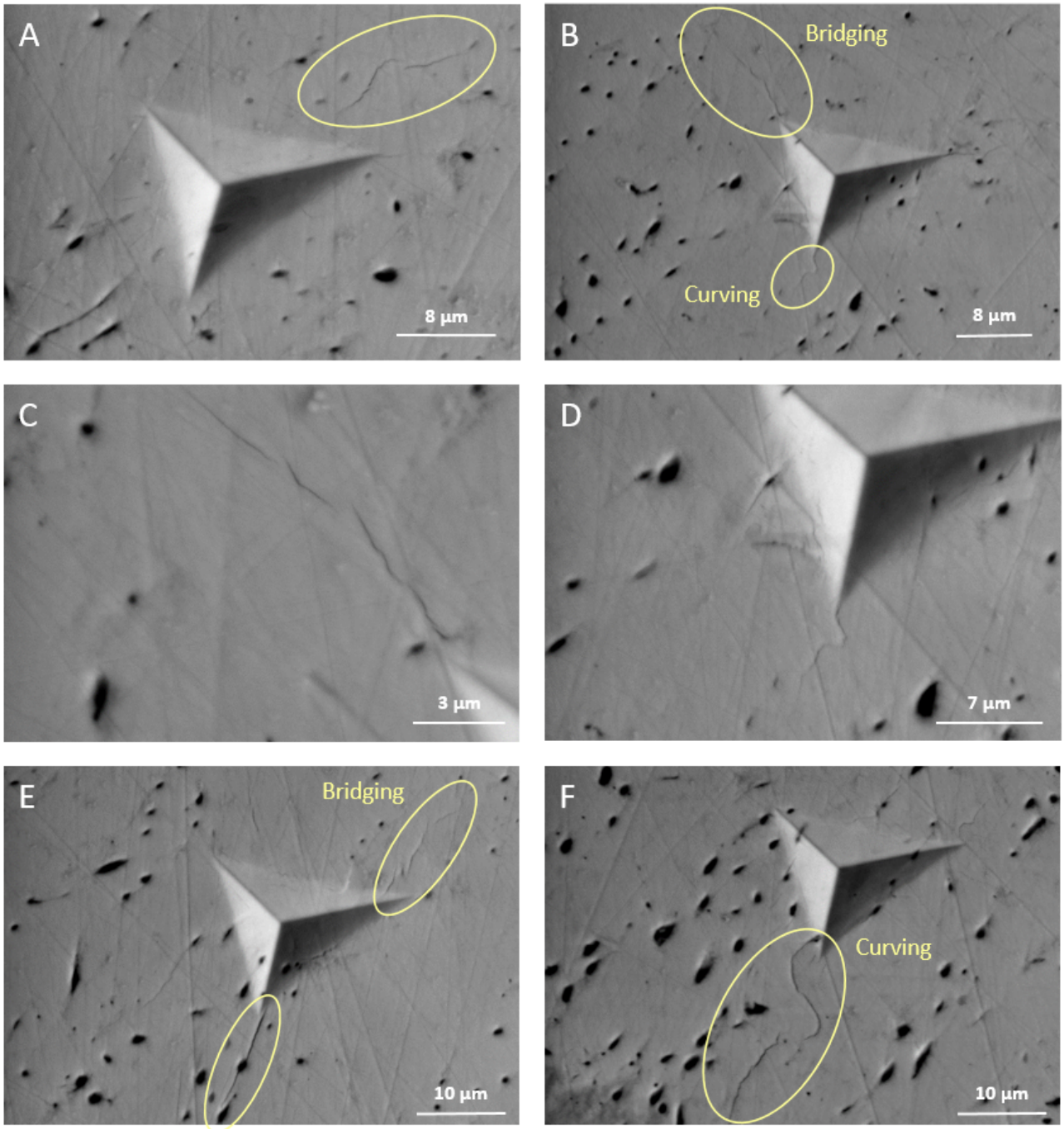

Figure 3.16: SEM−BSE images of the polished frontal section of the inner enameloid in the herbivorous *P. brachypomus* after indentations under (A) 600 mN, (B,C,D) 800 mN, (E) 900 mN and (F) 1000 mN load. The circled region in (A) denotes cracks located away from the indent. The circled regions in (B) denote crack bridging and crack curving, they are magnified in (C) and (D) respectively. The circled regions in (E) denote crack bridging and crack intercepting tubules. The circled region in (F) denotes cracks cruving.

Chapter 4

Discussion

In this chapter, the observations made in the previous section are discussed in relation to the literature in order to deduce features of the microstructure and to investigate fracture mechanical properties of the enameloid of the two fishes studied in this thesis. The main limitations of this thesis are then summarized and perspectives for future work are proposed.

4.1 Discussion

4.1.1 Dentin

The structure observed for the dentin of the two fishes studied is consistent with that observed by Delaunois et al. (2020) [21] with other methods in the same two fishes. The average diameter reported is, however, slightly larger than that observed by Delaunois et al. (2020) [21] in the dentin of the same two species (1.2 m versus 1 m).
Furthermore, it should be noted that the structure of the dentin of these fishes is also similar to that found in other species such as humans [4, 25, 26].

The small round structures observed around the dentinal tubules could correspond to non-oriented apatite microcrystals. Indeed, similar observations have been made in human dentin and these microcrystals have been described as apatite of lower crystallinity than those present in enamel [84].

4.1.2 Enameloid

Based on the results of the surface etching and fractured samples, we can suggest that the enameloid of the two species has a similar hierarchical structure in which the hydroxyapatite crystal fibers are aligned lengthwise and aggregate into bundles. These bundles are surrounded by a layer of organic matrix.
Note that the smaller hydroxyapatite crystal fibers composing the bundles do not seem to be enveloped by an organic matrix, as they are not visible on the etching images. Indeed, the average diameter of the bundles measured on the etching images is too large to correspond to the hydroxyapatite fibers composing the bundles.
The bundles are then arranged in two different organizations over the enameloid thickness, dividing the enameloid into two sub-layers: the inner and outer enameloid.
The inner enameloid is characterized by a well-disorganized arrangement with crossed and intertwined bundles forming a very complicated interlock structure. It also contains tubules that probably correspond to extensions of the dentinal tubules present in the dentin. These tubules are absent in the outer

enameloid. This latter possesses a well-organized arrangement with bundles aligned parallel to each other and oriented either perpendicular or parallel to the surface.
The bundles oriented parallel to the surface in the fractures seems, indeed, to correspond to those directed towards the top of the tooth observed with surface etching. There are therefore only two types of bundles, either parallel or perpendicular to the surface and the proportion of perpendicular or parallel bundles depends on the location within the tooth. The outer enameloid on the lingual side of the tooth has a greater proportion of large bundles parallel to the surface with few thinner bundles intercepting between the perpendicular bundles. The bundles perpendicular to the surface are predominant on the labial side of the tooth.

This organization of the enameloid is consistent with the findings reported by Delaunois et al. (2020) [21] in their paper about the same two fishes. Indeed, they also reported a two-layer organization of the enameloid and the presence of tubules in the inner enameloid. Moreover, only on the labial side of the tooth, the mineral fiber bundles show a similar organization to that of the collagen fibers reported by Delaunois et al. (2020) [21]. Indeed, collagen fibers have been shown to be aligned parallel and oriented perpendicular to the surface in the outer enameloid while they cross and intertwine in the inner enameloid. This corresponds well to the organization of the mineral bundles on the labial side of the tooth that has been revealed in this thesis. Remembering that collagen is the main constituent of the organic matrix, this observation validates the assumption that the bundles are surrounded by the organic matrix. Interestingly, in the outer enameloid on the lingual side of the tooth, the mineral bundles are not oriented in the same direction as the collagen fibers. Indeed, at this location, the collagen fibers are oriented perpendicular to the surface, according to Delaunois et al. [21], while the orientation of the mineral bundles, found in this thesis, is parallel to the surface.

This enameloid structure is different from that found in the enamel of humans and pandas whose structure consists of rods [38, 31, 2]. However, it is close to that found in other fishes such as the shortfin mako shark (*I. oxyrinchus*). Indeed, all these fishes have a two-layer organization of the enameloid as a result of the different mineral fiber bundles arrangement on the enameloid thickness [3]. The main structural difference lies in the organization of the bundles in the outer enameloid. In the shark, three types of bundles with different orientations are present, while the fishes of this study have only bundles oriented either parallel or perpendicular to the surface and, their proportions depend on the side of the tooth.

The finding of a similar structure for the enameloid in pacu and piranha although they have different diets may come from the fact that the enameloid of these two species has the same origin. This hypothesis is reinforced by the fact that the enameloid of these two fishes has a similar structure to that of the shark, which is also a lower vertebrate, while it differs from that of the panda and human, which are mammals. Indeed, as explained in Section 1.2.1, the enamel and the enameloid do not have the same origin.

The differences in orientation of the bundles depending on the side of the tooth in the enameloid of the two fishes may be linked to the functional demands placed on the tooth during eating. Indeed, during eating, one can expect more forces to be applied perpendicularly to the labial side of the tooth or to the top of the tooth due to lips pressure, contact with the teeth on the other jaw or with the food. The bundles are oriented to reinforce these more heavily stressed sides.

Moreover, in Figure 3.7 the organization of the bundles in the total enameloid seems to have an impact on the propagation of the fracture. It seems to propagate easily in the outer enameloid while the bundles of the inner enameloid seem to be mechanically organized in order to stop the propagation of the fracture.

4.1.3 Cuticle

It appears that the cuticle is easily eroded or detached when it is overstressed. Indeed, it was seen detaching in Figures 3.7.C and 3.7.D. Moreover, it is no longer present on the labial side of the tooth on the etching images of both species (Figures 3.1 and 3.2). This side of the tooth is located outside of the mouth and is therefore the one most likely to experience friction or impact with anything near its mouth and entering the mouth.

4.1.4 Fracture toughness

The effect of local microstructure on crack propagation was studied by analyzing the direction of crack propagation in relation to the structure of the inner and outer enameloid (Figure 3.3).

The fracture toughness varies between the two sub-layers of the enameloid with higher values in the inner enameloid than in the outer enameloid in both species. There also appears to be a species dependence of this property with higher fracture toughness in herbivorous species than in carnivorous species. However, these variations are not significant and should be analyzed with caution. As explained in Section 2.5.2.1, this method of fracture toughness has been implemented for brittle materials and not for biological materials containing a small amount of tough organic matrix, like enameloid.
It is also important to note that cracks were pre-existing in the outer enameloid of the carnivore sample, as shown in the circled area in Figure 3.14.B. Although pre-existing cracks can be avoided by careful experimentation, this damage can affect the fracture toughness of the material. Indeed, they can influence the Young's modulus but also the residual stress field around the indent [79].

However, it is interesting to note that the variation in toughness values obtained between the enameloid of the two species can be can probably be correlated with a variation in chemical composition between the two species. Indeed, it has been concluded previously that the two species have a similar enameloid structure, only the chemical composition varying from one species to the other. The higher fracture toughness computed for the pacu could therefore be due to the smaller amount of minerals present in this species. Indeed, Delaunois et al. (2020) [21] reported that the enameloid of the pacu has a mineral proportion of 88 wt% while the mineral content of the carnivorous species is 91 wt%. This assumption is consistent with the fact that in biological composite the mineral part brings the hardness while the organic matter brings the toughness.

Although the difference in fracture toughness values obtained between the inner and outer enameloid is not substantial, the representative indentation morphologies seem coherent with a greater toughness fracture in the inner enameloid compared to the outer one. Indeed, the inner enameloid generally presents less, smaller and thinner cracks than the outer enameloid for the same load. These qualitative observations of cracks are also in agreement with the lowest initiation load found in the outer enameloid.
It can therefore be concluded that the inner enameloid has a greater resistance to the initiation and propagation of cracks than the outer enameloid. This difference in mechanical behavior between the inner and outer enameloid is probably due to the structural specificities since the two sub-layers have a similar chemical composition [21].

High load indentations have been applied to evaluate the fracture toughness of many biological materials in literature. However, the formula used differs from one study to another due to the type of tip geometry used and the type of crack morphology created during indentations as explained in Section 2.5.2.1. To be convinced of the results, it can be interesting to compare them to those obtained in the enamel

of other species. The values obtained for the enameloid of the pacu and the piranha are of the same order of magnitude as those obtained in the human enamel. Indeed, the fracture toughness reported for the human enamel ranges from 0.4 to 1.5 MPa $m^{1/2}$ [40, 41, 42, 43]. It is also interesting to note that the values obtained for the fishes enameloid are closer to the lower range limit of values for the human enamel than to the upper limit. It means that the human enamel has a higher resistance to fracture than the enameloid of these two fishes. This can easily be explained by the fact that the human tooth renews at most once and must therefore resist throughout its entire life, which is not the case with the fish teeth that are renewed several times during its life.

The obtained fracture toughness values are also superior to the toughness of the hydroxyapatite which is equal to 0.3 MPa $m^{1/2}$ [2, 40]. This means that the low amount of organic matrix in combination with the enameloid structure allows increasing the fracture toughness of the material.

It was also observed in the previous section that some regions are favorable to the development of very large and extensive cracks. For example, the interface between the cuticle and the enameloid seems to be a preferential location for fracture propagation where crack spreads very easily. Indeed, Figure 3.12.A shows that a low load indentation causes a large crack at the interface between the cuticle and the enameloid. It can be deduced that this interface is very weak. This finding is, furthermore, in agreement with the images of the fractured teeth showing the cuticle is detaching from the rest of the tooth (Figures 3.7.C and 3.7.D) and with the images of the surface etching showing that the cuticle was present only on the lingual side of both species (Figure 3.1). All those results seem to confirm that the interface between the enameloid and its protective layer is weak, leading to the detachment of the latter or its erosion when it is too solicited.
In addition, large and extended cracks also appear at the interface between the inner and outer enameloid on the labial side of the carnivorous species tooth. Etching revealed that on this side in the carnivorous teeth, the bundles are oriented perpendicular to the surface in the outer enameloid and randomly but preferentially parallel to the surface of the inner enameloid adjacent to the outer enameloid (Figure 3.3.A). This difference in bundles orientation appears to create a weak interface favoring crack propagation, as shown in Figure 3.12.B.

Indentation cracks originate and develop preferentially in the direction given by the orientation of the bundles, along the interface between the bundles.
Indeed, first, it has also been observed earlier in the outer enameloid that cracks develop more easily in the direction perpendicular to the surface on the labial side and parallel to the surface on the lingual side. As described in Section 4.1.2, this sub-layer consists of aligned bundles oriented mainly perpendicular to the surface on the labial side of the tooth and mostly parallel on the lingual side. The preferential orientations of the cracks correspond therefore well with the orientation of the bundles. This leads to crack deflection of the larger cracks of the outer enameloid in the direction of the bundles.
Second, the smaller cracks also observed in the outer enameloid correspond to intra-bundle cracks as they are oriented in a direction different from that of the bundles (Figures 3.13 and 3.14). They are occasionally formed at the corner of the indenter due to stress concentration, but these cracks stop propagating rapidly due to the propagation of the crack that is more difficult within bundles.
Finally, in the inner enameloid, bundles are curved and intersected. The interfaces between bundles are therefore more complex than the straight longitudinal ones in the outer enameloid. This leads to marked curving and deflection of cracks. This also confirms that the crack propagation is related to the organization of the bundles and develops preferentially along the bundles.
Crack deflection and crack curving are extrinsic toughening mechanisms. They allow the crack paths to be directed away from the path of maximum mechanical driving force [2]. These two mechanisms as well as the crack bridging contribute to reducing the propagation of damage in the inner enameloid.

Another toughening mechanism observed in the two sub-layers of the enameloid is crack bridging. It can be noticed that the length scale at which it occurs both in the outer than in the inner enameloid corresponds to the size of the hydroxyapatite bundles, which means that it is certainly an un-cracked bundle that acts as a bridge to increase the resistance to fracture. Note that crack bridging is an extrinsic toughening mechanism that acts primarily to reduce the local stresses and strains experienced at the crack tip that serves to extend the crack [85].

The tubules present in the inner enameloid could be used to stop or reduce the propagation of the crack.

4.1.4.1 Structural dependence of indentation behavior

It has been concluded earlier that although the difference is not significant, the fracture toughness varies between the inner and outer enameloid with the inner part having a higher fracture resistance to crack initiation and propagation than the outer part and that this variation in toughness can only come from their structural differences. It appears therefore that the disordered architecture of the inner enameloid is more efficient in mitigating the tendency for crack formation during high-load indentations.

Structurally, cracks in enameloid are more prone to occur and propagate along the interfaces between bundles, where the organic content is less resistant to fracture than hydroxyapatite [86], rather than across them. These interfaces are therefore preferred paths for indentations damage which leads to the predominance of crack propagation along the bundles.
The outer enameloid contains bundles aligned parallel to each other and oriented parallel or perpendicular to the surface. This organization leads to an easy development of straight-line cracks along these aligned bundles.
The random organization of the inner enameloid where the bundles are intertwined and curved results in continuous deflection and curvature of cracks along the interfaces. This leads to increased fracture toughness and crack arrest. Thus, there is significant resistance to inward propagation of indentation damage.
If the cracks start from the outer surface on the labial side of the tooth, they are therefore easily directed to the inner enameloid where it is dissipated due to its very sophisticated interlocking structure. This mechanism prevents chipping of the enameloid surface while stopping cracks before they reach the dentin. This is well represented in Figure 3.7.

4.1.4.2 Toughening mechanisms

Enameloid of *P. nattereri* and *P. brachypomus* allows combining strength and toughness which are mutually exclusive properties. Indeed, although this material consists mainly of stiff and brittle mineral matter, different extrinsic mechanisms are used to reduce stresses at the crack tip and to counteract fracture propagation. These are induced by the hierarchical structure of the enameloid. The small portion of organic matter surrounding the bundles represents a preferential direction for crack propagation and this leads to several extrinsic toughening mechanisms allowing resisting the development of damage. In a first step, the deflection of the cracks at the crack corner in the direction of the bundles contributes to decreasing the intensity of the local stress at the crack tip. Secondly, the crack bridging formed by the un-cracked hydroxyapatite fibers or fiber bundles spans the cracks and reduces the intensity of the local stress at the crack tip. Finally, the cracks propagating along the disorganized bundles of the inner enameloid may curve resulting in an increase of the fracture resistance or be directed into a tubule which stops or reduces the crack propagation.

4.2 Limitations

A limitation encountered in the experiments was the resin used to embed the teeth used in the high load indentation tests. This resin was chosen based on the high quality results obtained by Ludwig Boltzmann Institute of Osteology in Vienna during their works on osteons. Despite having followed their protocol exactly, several problems were encountered when using this resin. The first was the evaporation of the resin in the incubator despite the use of paraffin to seal the mold. This evaporation led to the tooth being left in the oven for several hours without resin around it, which could have led to the formation of micro-cracks like those seen in the piranha tooth in Figure 3.14.B. However, no certainty concerning the origin of these cracks can really be made. Secondly, even after polymerization, the resin remained slightly soft at the base of the mold, which may have an influence on the mechanical tests because the tooth does not sit on a hard surface but on a slightly soft surface. Finally, during the observation of the scanning electron microscope, the voltage of the electron beam had to be decreased to avoid the resin to make bubbles during the passage of the beam on it.

A second limitation of this work is the fact that we did not etch the cross sections of the teeth to also have a clear idea of the orientation of the fibers in this section as well. However, the results of the fractures and etching in the frontal section seemed sufficient to identify the internal structure of the enameloid of these two species.

The small number of samples used in this study is also a limitation that does not allow extensive statistical testing between the species.

It is also important to remember that the samples were tested in a dehydrated state. Due to the water loss, it can therefore be expected that the experimental results will not accurately reflect the actual mechanical properties of tooth enameloid still functioning in vivo. For example, the stiffness and hardness will be higher than the ones found in its natural state while the toughness will be lower. However, due to the low percentage of organic matter present in the enameloid, these variations should not be significant.

4.2.1 Modulus mapping

In addition to mechanical testings with high load indentations, additional trials have been conducted using the modulus mapping technique. However, the application of the procedure to the samples can be considered has a limitation given the very high obtained values.

The modulus mapping technique is an extremely powerful instrument providing the elastic and viscoelastic moduli distributions across the surface of the sample with high spatial resolution. It consists of scanning the surface of the sample with diamond indenters with very sharp tips to which a static force is applied. In addition to this static force, a periodic force is superimposed onto the tip. By measuring the periodic displacement of the tip, it is then possible to obtain the complex stiffness in the near-surface zone and then to extract the storage and loss moduli locally [87].

Modulus mapping technique provided maps of the storage modulus of the enameloid of the carnivorous *P. nattereri* (Figures4.1, 4.2 and 4.3). In general, the values obtained correspond to those obtained by the ongoing study at the University of Liege using static indentation tests. Indeed, the storage modulus values are mainly located between 60 and 120 GPa. However, very high values were also obtained at some locations on the surface. This method is recent, complex and very sensitive and we are not able to

explain the reason for the high values obtained. However, this is a side aspect of this master thesis and therefore has not been investigated further.

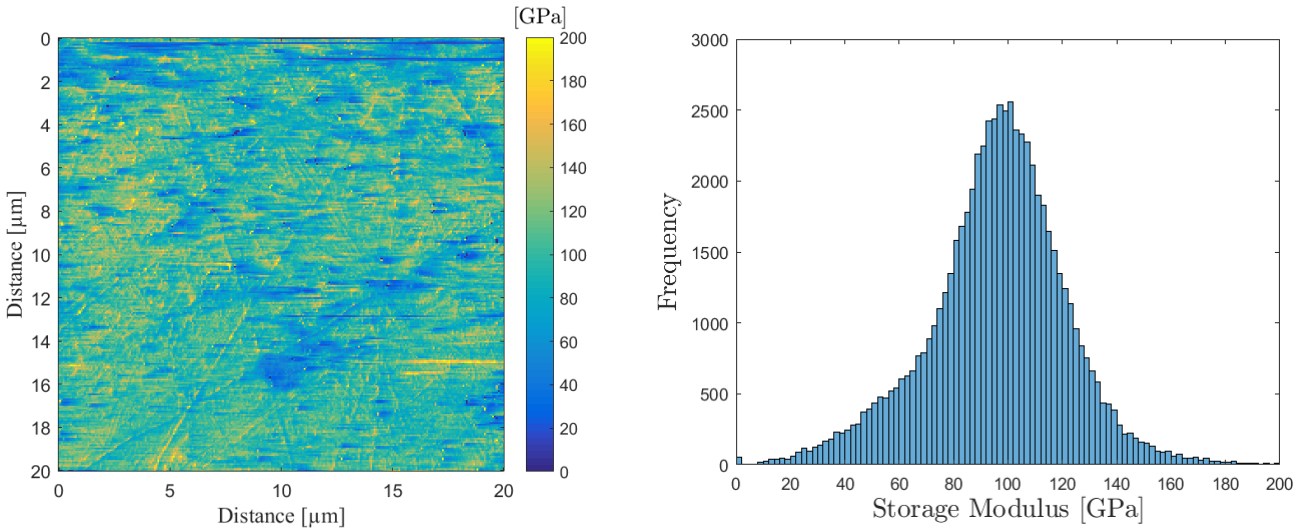

Figure 4.1: (A) Map (B) Histogram of the storage modulus [GPa] of the outer enameloid of the carnivorous *P. nattereri*.

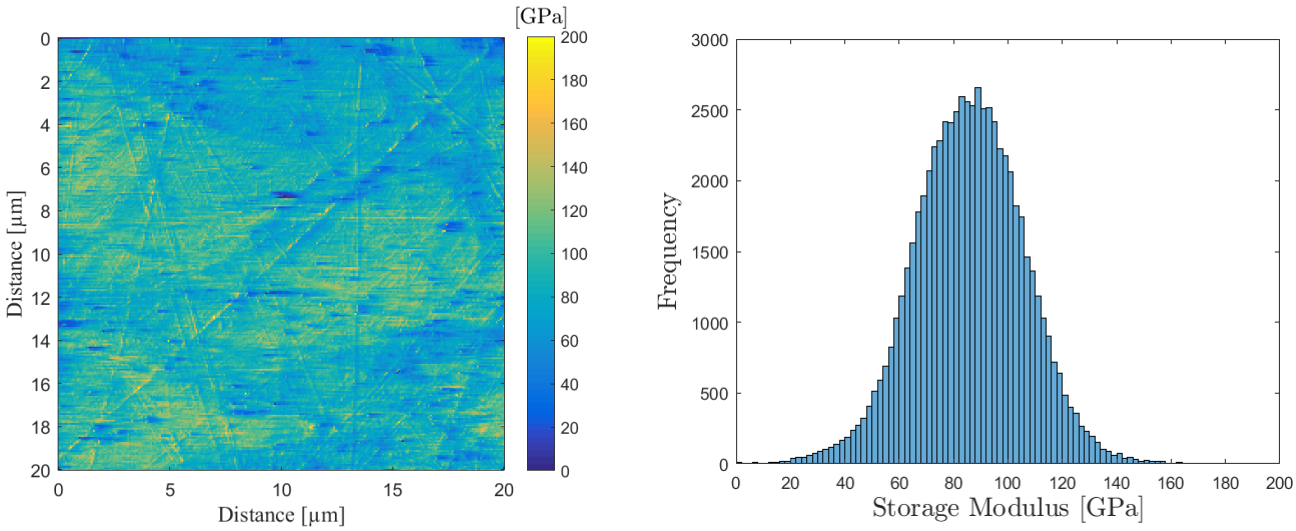

Figure 4.2: (A) Map (B) Histogram of the storage modulus [GPa] of the inner enameloid of the carnivorous *P. nattereri*.

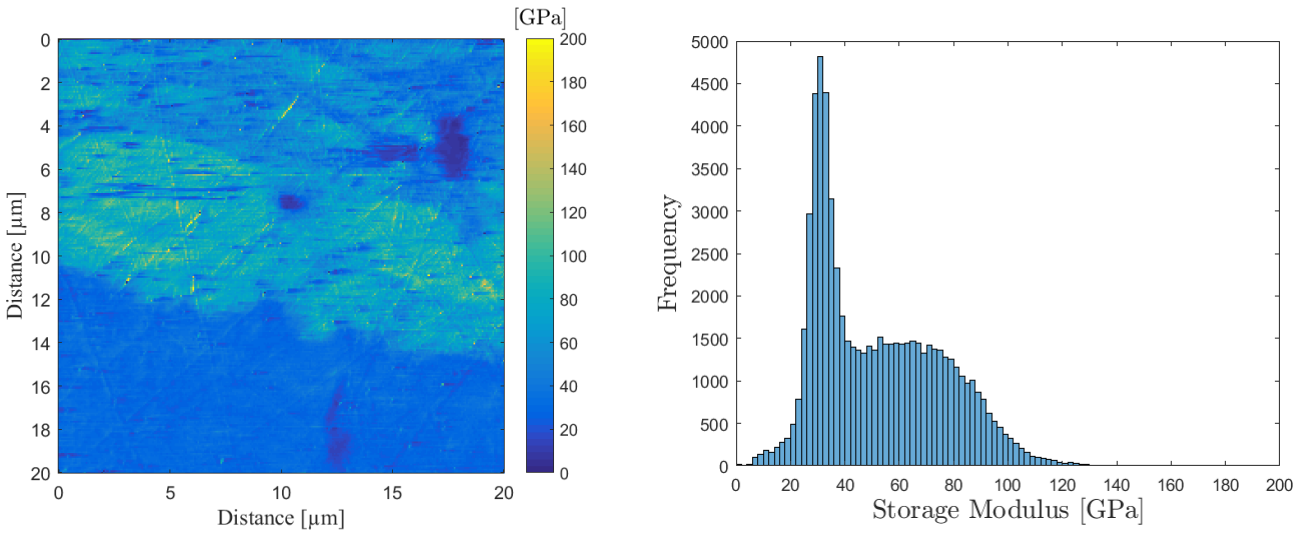

Figure 4.3: (A) Map (B) Histogram of the storage modulus [GPa] of the inner enameloid and the dentin of the carnivorous *P. nattereri*.

4.3 Future works

A first idea for future work related to the limitations of this thesis would be to attempt again a more in-depth modulus mapping over the entire thickness of both sides of the teeth in order to observe precisely if the elastic properties change from one side of the tooth to the other, but also over the enameloid thickness. Linking this technique with FEM simulations to verify the results would be insightful as well.

Another idea for future work could be to perform a slight etching on the high load indentations. This would make it possible to show the orientation and the organization of the bundles under the indents and thus to perfectly relate them to crack propagation phenomena observed.

Finally, another idea for future work would be to study fracture toughness using 3D printing. This technique could be used to generate and print a structure corresponding to the observed arrangement of the mineral bundles surrounded by the organic matrix in the two sub-layers of the enameloid. The influence of the arrangement on the fracture resistance could then be further visualized by performing a three-point bending test on the printed structure and following the cracks with high-speed cameras.

Chapter 5

Conclusion

The aim of this master thesis was first to identify the microstructure of the enameloid in two fishes of the Serrasalmidae family with different diets in order to determine if diet has an impact on the internal microstructure of the enameloid. The second goal of this thesis was to study the fracture toughness of this layer and the link between this mechanical property and the structure.

By analyzing the structure and local fracture behavior of *P. nattereri* and *P. brachypomus* teeth, the following conclusions can be drawn:

- The teeth of piranha and pacu present different external morphology, as already exposed by Delaunois et al. (2020) [21] and the distribution of enameloid within the tooth varies according to the species with a concentration of enameloid mainly at the top of the tooth in pacu and over the whole height of the tooth in carnivores.
- The interface between the enameloid and the cuticle, present in both fishes and having a role in the protection according to Delaunois et al. (2020) [21], seems to be weak, leading to the detachment or the erosion of the latter when it is too solicited.
- Despite their different diet, the enameloid of both fishes have a similar microstructure. Both fish tooth enameloid possesses a hierarchical structure with aligned hydroxyapatite fibers assembled in larger bundles covered with an organic matrix layer. These bundles are arranged in two different organizations through the thickness of the enameloid, dividing this one into two structurally different sub-layers. The inner enameloid contains crossed, oriented and curved bundles in a random manner forming a very complicated interlock structure. While the outer enameloid is well-organized with bundles aligned parallel to each other and oriented either parallel and perpendicularly to the surface depending on the region analyzed (lingual or labial side).
- This structural complexity gives enameloid a higher resistance to fracture than its main component, the mineral hydroxyapatite, allowing the enameloid and, in general, the tooth to avoid catastrophic failure when cracks nucleate on the outer surface due to repeated cycles of chewing.
- The mechanical behavior under the indentation of the enameloid depends on the location within the enameloid. Despite similar values of Young's modulus and hardness, the inner and outer enamel have different fracture properties. Although the difference is not significant, greater fracture toughness is nevertheless observed in the inner enameloid than the outer enameloid.
- Cracks propagate preferentially along the interfaces between hydroxyapatite bundles or different layers (cuticle, inner and outer enameloid). Several extrinsic toughening mechanisms are used by the enameloid to increase its fracture toughness such as crack deflection/curvature and un-cracked hydroxyapatite bundles.

Appendices

Appendix A: Surface etching

Outer enameloid

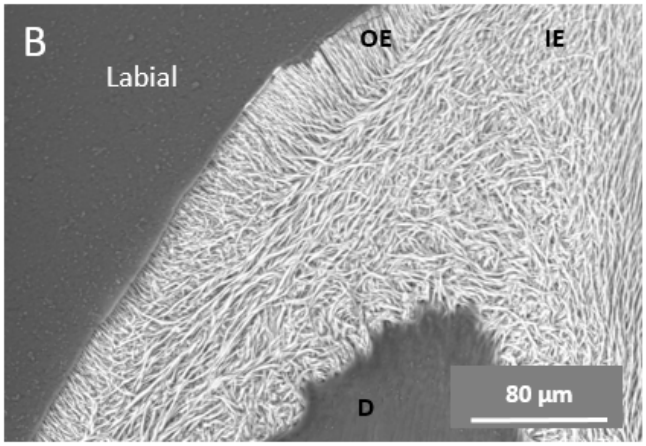

Figure 5.1: SEM−BSE images of frontal sections of an oral tooth of the carnivorous P. nattereri after HCl etching. *Abbreviations: D, dentin; OE, outer enameloid; IE, inner enameloid.*

Appendix B: Fractures

Outer enameloid

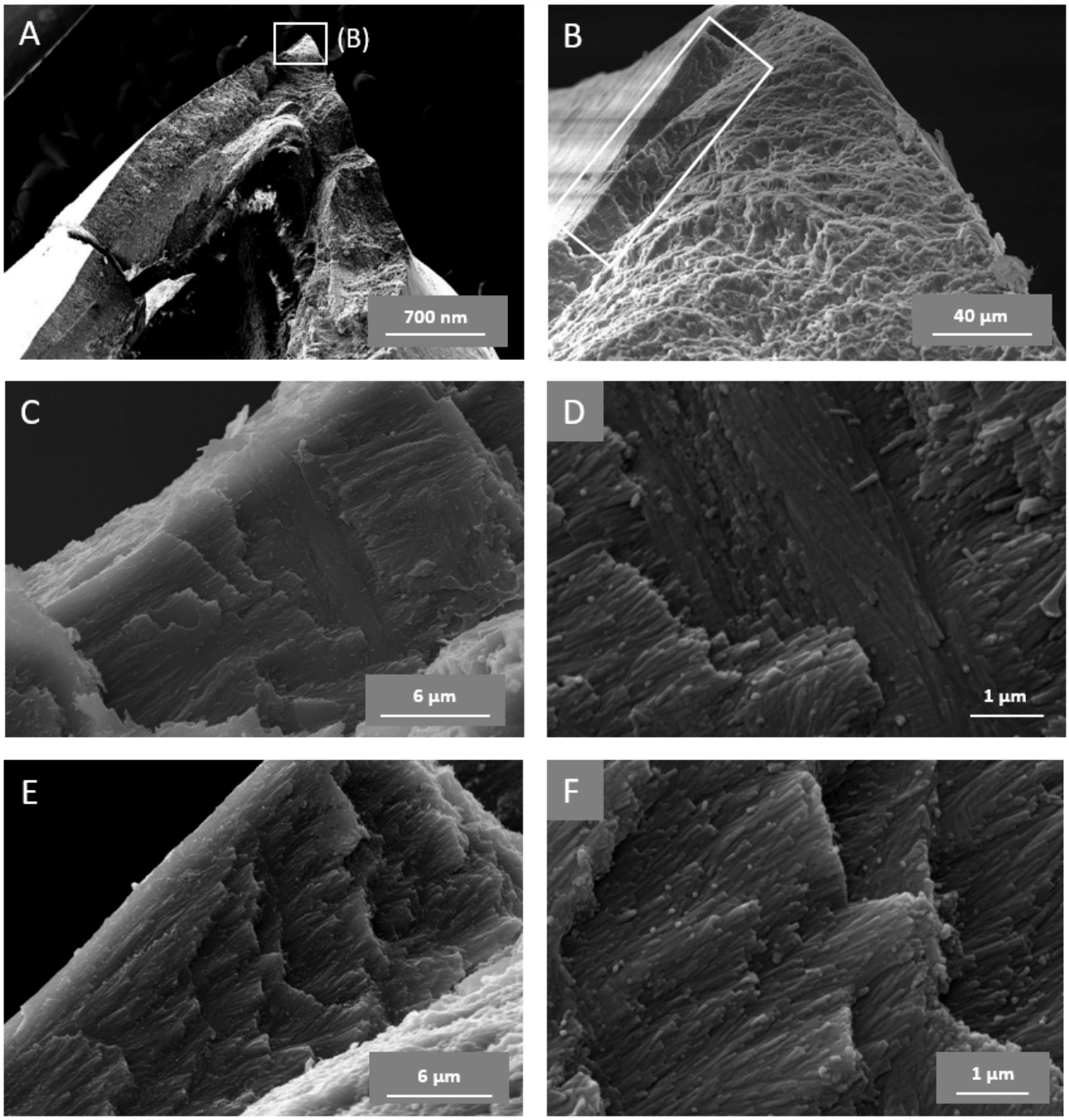

Figure 5.2: SEM−SE images of frontal section fractures of an oral tooth of the herbivorous *P. brachypomus*. (B) Zoom in the region B of (A); (C,D),(E,F) Zooms in different regions in the rectangle of (B) showing two different zones of the outer enameloid.

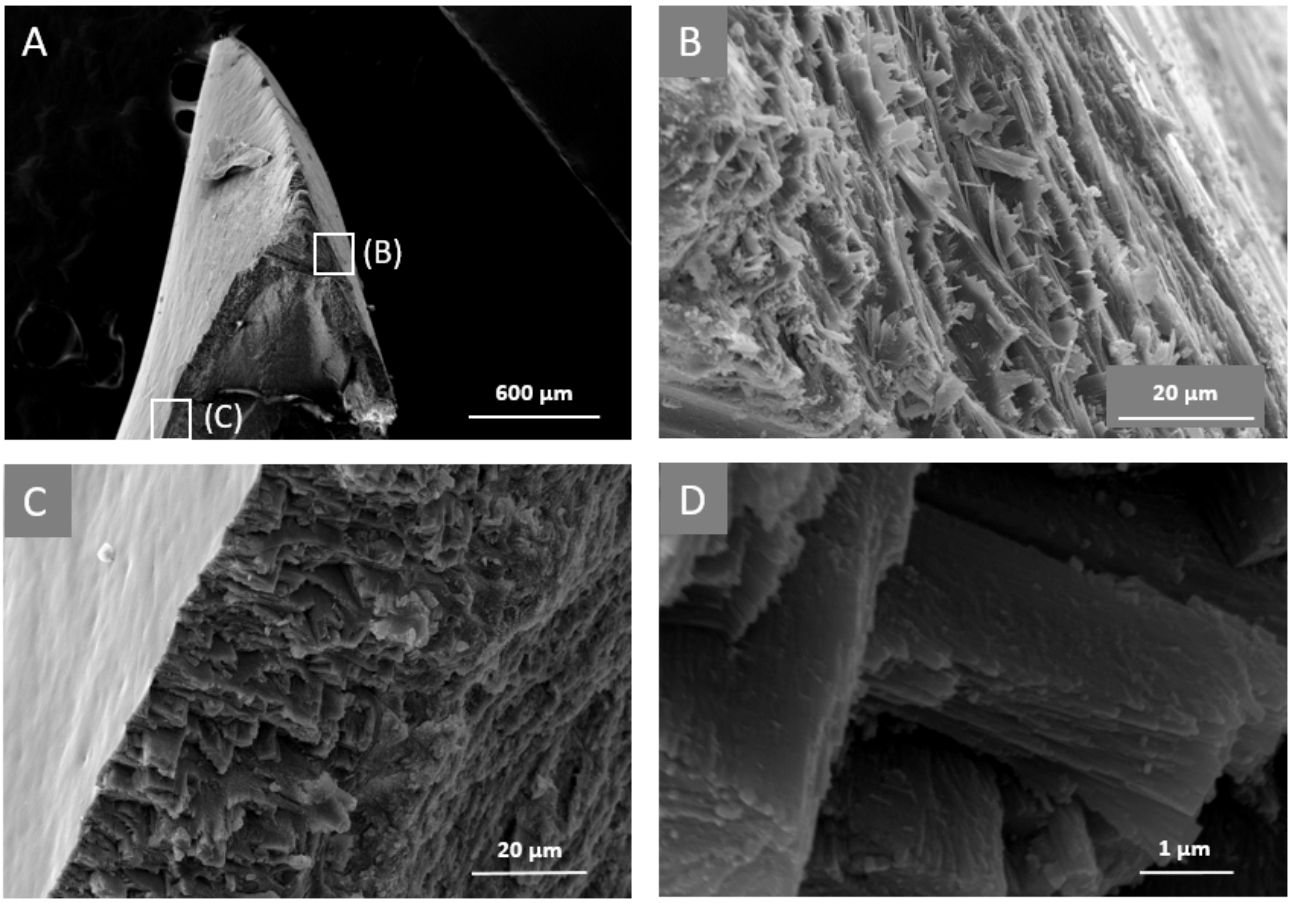

Figure 5.3: SEM−SE images of section fractures of an oral tooth in the carnivorous *P. nattereri*. (B) Zoom in the region B of (A) showing the outer enameloid above which the cuticle has been peeled; (C,D) Zooms in the region C of (A) showing the outer enameloid.

Inner enameloid

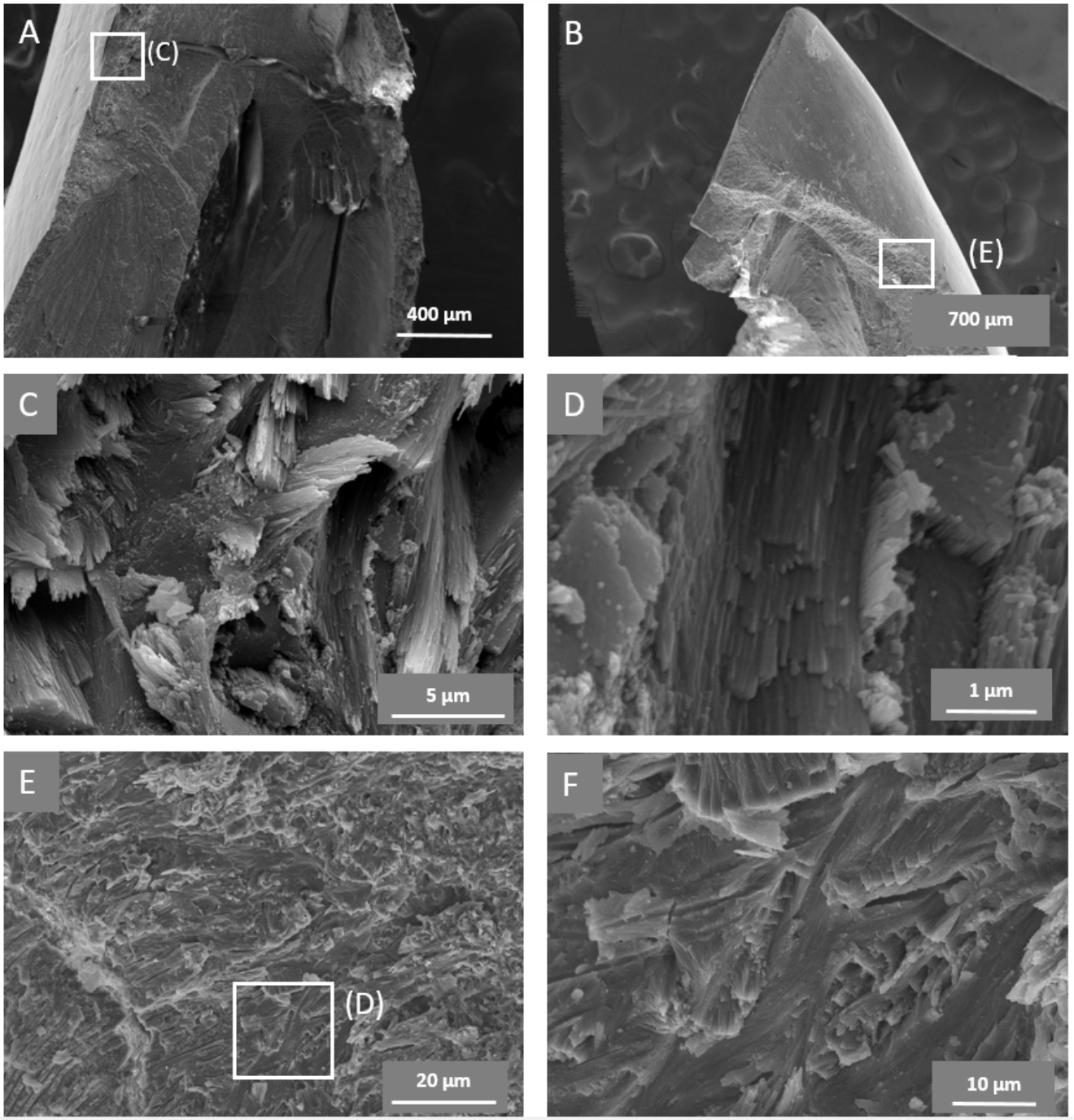

Figure 5.4: SEM−SE images of section fractures of oral teeth in the (A,D,F) carnivorous *P. nattereri* and the (B,C,E) herbivorous *P. brachypomus*. (C,D) Zooms in the region C of (A) showing the inner enameloid of the carnivorous species; (E,F) Zooms in different regions in the region E of (B) showing inner enameloid of the herbivorous species.

Dentin

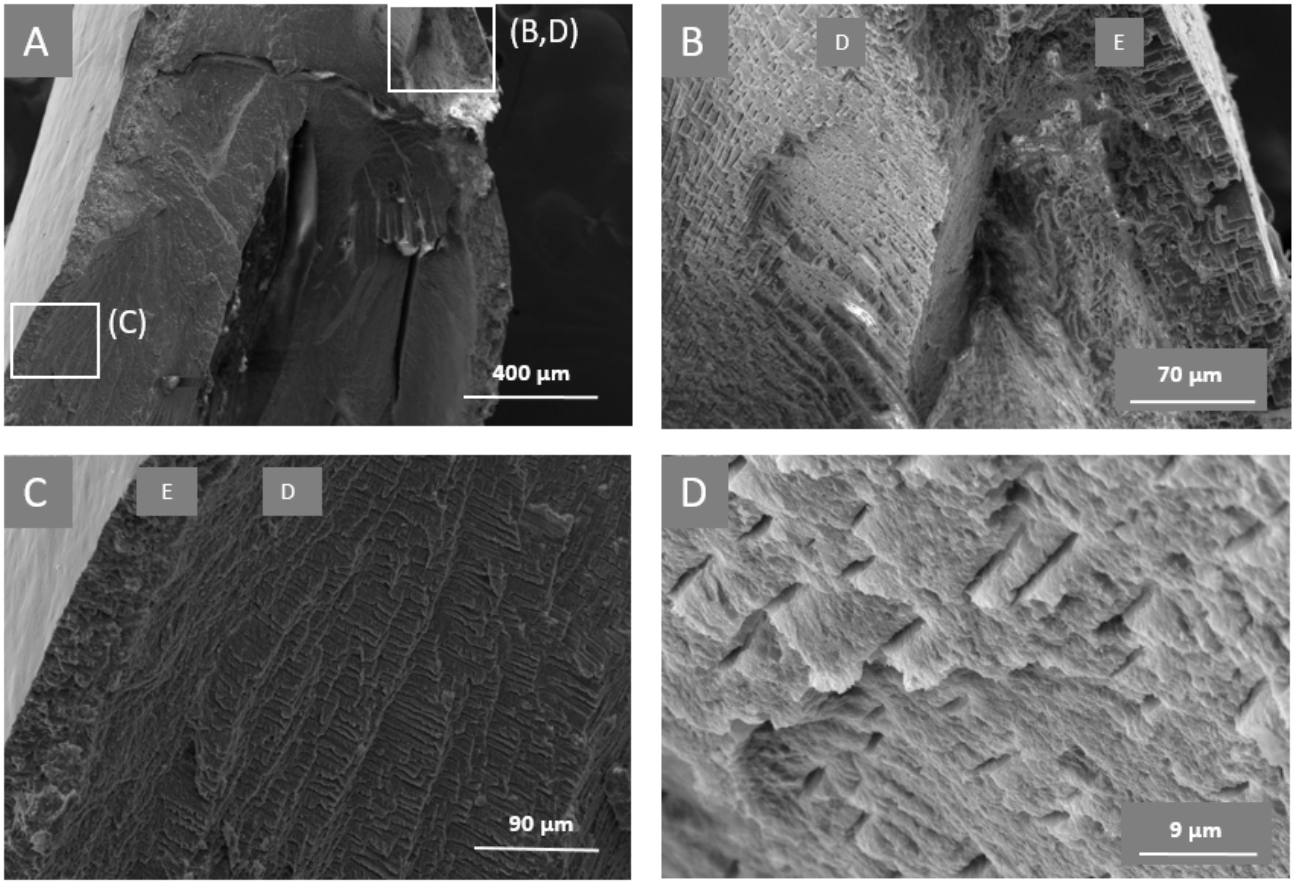

Figure 5.5: SEM−SE images of frontal section fractures of an oral tooth of the carnivorous *P. nattereri*. (B,D) Zooms in the region B, D of (A) showing the enameloid and the dentin; (D) shows cross sections of dentin tubules; (C) Zoom in the region C of (A) showing the enameloid and the dentin; *Abbreviations: E, enameloid; D, dentin*.

Bibliography

[1] P. Y. Chen, A. Y. M. Lin, Y. S. Lin, Y. Seki, A. G. Stokes, J. Peyras, E. A. Olevsky, M. A. Meyers, and J. McKittrick. Structure and mechanical properties of selected biological materials. *Journal of the Mechanical Behavior of Biomedical Materials*, 1(3), 2008.

[2] Z.Y. Weng, Z.Q. Liu, R.O. Ritchie, D. Jiao, D.S. Li, H.L. Wu, L.H. Deng, and Z.F. Zhang. Giant pandas tooth enamel: Structure, mechanical behavior and toughening mechanisms under indentation. *Journal of the Mechanical Behavior of Biomedical Materials*, 64:125–138, 2016.

[3] J Enax, A M. Janus, D Raabe, M Epple, and HO Fabritius. Ultrastructural organization and micromechanical properties of shark tooth enameloid. *Acta Biomaterialia*, 10(9):3959–3968, 2014.

[4] Barry K. B Berkovitz. *Nothing but the Tooth: A Dental Odyssey*. Elsevier Insights, 2013.

[5] J. Jernvall and I. Thesleff. Tooth shape formation and tooth renewal: evolving with the same signals. *Development*, 139(19):3487–3497, 2012.

[6] J. Huber, E. Griesshaber, F. Nindiyasari, W. W. Schmahl, and A. Ziegler. Functionalization of biomineral reinforcement in crustacean cuticle: Calcite orientation in the partes incisivae of the mandibles of Porcellio scaber and the supralittoral species Tylos europaeus (Oniscidea, Isopoda). *Journal of Structural Biology*, 190(2):173–191, May 2015.

[7] Teaford; Mark F and Smith; Moya Meredith. *Development, Function and Evolution of Teeth*. Cambridge University Press, 2007.

[8] Zackary A. Graham, Eva Garde, Mads Peter Heide-Jørgensen, and Alexandre V. Palaoro. The longer the better: evidence that narwhal tusks are sexually selected. *Biology Letters*, 16(3):20190950, March 2020. Publisher: Royal Society.

[9] S. J. Carlson. Vertebrate Dental Structures. In J. G. Carter, editor, *Short Courses in Geology*, pages 235–260. American Geophysical Union, Washington, D. C., March 2013.

[10] A. Sadier, W. R. Jackman, V. Laudet, and Y. Gibert. The Vertebrate Tooth Row: Is It Initiated by a Single Organizing Tooth? *BioEssays*, 42(6):1900229, June 2020.

[11] J. P. Malfay. Les dents des vertébrés fossiles. *Minéraux et fossiles, le guide du collectionneur*, (205):13–19, 1993.

[12] A. H. Thompson. The Homology of the Dental Tissues, Etc. *The Dental Register*, 31(6):249–258, June 1877.

[13] month = may year = 1869 pmid = 17230805 pmcid = PMC1318682 pages = 262–278 Flower, W. H. The Homologies and Notation of the Teeth of Mammalia. *Journal of Anatomy and Physiology*, 3(Pt 2).

[14] A. Huysseune and I. Thesleff. Continuous tooth replacement: the possible involvement of epithelial stem cells. *BioEssays*, 26(6):665–671, June 2004.

[15] B. K. B. Berkovitz and R. P. Shellis. *The teeth of non-mammalian vertebrates*. Academic Press is an imprint of Elsevier, London, United Kingdom ; San Diego, CA, United States, 2017.

[16] P. S. Ungar. Tooth form and function: insights into adaptation through the analysis of dental microwear. *Frontiers of Oral Biology*, 13:38–43, 2009.

[17] P. S. Ungar and H.-D. Sues. Tetrapod Teeth: Diversity, Evolution, and Function. In V. Bels and I. Q. Whishaw, editors, *Feeding in Vertebrates: Evolution, Morphology, Behavior, Biomechanics*, Fascinating Life Sciences, pages 385–429. Springer International Publishing, Cham, 2019.

[18] toppr Answr. Teeth. `https://www.toppr.com/ask/content/concept/teeth-200888/`.

[19] S. R. P. Line and P. D. Novaes. THE DEVELOPMENT AND EVOLUTION OF MAMMALIAN ENAMEL: STRUCTURAL AND FUNCTIONAL ASPECTS. page 6, 2005.

[20] ClipArt ETC. Structure of canine tooth.

[21] Y Delaunois, A Huby, C Malherbe, G Eppe, E Parmentier, and P Compère. Microstructural and compositional variation in pacu and piranha teeth related to diet specialization (Teleostei: Serrasalmidae). *Journal of Structural Biology*, 210(3):107509, 2020.

[22] D. S. Koussoulakou, L. H. Margaritis, and S. L. Koussoulakos. A Curriculum Vitae of Teeth: Evolution, Generation, Regeneration. *International Journal of Biological Sciences*, pages 226–243, 2009.

[23] J. Catón and A. S. Tucker. Current knowledge of tooth development: patterning and mineralization of the murine dentition. *Journal of Anatomy*, 214(4):502–515, 2009.

[24] M. A. Meyers, P.-Y. Chen, A. E. W. Lin, and Y. Seki. Biological materials: Structure and mechanical properties. *Progress in Materials Science*, 53(1):1–206, 2008.

[25] S Isokawa, M Yoshida, K Ikeda, K Yamaguchi, and N Chikazawa. Tooth Enameloid Formation of a Fish (Hoplognathus fasciatus). Chronological relationship of matrix formation and mineralization of the enameloid and dentin. *The Journal of Nihon University School of Dentistry*, 14(1):1–11, 1972.

[26] K. Kubota, M. Kabasawa, K. Morimoto, T. Oyanagi, and Y. Toda. Scanning electron microscope study of fish tooth dentin. (Serrasalmus nattereri KNER). *The Journal of Nihon University School of Dentistry*, 13(2):63–70, 1971.

[27] I. Thesleff. Chapter 22 - Molecular Genetics of Tooth Development. In S. A. Moody, editor, *Principles of Developmental Genetics (Second Edition)*, pages 393–405. Academic Press, Oxford, January 2015.

[28] R. P. Shellis, A. E. W. Miles, and Richard John Harrison. Observations with the electron microscope on enameloid formation in the common eel (Anguilla anguilla; Teleostei). *Proceedings of the Royal Society of London. Series B. Biological Sciences*, 194(1115):253–269, October 1976. Publisher: Royal Society.

[29] DentoMedia. Understand development of tooth stages with diagrams and charts, 2020.

[30] I. Sasagawa, M. Ishiyama, and J. Akai. Cellular influence in the formation of enameloid during odontogenesis in bony fishes. *Materials Science and Engineering: C*, 26(4):630–634, 2006.

[31] N. Biswas, A. Dey, S. Kundu, H. Chakraborty, and A. K. Mukhopadhyay. Orientational Effect in Nanohardness of Functionally Graded Microstructure in Enamel. *Journal of The Institution of Engineers (India): Series D*, 93(2):87–95, 2012.

[32] P.-Y. Chen, J. Schirer, A. Simpson, R. Nay, Y.-S. Lin, W. Yang, M. I. Lopez, J. Li, E. A. Olevsky, and M. A. Meyers. Predation versus protection: Fish teeth and scales evaluated by nanoindentation. *J. Mater. Res.*, 27(1):13, 2012.

[33] Y. Miake, T. Aoba, E. C. Moreno, S. Shimoda, K. Prostak, and S. Suga. Ultrastructural studies on crystal growth of enameloid minerals in elasmobranch and teleost fish. *Calcified Tissue International*, 48(3):204–217, March 1991.

[34] J.C. Elliott, R.M. Wilson, and S.E.P. Dowker. Apatite structures. *Advances in X-ray Analysis*, 45:172–81, 2002.

[35] J. Enax, O. Prymak, D. Raabe, and M. Epple. Structure, composition, and mechanical properties of shark teeth. *Journal of Structural Biology*, 178(3):290–299, 2012.

[36] R Z Legeros and J P Legeros. 16 - Hydroxyapatite. In T. Kokubo, editor, *Bioceramics and their Clinical Applications*, Woodhead Publishing Series in Biomaterials, pages 367–394. Woodhead Publishing, 2008.

[37] R. Z. LeGeros and S. Suga. Crystallographic nature of fluoride in enameloids of fish. *Calcified Tissue International*, 32(1):169–174, 1980.

[38] Fu-Zhai Cui; Jun Ge. New observations of the hierarchical structure of human enamel, from nanoscale to microscale. *Tissue engineering and regenerative medicine*, 1(3):722–741, 2007.

[39] J.L. Cuy, A.B. Mann, K.J. Livi, M.F. Teaford, and T.P. Weihs. Nanoindentation mapping of the mechanical properties of human molar tooth enamel. *Archives of Oral Biology*, 47(4):281–291, April 2002.

[40] Park S. Quinn G.D. Arola D. Bajaj, D. Fracture processes and mechanisms of crack growth resistance in human enamel. *JOM*, 62:76–82, 2010.

[41] S.N. White, W. Luo, M.L. Paine, H. Fong, M. Sarikaya, and M.L. Snead. Biological Organization of Hydroxyapatite Crystallites into a Fibrous Continuum Toughens and Controls Anisotropy in Human Enamel. *Journal of Dental Research*, 80(1):321–326, January 2001. Publisher: SAGE Publications Inc.

[42] R. Hassan, A.A. Caputo, and R.F. Bunshah. Fracture Toughness of Human Enamel. *Journal of Dental Research*, 60(4):820–827, April 1981. Publisher: SAGE Publications Inc.

[43] S. Park, J. B. Quinn, E. Romberg, and D. Arola. On the brittleness of enamel and selected dental materials. *Dental Materials: Official Publication of the Academy of Dental Materials*, 24(11):1477–1485, November 2008.

[44] Z.-J. Cheng, J. Wang, X.-M.and Ge, J.-X. Yan, N. Ji, L.–L. Tian, and F.-Z. Cui. The mechanical anisotropy on a longitudinal section of human enamel studied by nanoindentation. *Journal of Materials Science: Materials in Medicine*, 21(6):1811–1816, 2010.

[45] A W. Thompson, R Betancur-R., H López-Fernández, and G Ortí. A time-calibrated, multi-locus phylogeny of piranhas and pacus (Characiformes: Serrasalmidae) and a comparison of species tree methods. *Molecular Phylogenetics and Evolution*, 81:242–257, 2014.

[46] M A Kolmann, L C Hughes, L P Hernandez, D Arcila, R Betancur-R, M H Sabaj, H López-Fernández, and G Ortí. Phylogenomics of Piranhas and Pacus (Serrasalmidae) Uncovers How Dietary Convergence and Parallelism Obfuscate Traditional Morphological Taxonomy. *Systematic Biology*, 2020.

[47] N T.B. Mateussi, B F. Melo, R P. Ota, F F. Roxo, L E. Ochoa, F Foresti, and C Oliveira. Phylogenomics of the Neotropical fish family Serrasalmidae with a novel intrafamilial classification (Teleostei: Characiformes). *Molecular Phylogenetics and Evolution*, 153:106945, 2020.

[48] B Freeman, LG. Nico, M Osentoski, H L. Jelks, and T M. Collins. Molecular systematics of Serrasalmidae: Deciphering the identities of piranha species and unraveling their evolutionary histories. *Zootaxa*, 1484(1):1–38, 2007.

[49] G Ortí, A Sivasundar, K Dietz, and M Jégu. Phylogeny of the Serrasalmidae (Characiformes) based on mitochondrial DNA sequences. *Genetics and Molecular Biology*, 31(1):343–351, 2008.

[50] F. Duponchelle, F. Lino, N. Hubert, J. Panfili, J.-P. Renno, E. Baras, J.-P. Torrico Ballivian, R. Dugué, and J. Núñez-Rodriguez. Environment-related life-history trait variations of the red-bellied piranha Pygocentrus nattereri in two river basins of the Bolivian Amazon. *Journal of Fish Biology*, 71:1113–1134, 2007.

[51] D. Pauly. Quantitative analysis of published data on the growth, metabolism, food consumption, and related features of the red-bellied piranha,Serrasalmus nattereri (Characidae). *Environmental Biology of Fishes*, 41(1):423–437, 1994.

[52] J. R. Grubich, S. Huskey, S. Crofts, G. Orti, and J. Porto. Mega-Bites: Extreme jaw forces of living and extinct piranhas (Serrasalmidae). *Scientific Reports*, 2(1):1009, 2012. Number: 1 Publisher: Nature Publishing Group.

[53] J Joseph. Etude morpho-fonctionnelle des mâchoires buccales supérieures et de la dentition chez différentes espèces de Serrasalmidae. page 40.

[54] M. Goulding and M. Goulding. *The Fishes and the Forest: Explorations in Amazonian Natural History*. University of California Press, January 1980. Google-Books-ID: krIsP5RbFx0C.

[55] M. Goulding and M.L. Carvalho. Life history and management of the tambaqui (Colossoma macropomum, Characidae): an important Amazonian food fish. *Revista Brasileira de Zoologia*, 1(2):107–133, 1982.

[56] M. Jégu. Subfamily Serrasalminae (Pacus and piranhas). In R.E. Reis, S.O. Kullander, and C.J. Ferraris, editors, *Check list of the freshwater fishes of South and Central America*, pages 182–196. Edipucrs, Porto Alegre, 2003. Accession Number: fdi:010036914 Source: IRD - Base Horizon / Pleins textes.

[57] Seriously fish. Pygocentrus nattereri. `https://www.seriouslyfish.com/species/pygocentrus-nattereri/`.

[58] Imperial tropical. Red bellied pacu (piaractus brachypomus). `https://imperialtropicals.com/products/red-bellied-pacu`.

[59] W. L. Fink. Revision of the Piranha Genus Pygocentrus (Teleostei, Characiformes). *Copeia*, 1993(3):665–687, 1993. Publisher: [American Society of Ichthyologists and Herpetologists (ASIH), Allen Press].

[60] M. Uetanabaro, T. Wang, and A. Abe. Breeding behavior of the red-bellied piranha Pygocentrus nattereri in nature. *Environmental Biology of Fishes*, 38:369–371, 1993.

[61] P. Fuller, L. Nico, and J. Williams. *Non-Indigenous Fishes Introduced into Inland Waters of the United States*, volume 27. 1999. Journal Abbreviation: American Fisheries Society Special Publication Publication Title: American Fisheries Society Special Publication.

[62] Red piranha - Encyclopedia of Life.

[63] I. Sazima and F. Machado. Underwater observation of piranhas in western Brazil. *Environmental Biology of Fishes*, 28:17–31, 1990.

[64] M. Escobar Lizarazo, R. Ota, A. Machado-Allison, I. Farias, and T. Hrbek. A new species of Piaractus (Characiformes: Serrasalmidae) from the Orinoco Basin with a redescription of Piaractus brachypomus. *Journal of Fish Biology*, 95, 2019.

[65] A. F. Nascimento, A. N. Maria, N. O. Pessoa, M. a. M. Carvalho, and A. T. M. Viveiros. Out-of-season sperm cryopreserved in different media of the Amazonian freshwater fish pirapitinga (Piaractus brachypomus). *Animal Reproduction Science*, 118(2-4):324–329, 2010.

[66] K. Roshni, R. Cr, and M. Kurup. Record of a newly introduced fish, red-bellied pacu Piaractus brachypomus (Cuvier, 1818) (Characiformes, Serrasalmidae), in a tropical wetland system, India. *Journal of Applied Ichthyology*, 30, June 2014.

[67] G.R. Reenamole and F. George D'Cruz. New record of exotic fish red bellied pacu, piaractus brachypomus (cuvier, 1818) from vellayani fresh waterlake, southwest coast of india. *Int. J. Sci. Res.*, 4(12):1106–1110, 2014.

[68] S. T. Ross and W. M. Brenneman. *The Inland Fishes of Mississippi*. Univ. Press of Mississippi, 2001. Google-Books-ID: WEaKXWRt10kC.

[69] D. Schleser. *Piranhas: A Complete Owner's Manual*. Barron's Educational Series, 1997.

[70] J. B. K. Fernandes, R. Lochmann, and F. A. Bocanegra. Apparent Digestible Energy and Nutrient Digestibility Coefficients of Diet Ingredients for Pacu Piaractus brachypomus. *Journal of the World Aquaculture Society*, 35(2), 2004.

[71] Elia Beniash; Cayla A. Stifler; Chang-Yu Sun; Gang Seob Jung; Zhao Qin; Markus J. Buehler Pupa U.P.A. Gilbert. The hidden structure of human enamel. *Nature Communications*, 10(1):4383, 2019.

[72] Alessia Huby, A Lowie, A Herrel, R Vigouroux, Bruno Frédérich, X Raick, G Kurchevski, A L Godinho, and E Parmentier. Functional diversity in biters: the evolutionary morphology of the oral jaw system in pacus, piranhas and relatives (Teleostei: Serrasalmidae). *Biological Journal of the Linnean Society*, 127(4):722–741, 2019.

[73] N. A. Yaraghi, N. Guarín-Zapata, L. K. Grunenfelder, E. Hintsala, Sanjit Bhowmick, J. M. Hiller, M. Betts, E. L. Principe, J.-Y. Jung, L. Sheppard, R. Wuhrer, J. McKittrick, P. D. Zavattieri, and D. Kisailus. A Sinusoidally Architected Helicoidal Biocomposite. *Advanced Materials*, 28(32):6835–6844, 2016. _eprint: https://onlinelibrary.wiley.com/doi/pdf/10.1002/adma.201600786.

[74] K. Akhtar, S. A. Khan, S. B. Khan, and A. M. Asiri. Scanning Electron Microscopy: Principle and Applications in Nanomaterials Characterization. In Surender Kumar Sharma, editor, *Handbook of Materials Characterization*, pages 113–145. Springer International Publishing, Cham, 2018.

[75] University of Cambridge. Rolls-royce utc - department of materials science and metallurgy - looking at materials up close - the scanning electron microscope.

[76] How to Mix Backscattered and Secondary Electron Images, July 2018. Section: Materials Article.

[77] Hysitron Ubi-1 Nanoindenter – Analytical Instrumentation Facility (AIF).

[78] N. Cuadrado, D. Casellas, M. Anglada, and E. Jiménez-Piqué. Evaluation of fracture toughness of small volumes by means of cube-corner nanoindentation. *Scripta Materialia*, 66(9):670–673, May 2012.

[79] J. J. Kruzic, D. K. Kim, K. J. Koester, and R. O. Ritchie. Indentation techniques for evaluating the fracture toughness of biomaterials and hard tissues. *Journal of the Mechanical Behavior of Biomedical Materials*, 2(4):384–395, 2009.

[80] A. Miserez, J. C. Weaver, P. J. Thurner, J. Aizenberg, Y. Dauphin, P. Fratzl, D. E. Morse, and F. W. Zok. Effects of Laminate Architecture on Fracture Resistance of Sponge Biosilica: Lessons from Nature: Effects of Laminate Architecture on Fracture Resistance of Biosilica. *Advanced Functional Materials*, 18(8):1241–1248, April 2008.

[81] R. D. Dukino and M. V. Swain. Comparative Measurement of Indentation Fracture Toughness with Berkovich and Vickers Indenters. *Journal of the American Ceramic Society*, 75(12):3299–3304, 1992. _eprint: https://ceramics.onlinelibrary.wiley.com/doi/pdf/10.1111/j.1151-2916.1992.tb04425.x.

[82] A. Datye, U.D. Schwarz, and H.-T. Lin. Fracture Toughness Evaluation and Plastic Behavior Law of a Single Crystal Silicon Carbide by Nanoindentation. *Ceramics*, 1(1):198–210, September 2018. Number: 1 Publisher: Multidisciplinary Digital Publishing Institute.

[83] Alexandra Tits and À Fin Université de Liège > Master ing. civ. biomed. Master thesis : WHERE TENDONS MEET BONES : STRUCTURAL AND MECHANICAL ANALYSIS OF ACHILLES TENDON INSERTION INTO CALCANEUS. June 2018. Accepted: 2018-06-30T02:05:15Z Publisher: Université de Liège, Liège, Belgique.

[84] Hong Hanlie, Tie Liyun, and Jian Tao. The crystal characteristics of enamel and dentin by XRD method. *Journal of Wuhan University of Technology-Mater Sci Ed*, 21:9–12, March 2006.

[85] Robert O. Ritchie. The conflicts between strength and toughness. *Nature Materials*, 10(11):817–822, November 2011. Number: 11 Publisher: Nature Publishing Group.

[86] J. Ge, F. Z. Cui, X. M. Wang, and H. L. Feng. Property variations in the prism and the organic sheath within enamel by nanoindentation. *Biomaterials*, 26(16), June 2005.

[87] Igor Zlotnikov, Emil Zolotoyabko, and Peter Fratzl. Nano-scale modulus mapping of biological composite materials: Theory and practice. *Progress in Materials Science*, 87:292–320, June 2017.

[88] Géry J. Poissons characoïdes des guyanes. i. généralités. ii. famille des serrasalmidae. *Zoologische Verhandelingen*, 122(1):1–250, 1972.

[89] DentoMedia. Understand development of tooth stages with diagrams and charts, 2020.

[90] Bianca Weiss, J. A. S. Zuanon, and M. T. F. Piedade. Viability of Seeds Consumed by Fishes in a Lowland Forest in the Brazilian Central Amazon. *Tropical Conservation Science*, 9(4), 2016.

[91] S. B. Correa, K. O. Winemiller, H. LóPez-Fernández, and M. Galetti. Evolutionary Perspectives on Seed Consumption and Dispersal by Fishes. *BioScience*, 57(9):748–756, 2007.

[92] Figure 2.3: Schematic of the Berkovich indenter (a) Indenter impression...

[93] J.-Y. Sun and J. Tong. Fracture Toughness Properties of Three Different Biomaterials Measured by Nanoindentation. *Journal of Bionic Engineering*, 4(1):11–17, March 2007.

[94] M. T. Laugier. New formula for indentation toughness in ceramics. *Journal of Materials Science Letters*, 6(3):355–356, March 1987.